Renewable Energy Systems and Power Electronics: Advances, Applications, and Integration

Editor: Dr. Muhammet Raşit Sancar

ÖZGÜR YAYINLARI

Renewable Energy Systems and Power Electronics: Advances, Applications, and Integration

Editor:

Dr. Muhammet Raşit Sancar

ÖZGÜR YAYINLARI

Published by
Özgür Yayın-Dağıtım Co. Ltd.
Certificate Number: 45503

15 Temmuz Mah. 148136. Sk. No: 9 Şehitkamil/Gaziantep
+90.850 260 09 97
+90.532 289 82 15
www.ozguryayınlari.com
info@ozguryayinlari.com

Renewable Energy Systems and Power Electronics: Advances, Applications, and Integration

Editor: Dr. Muhammet Raşit Sancar

Language: English
Publication Date: 2023
Cover design by Mehmet Çakır
Cover design and image licensed under CC BY-NC 4.0
Print and digital versions typeset by Çizgi Medya Co. Ltd.

ISBN (PDF): 978-975-447-675-0

DOI: https://doi.org/10.58830/ozgur.pub186

Suggested citation:
Sancar, M. R. (ed) (2023). *Renewable Energy Systems and Power Electronics: Advances, Applications, and Integration.* Özgür Publications. DOI: https://doi.org/10.58830/ozgur.pub186. License: CC-BY-NC 4.0

The full text of this book has been peer-reviewed to ensure high academic standards. For full review policies, see https://www.ozguryayinlari.com/

ÖZGÜR YAYINLARI

Foreword

Dear Readers,

Renewable Energy Systems and Power Electronics: Advances, Applications, and Integration, aims to provide a comprehensive resource on renewable energy systems and power electronics. Meeting the energy demand in a sustainable and environmentally friendly manner has become increasingly important in today's world. Therefore, renewable energy-based systems and power electronics technologies have garnered significant attention.

This book consists of articles written by expert authors in the field. The authors address various topics, including solar energy, thin film deposition techniques, ultrasonic spray pyrolysis technique, dual active bridge DC/DC converters, and other important subjects. The book aims to serve as a valuable reference for students, researchers, and industry professionals who wish to grasp the fundamentals of these topics.

The first section of the book provides a general overview of renewable energy sources. Solar energy, thin film deposition techniques, and other current topics are discussed in detail. Subsequently, the ultrasonic spray pyrolysis technique and its parameters, CdTe thin film solar cell structures and production methods, and other related subjects are examined. Additionally, the working principles and applications of emerging technologies such as Dye Sensitized Solar Cells (DSSCs) and Dual Active Bridge DC/DC Converters are also addressed.

I believe that this book will provide readers with a broad perspective on renewable energy systems and power electronics. Each chapter contains detailed information to provide an in-depth understanding. Moreover, current research and applications are taken into account when discussing each topic.

Lastly, I would like to express my gratitude to all the authors who contributed to the creation of this book. This work has been made possible through their willingness to share their knowledge and experience in the field of renewable energy systems and power electronics.

In conclusion, I hope that this book will serve as a valuable resource for anyone interested in renewable energy systems and power electronics. Enjoy your reading.

Best regards,

Contents

Chaphter 1

Renewable Energy Source And Energy Production

Hüsam Emre Kuzdere[1]

INTRODUCTION

Renewable energy can be defined as "energy that can be replenished within a short period of time through natural cycles occurring in the environment." It is an energy source that starts with the energy coming from the Sun to the Earth and is continuously renewed and inexhaustible. Renewable energy sources have minimum negative impact on the environment compared to non-renewable energy sources. Energy derived from renewable energy sources can be converted into different forms of energy or used directly(Sancar&Altınkaynak, 2021).

Renewable energy sources are of particular importance for countries not only in overcoming the environmental problems encountered in energy production but also in another aspect(Sancar&Bayram, 2023). Although countries may acquire the technology used in power plants from abroad, they will eventually use their own energy resources in renewable energy power plants, thus reducing their dependence on foreign countries and preventing the outflow of money from the country caused by fuel imports for electricity production from traditional energy sources(Sancar&Yakut, 2023).

Global electricity generation capacity from renewable energy sources was 2,813,159 MW at the end of 2020 and reached 3,077,238 MW in 2021, and by the end of 2022, it reached a level of 3,371,793 MW. In Turkey, the capacity of electricity generation from renewable energy sources was 49,195 MW at the end of 2020, increased to 53,230 MW at the end of 2021, and reached 55,998 MW by the end of 2022. When looking at the given figures

1 Isparta University of Applied sciences,Institute of Postgraduate Education, Energy Systems Engineering, Isparta, Turkiye, ORCID Code: (0000-0002-4488-8393) d1840640001@isparta.edu.tr

and the mentioned reasons, it can be seen that the transition to renewable energy continues to increase both globally and in Turkey (IRENA, 2023).

Solar, wind, geothermal, hydroelectric, biogas, and wave energy are renewable energy sources. As important as the existence of these sources is, their utilization in electricity generation is equally important. In Turkey, while hydroelectric sources were predominantly used as renewable energy sources in electricity generation before the 2000s, electricity generation with other renewable energy sources such as wind, solar, biogas, geothermal, etc. became widespread in the 2000s, and as of the end of May 2023, the installed capacity in our country reached 104 672 MW.

As of the end of May 2023, the distribution of our installed capacity by sources is as follows: 30.2% hydropower, 24.2% natural gas, 20.8% coal, 11% wind, 9.6% solar, 1.6% geothermal, and 2.5% other sources (ETKB, 2023).

Furthermore, the number of electricity generation power plants in our country has reached 12 057 (including unlicensed power plants) as of the end of May 2023. Out of the existing plants, 751 are hydroelectric, 67 are coal-fired, 361 are wind, 63 are geothermal, 346 are natural gas, 9 979 are solar, and 490 are other source-based plants.

Hydrolic Energy

Solar energy provides the energy required to sustain the energy cycle that constitutes renewable energy sources. Therefore, solar energy is the primary source of all renewable energy sources. While solar energy was initially used for water heating with the use of collectors, it has also been used for electricity generation through ongoing research and development. Solar energy-based electricity generation has been widely used in Europe for a long time and has started to become more common in Turkey in recent years.

Just as solar energy is the energy source that forms the energy cycle of other renewable energy sources, the factor that allows the formation of water masses that constitute hydraulic energy is also the sun. Water particles, when combined, possess potential energy relative to reference points and kinetic energy due to their velocity. Rivers with qualified energy content are transported to turbines through pipes or channels. The collision of water with the turbine enables the transfer of the water's energy to the turbine shaft. Thus, the potential or kinetic energy of water is converted into mechanical energy. The resulting mechanical energy is then converted into electrical energy through generators (Figure 1).

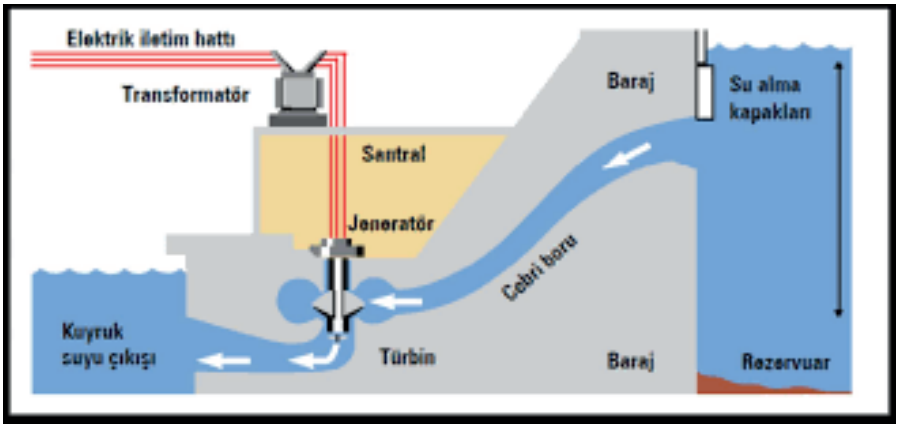

Figure 1. Schematic representation of a hydroelectric power plant (EROĞLU, 2016)

With the advancement of technologies facilitating the transmission of electricity, the proliferation of power plants generating electricity has increased. The first power plants to generate electricity from renewable energy sources were hydroelectric power plants, which are the most widely used and highest electricity-producing source among renewable energy sources. Globally, the installed capacity dependent on hydraulic energy is 1,392,598 MW. The ratio of this value to all renewable energy sources is 37%. In Turkey, there is an installed capacity of 31,572 MW in hydraulic energy (IRENA, 2023).

Turkey is a country rich in hydraulic energy based on water power and has an alternative energy source. Hydroelectric energy production is influenced by precipitation patterns, and consequently, our country, which receives irregular rainfall, can vary in energy production from year to year. Based on long-term meteorological observations and hydraulic data, theoretically, the average annual precipitation of 643 mm corresponds to 501 billion cubic meters. According to current research for the regulation of rivers and maximizing benefits, it is necessary to construct 702 dams. As of 1997, it was determined to be 124.5 billion kWh in Turkey. The first phase of studies on Turkey's hydroelectric potential was carried out by the Electricity Works Research Institute, and the second phase continued with measurements and evaluations conducted in selected basins by the State Hydraulic Works. As a result of the study, it was determined that 3,948 MW of installed capacity could be established on small water sources covering less than 1,000 square kilometers in Turkey, and the technical energy potential with this capacity is 13.9 billion kWh/year, while under average flow conditions, an average

electricity production of 32.4 billion kWh/year could be achieved. In the same study, considering Turkey's hydraulic characteristics and environmental issues, it was stated that small-scale hydroelectric plants should be river-type facilities (Figure 2) (GEZER, 2013).

Figure 2. Hydroelectric power plant (ONZATECH, 2014)

Wind Energy

Wind energy is a renewable energy source that has been used for centuries. It has been utilized in various places, such as moving ships and windmills. Like other renewable energy sources, the primary source of wind energy is solar energy. However, due to uneven heating by the sun, temperature differences occur, which result in the formation of air currents known as "wind." Wind energy is a clean, natural, and renewable form of energy (Sancar, 2023a).

Wind energy refers to the energy possessed by moving air (kinetic energy). Although wind energy utilizes only 1% of the energy received from the Sun, the amount of energy generated is 50-100 times greater than the energy that could be obtained if all the biomass energy from plants were converted. It is expected that this power that can be obtained from wind energy will further increase in the coming years, depending on the technology used (ERDOĞAN, 2014).

The utilization of wind energy dates back to ancient times. Wind energy has been harnessed from ancient times until today. Initially, wind energy was only converted into mechanical energy, but with technological

advancements, especially in the 21st century, it has been extensively used to generate electricity.

Wind turbines and generators are used to convert wind energy into electrical energy. Wind turbines are systems that convert the kinetic energy of the air into mechanical energy. Wind turbines generally consist of:

Wind blades

Hub that holds the blades together

Structure where the mechanical energy extracted from the blades is converted into high-quality mechanical energy

Tower that supports all these components and ensures sufficient height (Figure 3).

After obtaining high-quality mechanical energy in the gearbox located in the structure, this energy is converted into electrical energy in the generator.

Figure 3. Design of an offshore wind energy plant (enerjienstitusu, 2015)

With the rapid advancement of technology and the increasing demand for electricity, the proliferation of wind energy systems for electricity generation has also increased. Globally, electricity generation from wind energy reached 731,656 MW by the end of 2020, 824,171 MW in 2021, and reached 898,824 MW by the end of 2022. In our country, electricity generation from wind energy was 8,832 MW by the end of 2020, 10,607 MW by the end of 2021, and reached 11,396 MW by the end of 2022 (IRENA, 2023).

Geothermal energy, also known as underground heat, refers to the energy generated by the heat within the Earth's crust, which produces various steam and gas containing chemicals. Geothermal energy is derived from the direct or indirect utilization of these resources.

Geothermal energy emerged as one of the popular renewable energy sources in the 20th century, particularly with the energy crisis. Its significantly lower air pollution compared to fossil fuels has positioned it ahead of other systems that produce energy using thermal energy. Additionally, being a domestic and renewable energy source, it is supported by governments as it reduces dependency on external sources.

While heat energy is extracted from the depths of the Earth's crust, the total potential of this heat energy is not known. The temperature and heat capacity of the Earth's core are much greater than the heat capacity of the depths of the Earth's crust. However, reaching these depths is impossible, and therefore, capacity values have not yet been determined.

The renewability of the source and the formation of geothermal fluids rely on the meteoric origin of the waters and their continuous supply to the underground reservoirs. Therefore, as long as the utilization does not affect the replenishment, the depletion of resources is not possible. Geothermal reservoirs are formed as a result of the feeding of porous rock masses by rain, snow, seawater, and magmatic waters. As long as the production values remain within the sustainable limits, geological conditions are preserved, and reinjection processes are carried out, the renewability and sustainability of geothermal reservoirs will be maintained. (Reinjection refers to the process of returning the entire or remaining portion of the produced geothermal fluids back into the Earth's crust after their artificial utilization.) In other words, the water resources that reach underground are heated in suitable locations near the hot rock and magma layers and resurface again. Geothermal energy owes its renewability to this cycle. (GEZER, 2013).

Geothermal Energy

Electricity generation from geothermal energy cannot be achieved from low-temperature geothermal sources; therefore, the energy obtained from low-temperature sources is mainly used for heating purposes. Energy extracted from medium and high-temperature sources is used for electricity generation. Geothermal energy is utilized for electricity production in two different ways: steam-dominated systems and liquid-dominated systems (Figure 4).

In steam-dominated systems, a mixture of steam and water flows into separators where the water and steam are separated. The obtained steam is then sent to turbines to extract mechanical energy, which is further converted into electrical energy through generators.

Steam-dominated systems are named according to the number of separators present in the system. If there is a single separator, it is called a single-flash system; if there are two separators, it is referred to as a double-flash system, and if there are more than two separators, it is known as a multiple-flash system. In systems with multiple separators, the hot water passes through a second separation after the initial separation, and the resulting steam is directed to the turbines. Double-flash systems generally achieve 15-20% higher efficiency compared to single-flash systems. (GÜLAY, 2008)

The second method of electricity generation from geothermal energy is through liquid-dominated systems. Among these systems, the most well-known are binary power plants. In these plants, there is no steam separation; instead, heat is transferred to a second working fluid through a heat exchanger to generate electricity. This allows for easier utilization of medium-temperature sources. (Figure 4)

Figure 4. A geothermal power plant (Wikipedia, 2006)

Continuous research and efforts are being made worldwide, including in Turkey, to harness geothermal energy sources. Globally, the capacity for electricity generation from geothermal energy was 14,417 MW at the end of 2020, which increased to 14,696 MW in 2021 and reached 14,877 MW by the end of 2022. In Turkey, the capacity for electricity generation from geothermal energy was 1,613 MW at the end of 2020, which increased to 1,676 MW in 2021 and further rose to 1,691 MW by the end of 2022 (IRENA, 2023).

Biomass Energy

Biomass energy, like other renewable energy sources, is environmentally friendly. The source of biomass energy consists of animal and plant residues containing carbon compounds that are continuously found in nature. Biomass energy can be defined as the energy obtained from these sources. Unlike other renewable energy sources, biomass energy can be developed by harnessing the existing potential of biomass sources for energy production.

Biomass energy sources can be used for various purposes, such as heating, fuel, and electricity generation. The term "bioenergy" refers to systems that produce electricity or heat using biomass, while the term "biofuel" is used to refer to solid, liquid, and gas fuels obtained from biomass. (GÜLAY, 2008)

Biomass energy can be categorized into two groups: traditional and modern. The first group includes firewood obtained from traditional forests and plant and animal residues used as fuel (such as dung). The second group includes modern biomass energy derived from energy forestry and forest/tree industry residues, agricultural crop residues, urban waste, and agricultural industry residues. Some trees (such as poplar, eucalyptus, willow, Paulownia princess tree, etc.) have a higher growth rate compared to natural forests. Plants such as sweet sorghum, sugar cane, and corn, which grow in regions with abundant sunlight, efficiently utilize water, perform photosynthesis even at low carbon dioxide concentrations, and are more resistant to seasonal drought compared to other plants, are referred to as C4 (carbon) plants (Figure 5). (GEZER, 2013)

Figure 5. A biomass power plant (Piyasaanketi, 2015)

Biogas is a combustible, colorless gas with a high heat value that is produced by the anaerobic (oxygen-free) digestion of various plant residues, animal and human waste, and organic-rich wastewater in specially designed tanks at a constant temperature and without the presence of air. In other words, the composition of biogas consists of approximately 60-70% methane, 30-40% carbon dioxide, and small amounts of hydrogen sulfide, hydrogen, water vapor, ammonia, carbon monoxide, and nitrogen. The heating value of biogas varies depending on the methane content and is generally around 4700-6000 kcal/m^3. Therefore, biogas can be an alternative energy source to basic energy sources that can be easily used for purposes such as heating, lighting, and water heating. (GEZER, 2013)

Biomass can be converted into electricity by obtaining steam from the direct combustion of organic matter and using it to turn turbines, similar to a thermal power plant system. Additionally, electricity can be generated by using biogas obtained through various techniques, similar to combined cycle gas power plants. Waste-to-energy plants operate by utilizing combustible biogas, mainly methane gas, which is produced through the decomposition and anaerobic fermentation of waste. This simultaneously solves the problem of urban waste disposal and provides energy utilization. Urban waste is a good source of biomass energy, but its separation is costly due to the presence of organic and inorganic materials. (GEZER, 2013)

Biodiesel is a fuel that can be used and mixed in any proportion with petroleum-based diesel, or used pure, in any application where diesel is used,

especially in transportation. Biodiesel is produced by the reaction of oils derived from oilseed plants such as rapeseed (canola), soybean, sunflower, and mustard, or animal fats, with a short-chain alcohol (methanol or ethanol), in the presence of a catalyst. Used cooking oils and animal fats can also be used as feedstock for biodiesel production. (GEZER, 2013)

Biodiesel, which is obtained from oil-rich seeds where the majority of its energy content is stored, does not contain petroleum. It can be used as a diesel fuel substitute and can be blended with petroleum-based diesel in any ratio. Biodiesel is noteworthy for its economic viability, waste management benefits, and positive environmental impact. Numerous studies have been conducted on the use of vegetable oils and vegetable oil-based waste frying oils as motor fuels. Some of the leading vegetable oils that can be used in this way are soybean oil, sunflower oil, mustard oil, rapeseed oil, peanut oil, flaxseed oil, hazelnut oil, cottonseed oil, and waste frying oils. Research has shown that biodiesel is more environmentally friendly than diesel fuel, with emission values similar to diesel fuel and even better in some aspects (GEZER, 2013).

Countries are increasing their utilization of biomass energy to generate their own energy and utilize their waste. Globally, the capacity of electricity generation from biomass energy was 133,236 MW at the end of 2020, which increased to 141,302 MW in 2021 and reached 148,912 MW by the end of 2022. In Turkey, the capacity of electricity generation from biomass energy was 1,097 MW at the end of 2020, which increased to 1,637 MW in 2021 and further rose to 1,912 MW by the end of 2022 (IRENA, 2023).

Waves Energy

Waves are formed through the friction between wind and the water surface, which is influenced by the sun. The energy generated by these waves can be converted into usable energy through various methods, and it is referred to as wave energy. Wave energy can be a significant resource, particularly for countries with coastlines, if effectively harnessed.

The production of electricity from wave energy is a system that has been recently attempted. Seas are generally chosen as the application area for wave energy. The amount of electricity that can be generated from wave energy depends on the wave's potential. In some large lakes, waves with electricity generation potential occur, allowing for electricity production from wave energy.

The conversion of wave energy into electrical energy can be achieved through different systems, but the most commonly used system is the

turbine system. The potential energy generated by the wave striking specially designed blades is stored. The continuously produced energy is balanced with the stored energy to generate linear electrical energy. This energy is then converted into electrical energy through the created systems.

While the daily flow of solar energy varies depending on the location, the energy amount per meter is approximately 100 W. For example, in ideal conditions, 1 kW of electricity production can be obtained from a surface area of 10 square meters using solar energy. The same amount of electricity production requires 2 square meters of space when using wind energy. However, for wave power, this area is only 1 square meter. Moreover, in large seas and oceans, this power has the potential to meet more than five times the current global energy demand (Figure 6) (ERDOĞAN, 2014).

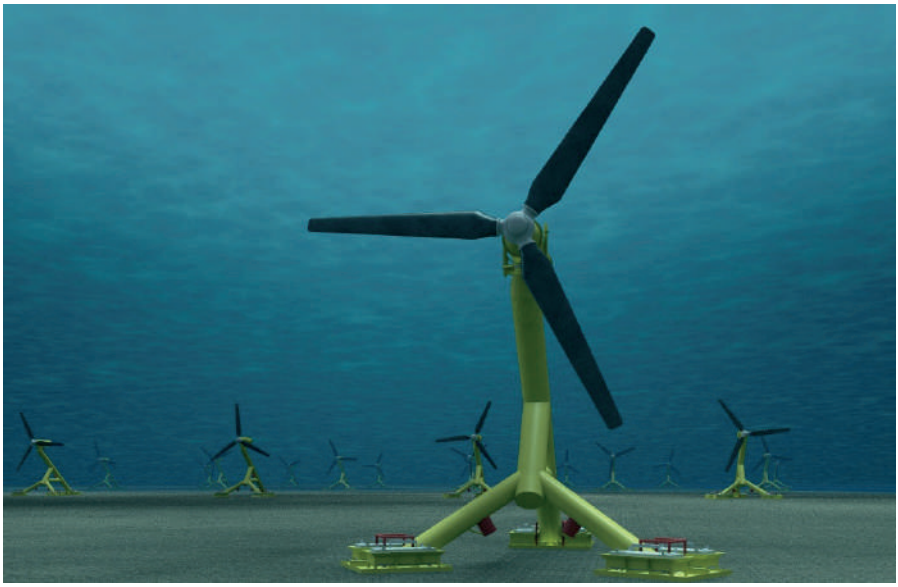

Figure 6. A Wave Energy Turbine Model (Subsea, 2012)

Using wave energy is a great opportunity for countries with coastlines to generate their own energy. Worldwide, the capacity for electricity production from wave energy was 523 MW at the end of 2020 and reached 524 MW by the end of 2022 (IRENA, 2023). In our country, there is currently no electricity production from wave energy. Considering that Turkey is surrounded by seas on three sides and faces increasing energy demand and dependence on external sources, utilizing wave energy for electricity production could be one of the steps taken to solve these problems.

Solar Energy

The Sun plays a crucial role in both warming and illuminating our Earth with its high amount of heat and light energy. The Sun, with a diameter of 1.39 million km and located approximately 150 million km away from Earth, is a mass composed of hot gases (primarily 95% hydrogen). Solar energy is a powerful source of energy resulting from the fusion (splitting) reaction in the Sun's core, where hydrogen gas is converted into helium. The energy released in this reaction is spread into space through heating. A small portion of this energy reaching Earth is more than enough to meet all of humanity's energy needs.

According to measurements, the energy created by the Sun's rays reaching Earth amounts to an average of 1.35 KW per square meter, and the solar energy obtained from a 10 square meter area is 1 KW. Based on this calculation, the energy generated by the Sun's rays reaching Earth in one year is approximately 50 times greater than the energy that can be obtained from known coal reserves (GÜLAY, 2008).

Solar energy is the energy source that gives rise to all renewable energy sources. However, the direct utilization of solar energy rays or heat for electricity production has not yet become widely prevalent. For many years, solar energy has been used primarily for heat generation. In recent years, with advancements in technology, methods of generating electricity from solar energy have been made more efficient and have become more widespread(Sancar, 2023b).

Countries are increasing their utilization of solar energy to generate their own power. Globally, the capacity of solar energy-based electricity production was 720,429 MW at the end of 2020, which increased to 861,537 MW in 2021, and reached 1,053,115 MW by the end of 2022 (IRENA, 2023). In our country, the solar energy-based electricity production capacity was 6,668 MW at the end of 2020, which increased to 7,817 MW in 2021, and reached 9,426 MW by the end of 2022 (IRENA, 2023).

CONCLUSION

In this chapter, we have explored various forms of renewable energy, including hydraulic energy, wind energy, geothermal energy, biomass energy, wave energy, and solar energy. These renewable energy sources play a crucial role in addressing the global energy challenges we face today.

Hydraulic energy, harnessed from the power of flowing water, offers a reliable and widely used renewable energy option. It has the potential to

generate significant amounts of electricity and provide various benefits such as flood control and irrigation. Wind energy, derived from the kinetic energy of moving air, has witnessed remarkable growth in recent years. Wind turbines have become increasingly efficient and cost-effective, making wind power a viable solution for electricity generation in many regions worldwide. Geothermal energy taps into the Earth's heat reservoirs, utilizing the natural heat from the Earth's core to produce electricity and heat. It is a clean and continuous source of energy that can contribute to reducing greenhouse gas emissions and meeting heating and cooling needs. Biomass energy utilizes organic materials, such as agricultural waste, forest residues, and dedicated energy crops, to produce heat, electricity, and biofuels. It offers a sustainable alternative to fossil fuels and helps in waste management while reducing carbon emissions. Wave energy, obtained from the power of ocean waves, has enormous potential as a renewable energy source, particularly for coastal countries. Developing efficient wave energy conversion technologies can lead to a significant contribution to the global energy mix. Solar energy, harnessed from the Sun's radiation, is abundant and widely available. Photovoltaic systems and solar thermal technologies have advanced significantly, enabling the widespread adoption of solar power for electricity generation, heating, and cooling applications. The integration of these renewable energy sources into the global energy mix is crucial for reducing dependence on fossil fuels, mitigating climate change, and achieving a sustainable future. However, challenges such as intermittency, scalability, and cost must be addressed to fully maximize their potential.

As we continue to advance renewable energy technologies and promote supportive policies, the transition to a clean energy future becomes increasingly feasible. By embracing these diverse renewable energy options, we can create a more sustainable and resilient energy system that benefits both present and future generations.

REFERENCES

IRENA (2023). Renewable capacity statistics 2023. *International renewable energy agency*.

ERDOĞAN, M.,2014. Türkiye'nin Yenilenebilir Enerji Potansiyelinin Termodinamik Analiz Yöntemi İle İncelenerek, Yenilenebilir Enerji Kullanımının Gelecek Projeksiyonlarının Değerlendirilmesi. İstanbul Aydın Üniversitesi, Fen Bilimleri Enstitüsü, Yüksek Lisans Tezi, 14s, İSTANBUL

EROĞLU, V. 2016. Çevre Ve Temiz Enerji, Hidrolik Enerji, Erişim Tarihi: 25.05.2016. http://docplayer.biz.tr/5499040-Cevre-ve-temgz-enerjg-hgdroelektrgk-enerjg.html

GEZER, E.H., 2013. Yenilenebilir Enerji Kaynakları ve Türkiye. Gazi Üniversitesi, Sosyal Bilimler Enstitüsü, Yüksek Lisans Tezi, 35s, 36s, ANKARA

GÜLAY, A.N., 2008. Yenilenebilir Enerji Kaynakları Açısından Türkiye'nin Geleceği ve Avrupa Birliği İle Karşılaştırılması. Dokuz Eylül Üniversitesi, Sosyal Bilimler Enstitüsü, Yüksek Lisans Tezi, 75s, İZMİR

Piyasaanketi, 2015. Erişim Tarihi: 25.05.2015. http://piyasaanketi.com/yenilenebilir-enerji/

Besconj, 2016. Erişim Tarihi:25.05.2016. http://besconj.com/off-grid-solar-energy-solutions/

Enerjienstitusu, 2015 Erişim Tarihi: 25.05.2016. http://enerjienstitusu.com/2015/12/25/turkiyenin-ilk-deniz-ustu-ruzgar-gulu-ciftligi-projesine-2016-yilinda-baslanacak/

ONZATECH, 2014. Erişim Tarihi: 25.05.2016. http://www.onzatech.com/wp-content/uploads/2014/05/akarsu.jpg

Subsea, 2012. Erişim Tarihi: 25.05.2016. http://subseaworldnews.com/2012/10/08/uk-government-encourages-marine-energy-generation/

Wikipedia, 2006. Erişim Tarihi: 25.05.2016. https://tr.wikipedia.org/wiki/%C4%B0zlanda#/media/File:NesjavellirPowerPlant_edit.jpg

Sancar, M. R. (2023a). Renewable Energy Sources and Energy Storage. In: Çakoğlu, A. H. & Sancar, M. R. (eds.), Versatile Approaches to Engineering and Applied Sciences: Materials and Methods (pp. 131-140). Özgür Publications. DOI: https://doi.org/10.58830/ozgur.pub50.c69

Sancar, M. R. (2023b). The Effect of Dust Deposition on Photovoltaic Systems' Electricity Generation and Its Economical Analysis. In: Çakoğlu, A. H. & Sancar, M. R. (eds.), Versatile Approaches to Engineering and Applied Sciences: Materials and Methods. Özgür Publications. DOI: https://doi.org/10.58830/ozgur.pub50.c43

Sancar, M. R. & Altınkaynak, M. (2021). Isparta İli İçin Farklı Çatı Tiplerinde Tasarlanan Fotovoltaik Sistemlerin Karşılaştırılması . Avrupa Bilim ve Te-

knoloji Dergisi , Ejosat Özel Sayı 2021 (RDCONF) , 1024-1028 . DOI: 10.31590/ejosat.1047453

Sancar, M. R. & Bayram, A. B. (2023). Modeling and Economic Analysis of Greenhouse Top Solar Power Plant with Pvsyst Software . International Journal of Engineering and Innovative Research , 5 (1) , 48-59 . DOI: 10.47933/ijeir.1209362

Sancar, M. R. & Yakut, K. (2023). Comparative Analysis of SAM and PVsyst Simulations for a Rooftop Photovoltaic System . International Journal of Engineering and Innovative Research , 5 (1) , 60-76 . DOI: 10.47933/ijeir.1209413

Chaphter 2

Electricity Production Methods From Solar Energy and Parameters Affecting Efficiency in Solar Cells

Hüsam Emre Kuzdere[1]

INTRODUCTION

With the rapid increase in the world's population and advancements in technology, humanity's interest in comfort is also rapidly growing. As a result, the demand for energy is increasing day by day. Alongside the rapidly increasing energy consumption, resources are diminishing in the opposite direction (Sancar, 2023a). Fossil fuel sources, which are the most commonly used for energy production today, cause significant harm and pose a threat to the future of humans, nature, and all living beings. The damages, ranging from global warming and air pollution to water contamination and soil degradation, are beginning to manifest themselves in our present time, leading to the extinction of species. Furthermore, fossil fuel sources are no longer capable of meeting the world's energy needs alone and are on the verge of depletion. For these reasons, the search for alternatives to fossil fuels has begun, and there is a growing interest in renewable energy sources (Sancar, 2023b).

Considering the availability, cleanliness, renewability, and inexhaustibility among numerous alternative energy sources that can be utilized on Earth, solar energy emerges as a superior option. There are two different methods of harnessing energy from solar radiation, known as indirect systems and direct systems(Sancar&Yakut, 2023).

Direct systems, such as solar cells, directly convert solar radiation into electrical energy through the photovoltaic effect. Indirect systems, on

1 Isparta University of Applied sciences,Institute of Postgraduate Education, Energy Systems Engineering, Isparta, Turkiye, ORCID Code: (0000-0002-4488-8393) d1840640001@isparta.edu.tr

the other hand, utilize concentrator systems to focus solar radiation onto a fluid medium through large reflectors, enabling the transfer of thermal energy(Sancar&Bayram, 2023). This heated fluid passes through a turbine, converting its energy first into mechanical motion and then into electrical energy. Indirect systems suffer from significant losses due to multiple phase transformations of energy.

Solar cells, are silent, efficient, and require minimal maintenance. On the other hand, indirect systems, like concentrator systems, incur significant maintenance costs (such as seal degradation, corrosion formation, mechanical wear, etc.). Due to all these reasons, research on solar cells has gained importance in recent times and has yielded positive results. The main advantages of solar cells are as follows:

- Can be used anywhere in the world since they operate with solar radiation.
- Do not emit harmful waste or toxic gases.
- Quickly recoup the investment costs.
- Do not require significant maintenance costs.
- Operate silently and safely.

ELECTRICITY GENERATION METHODS FROM SOLAR ENERGY

The Sun, with a diameter of approximately $1{,}392 \times 10^6$ km, is about 109 times larger in diameter than the Earth (Öztürk, 2012). It is considered a fusion reactor due to its composition, which consists of approximately 92.8% hydrogen and 7.1% helium atoms.

The radiation energy resulting from the fusion process occurring in the core of the Sun is called "solar energy." Fusion (nuclear fusion) refers to the reaction where lighter particles combine to form heavier particles. In the Sun, about 657 million tons of hydrogen convert to helium every second, resulting in an excess mass of 4 million tons releasing an energy of 38×10^{22} kJ per second (Ültanır, 1987).

While the core of the Sun reaches temperatures of about 15 million degrees Kelvin, the surface temperature is around 6050 K. Only one two-billionth of the energy emitted by the Sun reaches our planet. Even this small portion exceeds the amount of energy we consume on Earth. The energy that reaches our atmosphere is approximately 1367 W per square meter, known as the "solar constant." However, not all of this energy reaches

the Earth's surface. About 30% is directly reflected back into space from the outer atmosphere, 20% is absorbed by clouds and dispersed into the atmosphere, and 50% reaches the Earth's surface, providing the necessary energy, heat, and resulting in atmospheric movements (Figure 1).

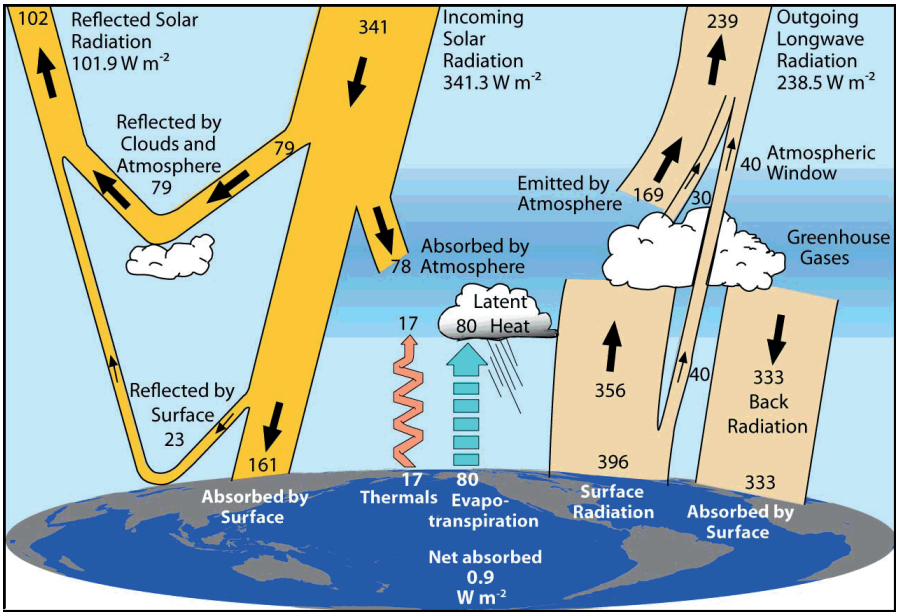

Figure 1. Distribution of radiant energy from the sun (W/m^2) (Bilici, 2019)

Electromagnetic waves are described using frequency (f or ν) and wavelength (λ). The electromagnetic waves emanating from the Sun propagate at different frequencies and wavelengths. These waves do not require any medium to propagate and their speed is known as the "speed of light" ($c=2.99792458 \times 10^8$ m/s). The equation relating the speed of light (c), frequency (f), and wavelength (λ) is given by:

$$\lambda = \frac{c}{f} \tag{1}$$

This equation (1) shows that the wavelength of an electromagnetic wave can be determined by dividing the speed of light by its frequency.

Exactly, electromagnetic waves are defined and categorized based on their wavelengths and frequencies, forming the "electromagnetic spectrum," as shown in Figure 2. Longer-wavelength rays have lower energy, while shorter-wavelength rays have higher energy. Visible light, which falls approximately

between 400 and 700 nm wavelengths, is the portion of the electromagnetic spectrum that is detectable by the human eye due to its sensitivity. Radiation refers to the process of electromagnetic waves or particles being emitted from a medium or substance.

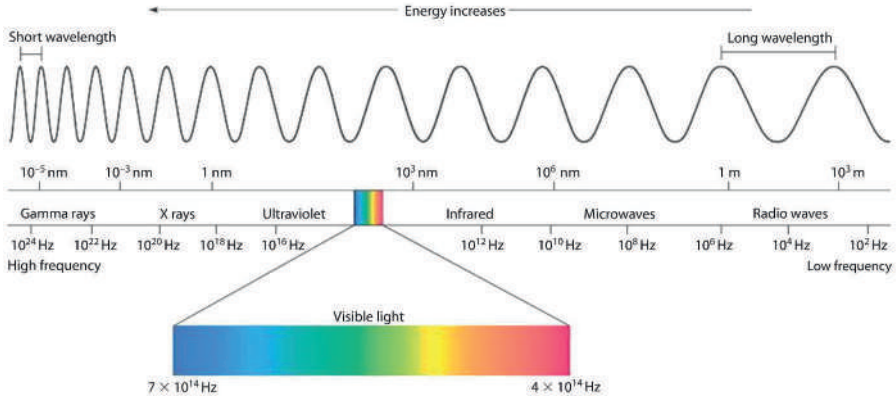

Figure 2. Electromagnetic spectrum (Khafagy, 2018)

As seen in Figure 2. the waves in the electromagnetic spectrum of the sun can be grouped according to their radiation and frequency as follows;

- Gamma rays
- X-rays
- Ultraviolet (UV) radiation
- Visible light
- Infrared radiation
- Microwaves
- Radio waves

Electricity Generation From Solar Energy By Indirect Methods

Thermal (heat) method is a method of generating electricity from solar radiation. The solar rays are concentrated using concentrator equipment and then the heat energy is transferred to a fluid, typically in a liquid phase, to produce high-temperature steam. The heat energy transferred to the high-temperature steam is first converted into mechanical motion in a turbine and then transformed into electrical energy. In some systems, steam generation is achieved directly with the primary fluid, while in others, the primary

fluid, which has absorbed energy through radiation, transfers its energy to a secondary fluid through heat exchange in an exchanger.

Solar thermal applications for solar energy can be categorized into three groups: low temperature (20-100 °C), medium temperature (100-300 °C), and high temperature (>300 °C). Low-temperature applications are used in areas such as water heating and residential heating, utilizing either non-concentrated or minimally concentrated collectors. However, they are not used for electricity generation.Medium-temperature applications are used to obtain high-temperature steam required for electricity generation by concentrating solar radiation using focused collectors.High-temperature applications involve systems that can achieve temperatures above 300 °C. These systems require the placement of numerous reflectors across a wide area, focusing the sunlight onto a single point to generate the necessary high-temperature steam for electricity production (Karamanav, 2007).

According to data from the International Renewable Energy Agency (IRENA) in 2018, the installed capacity of concentrated solar power systems, which are an indirect method of electricity generation from solar energy, reached approximately 5,469 MW worldwide. In Turkey, however, electricity production using these systems is not widespread, with a total installed capacity of around 1 MW (IRENA, 2019).

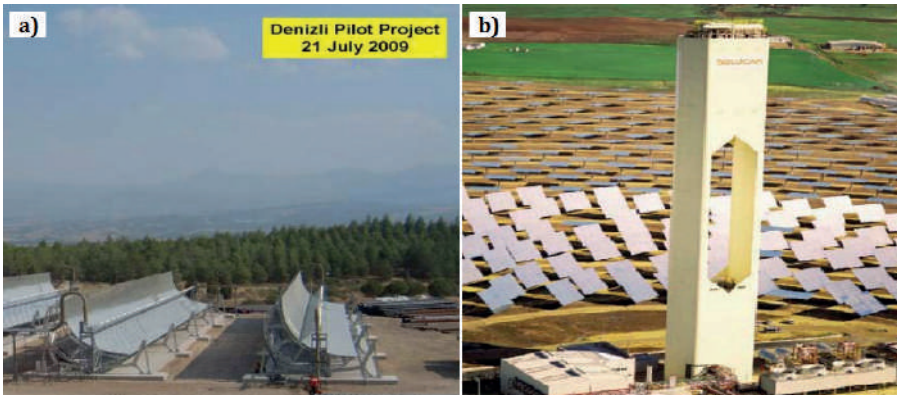

Figure 3. Examples of medium temperature parabolic system (a) and high temperature heliostat system (b) (Livatyalı, 2011)

Electricity Generation From Solar Energy By Direct Method

Direct method refers to the generation of electricity through the detachment of electrons from matter and the creation of current as a result

of the solar rays falling onto photovoltaic solar cells using the photoelectric effect and the concept of threshold energy (Sancar&Altınkaynak, 2021).

Photovoltaic systems, which are a direct method of generating electricity from solar radiation, were first investigated by Edmond Becquerel in 1839. Photovoltaic cells are systems that can directly convert solar radiation into electricity and do not have any moving parts. They generate voltage by absorbing the radiation that falls on their surfaces and causing electrons to be detached from the semiconductor materials they contain. Solar cells typically have a surface area of around 100 cm2 and can be produced in various geometric shapes.

According to data from the International Renewable Energy Agency (IRENA) in 2018, the installed capacity of photovoltaic systems, which are a direct method of generating electricity from solar energy, reached approximately 480 357 MW worldwide. In our country, electricity generation with these systems is highly prevalent, and in terms of installed capacity, Turkey ranks 11th among all countries worldwide. The total installed capacity of photovoltaic systems in Turkey reached 5 063 MW as of 2018 and continues to increase day by day (IRENA, 2019).

Photoelectric Effect And Threshold Energy

The phenomenon in which electrons are detached from a material surface as a result of an electromagnetic wave emitted from a source falling onto another material surface is called the "photoelectric effect." The electrons that are detached from the material are referred to as photoelectrons. The experimental observation of the photoelectric effect is attributed to Heinrich Rudolf Hertz, and therefore, this phenomenon is also known as the "Hertz effect" (Öztürk, 2013).

Under normal conditions, electrons are bound to the material and do not separate from it without external influence. In order for electrons to be detached from the material surface, the energy of the incoming radiation from the source must be greater than the energy of the electrons. The maximum energy required to detach electrons from the surface of the material is called the "threshold energy" or "binding energy."

$$E_K = h.\nu - \Phi \tag{2}$$

In the given formula (2) E_k represents the kinetic energy of the electron, h.ν denotes the energy of the emitted wave (photon), Φ is the energy required to detach the electron from the material.

Each photon that falls on the material surface transfers its energy to the electrons on the surface. If sufficient energy cannot be provided and the energy of the photon is smaller than the threshold energy ($h.\nu < \Phi$), the electron will not be detached. When sufficient energy is provided, the electrons spend a portion of that energy to overcome the binding energy and then separate from the surface. The remaining energy contributes to the kinetic energy of the photoelectron. Increasing the intensity of light does not affect the kinetic energy of the photoelectron, but it only increases the number of photoelectrons.

In this context, systems that can directly convert the energy of photons from the Sun into electrical energy through the photoelectric effect are called photovoltaic systems.

Semiconductors and Band Gap Theory

Atoms are composed of a positively charged heavy nucleus and electrons orbiting around the nucleus. All these charges are in balance with each other in the absence of external factors. Electrons carry potential and kinetic energy depending on the distance between their orbits and the nucleus. The first orbit can hold a maximum of 2 electrons, the second orbit can hold 8 electrons, the third orbit can hold 18 electrons, and the fourth orbit can hold 32 electrons. Electrons are found in consecutive energy bands. With an external influence, electrons in the valence band of semiconductors can transition to the conduction band, leaving behind a gap (hole). The gaps created in the valence band are seen as positive charges. When a gap is filled by another electron leaving a gap behind, the gaps behave as charge carriers (Serway, 2005).

Solid materials are divided into three groups: conductors, semiconductors, and insulators, based on their electrical conduction properties. Semiconductor materials have characteristics that lie between conductors and insulators in terms of electrical conductivity. The energy gap between the lower valence band and the upper conduction band is called the band gap (Eg). The band gaps of semiconductors are greater than those of metals but smaller than those of insulators. Semiconductor materials exhibit insulating properties at absolute zero temperature ($T=0$ K), but as the temperature increases, their ability to conduct electricity also increases. Figure 4 illustrates the band gaps of conductors, semiconductors, and insulators.

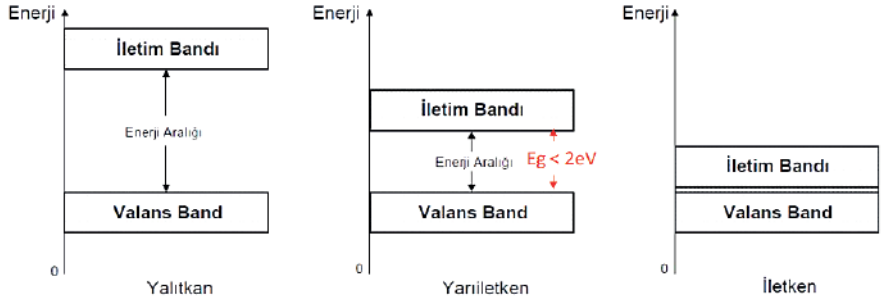

Figure 4. The band gaps (Eg) of insulators, semiconductors and conductors (Teşneli, 2015)

Pure and Doped Semiconductors

Pure or intrinsic semiconductors are perfect semiconductors that have an equal number of electrons and holes at any temperature, without containing any impurities. The valence band is completely filled with electrons, and there are no free electrons in the conduction band. At T=0 K, all electrons are in the valence band, and the conduction band is empty, so no electrical conduction is observed. In an intrinsic semiconductor, the number of electrons and holes is equal because a hole in the valence band can only be created when an electron moves to the conduction band, leaving a hole behind (Bhattacharyya, 1996).

Semiconductor materials cannot be used in their pure form for the production of photovoltaic cells. They need to be doped to become suitable for photovoltaic cell applications. Doping processes result in obtaining N-type or P-type doped semiconductors. Silicon, which is the most commonly used semiconductor in photovoltaic cells, has four electrons in its outermost shell. If each silicon atom forms covalent bonds with four other electrons, the silicon atom becomes stable and exhibits insulating properties. When silicon is doped with phosphorus, which is an element from the 5th group of the periodic table (with five electrons in its outermost shell), one electron remains unbound in phosphorus, and this electron is called a free electron. As a result, the doped semiconductor is called an N-type semiconductor.

To obtain P-type silicon, an element from the 3rd group of the periodic table is doped into it. For example, a boron atom has three electrons in its outermost shell, and when it is doped into silicon, one electron is missing from silicon, creating a hole. Holes are defined as positive charges,

and the semiconductors formed by this type of doping are called P-type semiconductors (Öztürk, 2013). The figure below (Figure 5) illustrates the structure of intrinsic silicon, N-type silicon doped with phosphorus, and P-type silicon doped with boron.

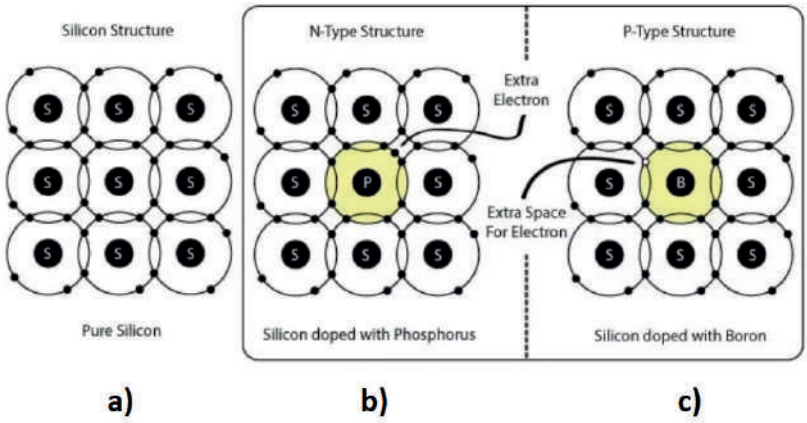

Figure 5. The structure of pure silicon (a), phosphorus-doped N-type silicon (b) and boron-doped P-type silicon (c) (Nextews, 2017)

P-N junction

When a P-type doped semiconductor and an N-type doped semiconductor are physically connected to each other, two natural carrier motion processes occur:

1-) Majority charge carriers, which are electrons in the N-type semiconductor, flow towards the P-type semiconductor.

2-) Majority charge carriers, which are holes in the P-type semiconductor, also flow towards the N-type semiconductor.

These transitions occur only in the region near the P-N junction. When both regions achieve charge balance, these movements cease. As electrons leave the P-type region, only positive (+) charges remain, while in the N-type region, only negative (-) charges remain as holes are leaving, resulting in a region without carriers. The remaining positive and negative charges create an electric field around the junction, which increases in the direction that inhibits the natural flow caused by carriers in the two separate regions. This junction region is called the depletion region.

When light falls on the junction, electron-hole pairs are created. If a photon with energy equal to or greater than the bandgap energy (Eg) is

absorbed by the semiconductor, it transfers its energy to an electron in the valence band, allowing the electron to move to the conduction band and creating an electron-hole pair (Yavuz, 2012). When these electron-hole pairs separate, with the electrons going to the negative side and the holes going to the positive side, an electric current is generated. Figure 6 below illustrates the step-by-step process from the formation of a P-N junction through the formation of the depletion region (charge-neutral region) in two doped semiconductor materials.

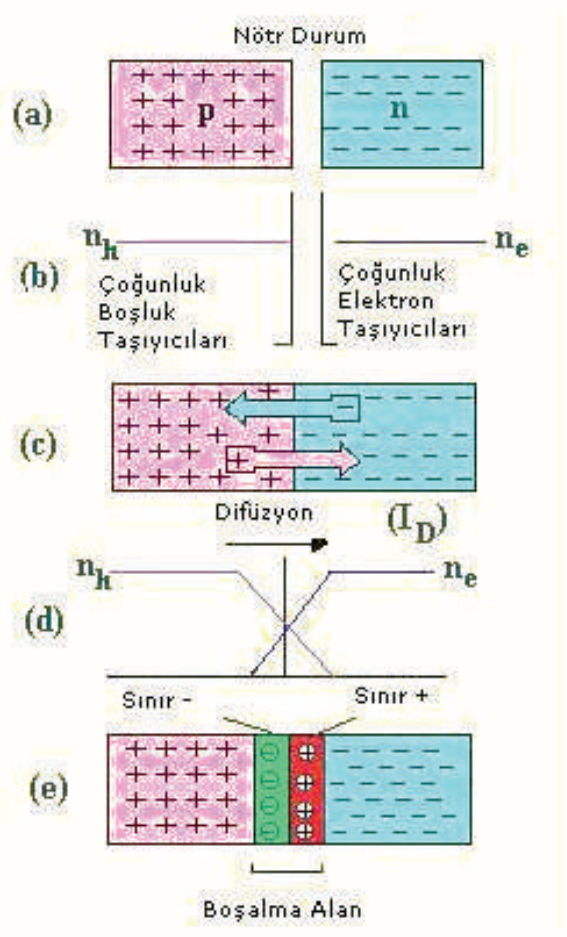

Figure 6. ***The process and displacement region after the formation of the P-N junction (ITU, 2007).***

PARAMETERS AFFECTING EFFICIENCY IN SOLAR CELLS

There are five parameters used to compare and evaluate photovoltaic cells. These parameters are crucial for calculating cell efficiency, conducting further research based on the obtained data, and designing efficient new cell architectures. The five parameters are listed below:

- Open-circuit voltage (Voc)
- Short-circuit current (Isc)
- Fill factor (FF)
- Maximum power point (MPP)
- Power conversion efficiency (PCE)

Open-Circuit Voltage (Voc) is one of the most important parameters of photovoltaic cells. It is the voltage measured across the terminals of a solar cell when no current is flowing (I=0). When the complementary circuit of the cell is open (terminals are unloaded), if light is incident on it, electrons and holes separate and flow in the respective directions of low and high work functions. The higher the value of open-circuit voltage, the higher the quality of the solar cell, and this parameter is highly affected by operating temperature.

Short-Circuit Current (Isc) is the current measured across the terminals of a photovoltaic cell when the voltage applied is zero (Volt=0) and it is under illumination. Short-circuit current is also defined as the current produced by the photovoltaic cell without any external load connected. The value of short-circuit current varies depending on the brightness of the irradiation.

Fill Factor (FF) is a measure of the power quality of a photovoltaic cell. It is the ratio of the maximum power to the product of the open-circuit voltage and short-circuit current of a solar cell. The fill factor can theoretically be a maximum of 1, and the closer it is to this value, the more ideal it indicates. It is an important factor in determining the maximum power in photovoltaic cells under weak illumination conditions. To indicate that a photovoltaic cell is of good quality, the fill factor value should be at least between 0.75 and 0.8 (Zafer, 2006).

$$FF = \frac{I_{max}\ V_{max}}{I_{SC}\ V_{OC}} = \frac{P_{max}}{I_{SC}\ V_{OC}} \tag{1.3}$$

The maximum power point (MPP) is the operating point of a photovoltaic cell where it achieves the highest efficiency. At this point, the power obtained from the cell will be maximum. The MPP is determined by the combination

of current and voltage that yields the maximum power output, and it depends on the amount of incoming light to the photovoltaic cell.

$$P_{max} = V_{max} \, x \, I_{max} \tag{1.4}$$

Power conversion efficiency (PCE) is the most commonly used parameter in comparing two photovoltaic cells. It represents the ratio of the energy obtained from the photovoltaic cell (Poutput) to the incident irradiation on the cell surface (Pinput). The power conversion efficiency varies depending on the energy of the incident irradiation and the temperature of the cell. Efficiency tests for cells are typically conducted under standard test conditions, which include an air mass (AM) of 1.5, irradiance of 1000 W/m2, and an ambient temperature of 25 °C. The air mass represents the path length of solar rays through the atmosphere and is expressed by the equation $1/\cos\theta$. In space, AM=0 when the solar rays are perpendicular to the Earth's surface, but due to the inclination of the Earth's axis, AM=1.5 is assumed in tests (Tan, 2004).

$$\eta = \frac{P_{max}}{P_{ışık}} = \frac{I_{SC} \, x \, V_{OC} \, x \, FF}{P_{ışık}} \tag{1.5}$$

CONCLUSION

Solar energy is a promising source for electricity generation, and various methods have been developed to harness this abundant resource. In this chapter, we discussed both indirect and direct methods of generating electricity from solar energy.

Indirect methods involve using solar energy to generate heat, which is then used to produce electricity through conventional thermal power plants or by using concentrated solar power (CSP) systems. These methods are well-established and widely used, but they have limitations in terms of efficiency and scalability.

On the other hand, direct methods of electricity generation from solar energy involve the use of photovoltaic (PV) systems, which directly convert sunlight into electricity through the photoelectric effect. We explored the principles behind the photoelectric effect, threshold energy, and the role of semiconductors in PV systems.

Semiconductors play a crucial role in PV systems, and we discussed the concept of band gap theory, which determines the energy levels that electrons can occupy in a material. Pure and doped semiconductors were explained,

along with the formation of P-N junctions, which create an electric field that separates charge carriers in a solar cell.

Several parameters affect the efficiency of solar cells, including the short-circuit current (Isc), fill factor (FF), maximum power point (MPP), power conversion efficiency (PCE), and open-circuit voltage (Voc). Understanding these parameters is essential for optimizing the performance of solar cells and improving their overall efficiency.

In conclusion, solar energy is a viable and renewable source for electricity generation. Indirect methods, such as thermal power plants and CSP systems, have their advantages but also limitations. Direct methods using PV systems offer a more direct and efficient approach, relying on the photoelectric effect and the properties of semiconductors. By optimizing the parameters affecting solar cell efficiency, we can further enhance the utilization of solar energy and contribute to a sustainable energy future.

REFERENCES

Bhattacharyya, D., & Carter, M. J. (1996). Effect of substrate on the structural and optical properties of chemical-bath-deposited CdS films. Thin Solid Films, 288(1-2), 176-181.

Bilici, M. S., 2019. Metal Katkılı TiO2 Öncülleri Kullanılarak Boya Duyarlaştırılmış Güneş Hücresi Üretimi ve Analizi. Isparta Uygulamalı Bilimler Üniversitesi, Lisansüstü Eğitim Enstitüsü, Yüksek Lisans Tezi, 68s, Isparta.

IRENA (2019), Renewable capacity statistics 2019, International Renewable Energy Agency (IRENA), Abu Dhabi.

ITU, 2007. Yarı-iletkenlerin katkılanması. Erişim Tarihi: 08.04.2019. https://web.itu.edu.tr/~kaymak/images/pv.html

Karamanav, M., 2007, Güneş Enerjisi ve Güneş Pilleri. Sakarya Üniversitesi, Fen Bilimleri Enstitüsü, Yüksek Lisans Tezi, 76s, Sakarya.

Khafagy, M., 2018. Geometrical and Physical Optics. Cairo University, Professor of Medicine and Ophthalmology Faculty of Medicine, 61s, Cairo.

Livatyalı, H., 2011. Yoğunlaştırılmış Güneş Enerjisi Teknolojileri. TÜBİTAK Marmara Araştırma Merkezi, Enerji Enstitüsü, 32s, Kocaeli.

Nextews, 2017. Exemplos de Semicondutores. Erişim Tarihi: 18.03.2019. http://pt.nextews.com/4f011e2c/

Öztürk, H. H., 2012. Güneş Enerjisi ve Uygulamaları. Birsen Yayınevi, 354s, İstanbul.

Öztürk, H. H., Kaya, D. 2013. Güneş Enerjisinden Elektrik Üretimi: Fotovoltaik Teknoloji. Umuttepe Yayınları, 432s, İstanbul.

Serway, R., Beichner, R., 2005. Fizik 3: Modern Fizik. Çev. Çolakoğlu, K. Palme Yayıncılık, 392s, İstanbul.

Tan, Y. T. (2004). Impact on the power system with a large penetration of photovoltaic generation. In Institute of Science and Technology (p. 160). The University of Manchester.

Teşneli, N.B., 2015. Yarıiletkenler, Bölüm 8, Sakarya Üniversitesi, 21s, Sakarya.

Ültanır, M. Ö., 1987. Termodinamik. Ankara Üniversitesi Ziraat Fakültesi Yayınları: 1023, Ders Kitabı: 296, 457s, Ankara.

Yavuz, N., 2012. Kadmiyum Sülfür (CdS) İnce Filmlerin Fotovoltaik Hücre Uygulamalarında Kullanılması. Yıldız Teknik Üniversitesi, Fen Bilimleri Enstitüsü, Yüksek Lisans Tezi, 138s, İstanbul.

Zafer, C., 2006. Organik Boya Esaslı Nanokristal Yapılı İnce Film Güneş Pili Üretimi. Ege Üniversitesi, Fen Bilimleri Enstitüsü, Doktora Tezi, 132s, İzmir.

Sancar, M. R. (2023a). Renewable Energy Sources and Energy Storage. In: Çakoğlu, A. H. & Sancar, M. R. (eds.), Versatile Approaches to Engi-

neering and Applied Sciences: Materials and Methods (pp. 131-140). Özgür Publications. DOI: https://doi.org/10.58830/ozgur.pub50.c69

Sancar, M. R. (2023b). The Effect of Dust Deposition on Photovoltaic Systems' Electricity Generation and Its Economical Analysis. In: Çakoğlu, A. H. & Sancar, M. R. (eds.), Versatile Approaches to Engineering and Applied Sciences: Materials and Methods. Özgür Publications. DOI: https://doi.org/10.58830/ozgur.pub50.c43

Sancar, M. R. & Altınkaynak, M. (2021). Isparta İli İçin Farklı Çatı Tiplerinde Tasarlanan Fotovoltaik Sistemlerin Karşılaştırılması . Avrupa Bilim ve Teknoloji Dergisi , Ejosat Özel Sayı 2021 (RDCONF) , 1024-1028 . DOI: 10.31590/ejosat.1047453

Sancar, M. R. & Bayram, A. B. (2023). Modeling and Economic Analysis of Greenhouse Top Solar Power Plant with Pvsyst Software . International Journal of Engineering and Innovative Research , 5 (1) , 48-59 . DOI: 10.47933/ijeir.1209362

Sancar, M. R. & Yakut, K. (2023). Comparative Analysis of SAM and PVsyst Simulations for a Rooftop Photovoltaic System . International Journal of Engineering and Innovative Research , 5 (1) , 60-76 . DOI: 10.47933/ijeir.1209413

Chaphter 3

Thin Film Depositing Techniques

Ahmet Buğrahan Bayram[1]

INTRODUCTION

Energy production from renewable energy sources has become very important due to increasing energy demand and global warming. Electricity production from solar energy, which is one of the renewable sources, can be achieved by harnessing both its thermal energy and photovoltaic potential(Sancar, 2023a).

Today, the limitations of energy resources and their environmental impacts have led people to search for more sustainable and cleaner energy sources(Sancar&Yakut, 2023). In this context, photovoltaic (PV) technologies have significant potential as systems that convert solar energy into electricity. PV technologies can reduce dependence on fossil fuels and significantly reduce carbon emissions(Sancar&Altınkaynak, 2021).

Photovoltaic cells are devices that convert sunlight directly into electrical energy. Traditionally, crystalline silicon-based photovoltaic cells have been widely used. However, the production of such cells is expensive and energy intensive. Therefore, thin film deposition techniques are gaining importance as a more economical and efficient option(Sancar, 2023b).

Thin film deposition techniques are the methods used in the production of photovoltaic cells. In these techniques, thin film layers are applied to substrates (substrates) and then used to convert sunlight into electrical energy. Thin film layers are usually composed of various semiconductor materials and affect the electrical performance of PV cells.

The advantages of photovoltaic thin-film deposition techniques include features such as lower cost, lighter weight and flexibility. These techniques can be produced on an industrial scale and can be tailored for various application

1 Isparta University of Applied sciences, Institute of Postgraduate Education, Energy Systems Engineering, Isparta, Turkiye, ORCID Code: (0000-0002-7364-8559)
d1940640016@isparta.edu.tr

areas. Furthermore, thin film deposition techniques use less material than conventional crystalline silicon-based cells, which reduces energy costs and environmental impacts.

There are different thin film deposition techniques, some of which include: amorphous silicon (a-Si), cadmium telluride (CdTe), copper indium gallium selenide (CIGS) and organic photovoltaic (OPV) technologies. Each technology has its own advantages and disadvantages, and these technologies are constantly being developed and improved.

This introduction highlights the importance and potential of photovoltaic thin film deposition techniques. Thin film technologies offer a more economical, efficient and environmentally sustainable option for solar electricity generation. Thin film deposition techniques can enable a wider deployment of PV technologies and improve conversion efficiency in power generation.

Amorphous silicon (a-Si) technology is one of the most widely used thin film deposition methods. Amorphous silicon cells are favored for their low-cost manufacturing processes and their ability to be applied on flexible substrates. However, low conversion efficiency and stability issues are aspects of a-Si technology that need improvement.

Cadmium telluride (CdTe) technology stands out with its high conversion efficiency and low cost advantage. CdTe cells are used on a commercial scale due to their easy manufacturability and high light absorbing capabilities. However, the environmental impact and toxic properties of CdTe cells need to be carefully studied.

Copper indium gallium selenide (CIGS) technology is of interest due to its high conversion efficiency and applicability to flexible substrates. CIGS cells can be fabricated by thin film deposition processes and have potential on an industrial scale. However, CIGS technology still requires further research and development for commercialization.

Organic photovoltaic (OPV) technology is characterized by advantages such as low cost, light weight and flexibility. OPV cells are composed of a combination of organic molecules and can be produced in low energy density environments. OPV technology offers potential applications in flexible electronic devices and integrated solar panels. However, the efficiency level of OPV cells is not yet competitive with conventional technologies and stability issues are still being studied.

In conclusion, photovoltaic thin film deposition techniques offer an alternative and sustainable option to conventional methods of converting solar

energy into electrical energy. The development and good communication of these technologies will encourage more widespread use of PV technologies and play an important role in meeting the demand for clean energy. Thin film deposition techniques have the potential to revolutionize the energy sector by offering advantages such as low cost, light weight, flexibility and industrial scale manufacturability.

Physical Vapor Deposition Method (PVD)

Physical vapor deposition method is the deposition of atoms atomically or ionically on the material to be coated by detaching atoms from the surface by evaporation or sputtering in a vacuum environment. With the physical vapor deposition method, the film thickness can be coated from a few nanometers to thousands of nanometers. In a typical physical vapor deposition process, the deposition rate is 10-100Å per second (Gürlük, 2009).

Sputter Deposition Method (Sputter)

Sputter deposition method is one of the oldest thin film deposition methods. Today, it is the most common deposition method used for a wide variety of purposes in different fields (Tavşanoğlu, 2009). This method has many application areas. Most of the elements in the periodic table can be deposited on a substrate by this method.

In this method, the atoms of the material to be used are detached from the surface of the material by ionized gas atoms (Ar etc.) and these detached atoms are deposited on the substrate. This method is non-thermal evaporation. When an ion hits the cathode (the source material used), many interactions occur on its surface. These interactions include the liberation of ionized atoms, the release of gas atoms from the surface of the material used. In the sputtering method, the surface atoms of the material used are physically detached by momentum transfer using energized particles (accelerated ions, electrons, etc.) from the ion gun. When the accelerated particle hits the surface of the material with sufficient energy, it breaks the bonds and causes the atoms to break away. The atom detached from the surface is referred to as a splattered atom. The coating process is realized when the atom detached from the surface is attached to the substrate to be coated (Başkurt, 2010; Tavşanoğlu, 2009). Sputtering technique is divided into four parts. These are radio frequency (RF), direct current (DC), magnetic sputtering and reactive sputtering techniques. The sputtering process is named according to the type of power source used, the target material and the growth rate of the desired film (Thornton,99 1983). If the voltage applied between the electrodes comes from a radio frequency generating source, this is the radio

frequency sputtering technique. If the voltage applied between the electrodes comes from a direct current generating source, this is the direct current sputtering technique. In the sputtering technique, the deposition process with the effect of a magnetic field is magnetic sputtering. If a reactive gas that can chemically interact with the target material is sent into the vacuum along with an inert gas, this is the reactive sputtering technique (Johnson, 2005).

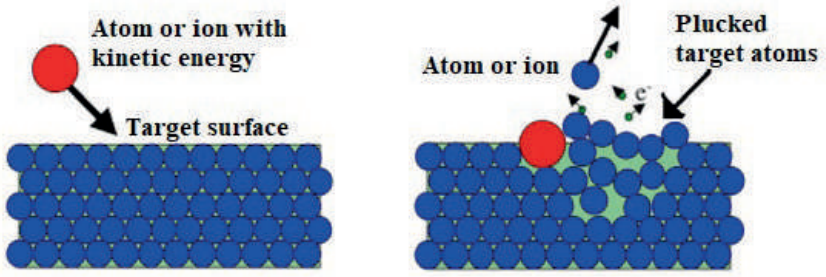

Figure 1. Show of sputter event (Caliskan, 2009)

Thermal Evaporation Method (Thermal Evaporation)

It is the simplest system among physical vapor deposition methods. The thermal evaporation method is realized by heating the source material used in a vacuum environment and separating the atoms on its surface and holding them on the substrate. Crucibles with high evaporation temperatures, current is passed through the crucible with the material to be used placed in it. The current passing through the crucible heats the crucible and when it reaches the temperature required for the evaporation of the material used, the material evaporates and moves upwards in the vacuum and is collected on the substrates. The temperature of the substrate can also be adjusted by the user. Thin film production by thermal evaporation method consists of three main units (Ceylan, 2013). These are respectively

a) Vacuum Chamber: Pump station and pressure measurement system

Figure 2. Vacuum circle

b) Magnification Sources and Controls: Sub-elements that make up thermal vaporization

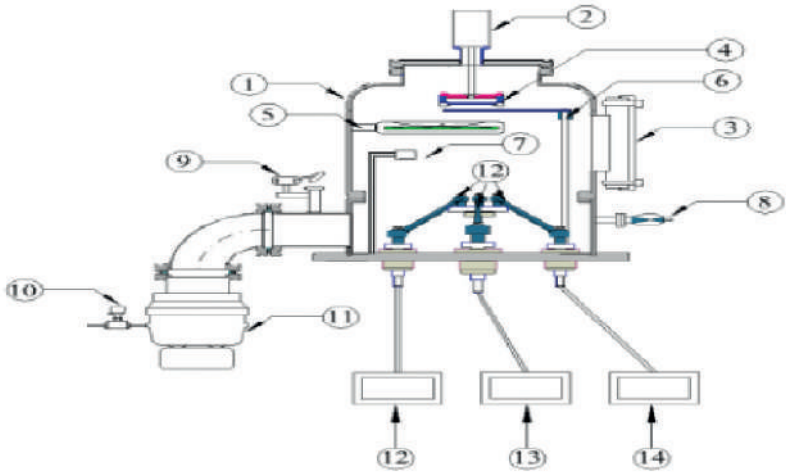

Figure 3. 1) Vacuum circle 2) 3) DC motor ISO 100 observation window 4) Substrate holder 5) Heater 6) Cutter 7) Dark monitor head 8) Pressure measuring head 9) The atmosphere key of the circle 10) Turbo pump vacuum break valve 11) Turbo pump 12-13-14) Thermal evaporation power sources (Ceylan, 2013)

b) Electronic Device Cabinet: Electronic controls for the items described in the computer and magnification sources section

Figure 4. 1) Control computer 2) Ammeters and thermal evaporation power supplies indicator 3) Peat pump control part 4) Temperature PID control part 5) Main switch 6) On/Off switch (Ceylan, 2013)

Electron beam method (E-Beam Evaporation)

In the electron beam system, the material used in a very high vacuum environment is heated by an electron beam generated by a filament source. The accelerated electron beam is focused on the material under the influence of the electromagnetic field created by a static magnet and an electrostatic electric field generator. The atoms on the surface of the material used are ruptured and are allowed to pass into the gas phase. The gas phase atoms are deposited on the substrate.

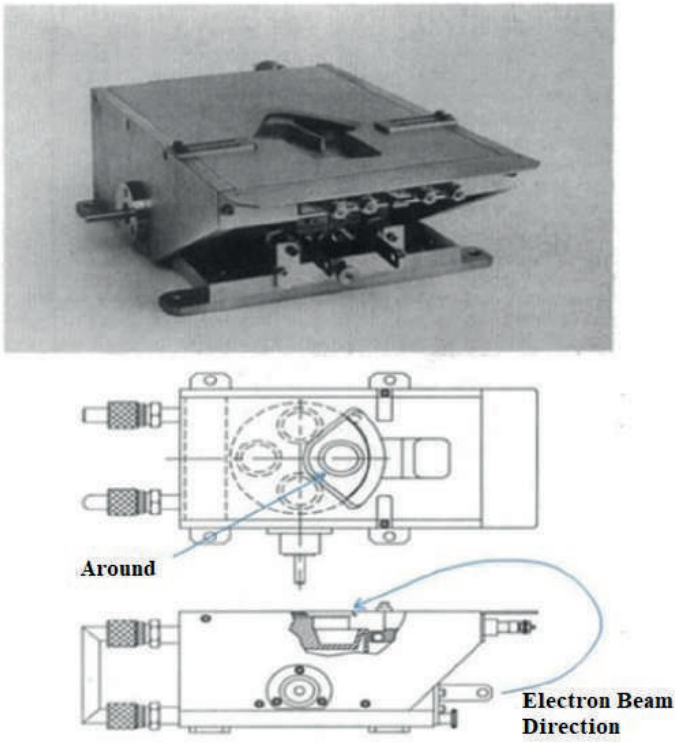

Figure 5. Electron beam evaporation unit

Flash evaporation method (Flash Evaporation)

In the vacuum flash evaporation method, the powders of the material to be used are baked for a while in an inert gas atmosphere. The obtained powders are slowly poured into a crucible heated to the sublimation temperature of the material we use under vacuum. The suddenly vaporized material is grown in amorphous (non-uniform) structure on glass substrates whose temperature is kept at 400 °C.

The average pressure of the environment during evaporation should be less than 10-4 Torr (Özdemir, 1992).

Flash evaporation method (Flash Evaporation)

In the vacuum flash evaporation method, the powders of the material to be used are baked for a while in an inert gas atmosphere. The obtained powders are slowly poured into a crucible heated to the sublimation temperature of the material we use under vacuum. The suddenly vaporized

material is grown in amorphous (non-uniform) structure on glass substrates whose temperature is kept at 400 °C.

The average pressure of the environment during evaporation should be less than 10-4 Torr (Özdemir, 1992).

Chemical Vapor Deposition Method (CVD)

Chemical vapor deposition is the process of depositing thin films on a substrate in a closed environment by a chemical reaction caused by the release of chemical gases. As a result of this method, very high quality thin films can be produced. Thin films in the range of 1 nm to 100 nm can be produced with this method.

Solution Based Augmentation Methods

Solution-Based Growth Method (SBGM) is one of the thin film deposition techniques and is widely used in the production of various semiconductor materials. In this method, thin film layers of semiconductor materials are formed by applying precursor materials in solution or suspensions to a surface.

The solution-based growth method offers advantages such as simple equipment requirements, low cost and wide-scale applicability. It also has flexibility advantages such as usability on a variety of substrates and the ability to produce flexible films.

In general, solution-based growth involves the following steps:

Precursor Solution/Suspension Preparation: The first step is the preparation of the precursor solution or suspension of the semiconductor material. In this process, the targeted components of the material and solvents are mixed in appropriate proportions.

Substrate Preparation: The substrate on which the thin film layer will be formed is cleaned and prepared. The surface of the substrate should be smooth and clean so that the precursor can spread homogeneously on the solution or suspension.

Application of Precursors: The prepared precursor solution or suspension is applied to the surface of the substrate by a coating method. These application methods may include techniques such as dip-coating, spray-coating, brush-coating and spin-coating.

Drying and Heat Treatment: After the precursor solution or suspension is applied on the substrate, the drying step is performed. In this step, a

thin film layer is formed as the solvents evaporate. Then, heat treatment (sintering) is applied to crystallize the film and ensure that it has a uniform structure.

Improving Thin Film Quality: The formed thin film layer can be subjected to a series of steps to improve its quality with additional processing if necessary. These steps can be diversified as optimizing the crystal structure, increasing the surface smoothness or forming a bonding layer. These steps are intended to optimize the electrical and optical properties of the thin film layer.

The solution-based growth method can be used in the production of various semiconductor materials. For example, in organic photovoltaic (OPV) cells, thin film layers are formed by applying a solution of polymer or organic molecules onto the substrate. Similarly, in perovskite-based solar cells, thin film layers are obtained by using solutions of perovskite materials.

Solution-based growth is generally a low-cost and easily scalable technique. However, it also presents some challenges. For example, it is important to control the thickness and uniformity of the thin film layer. Furthermore, mixing and stabilization of the components of the solution or suspension in appropriate proportions is also a critical factor.

In conclusion, solution-based growth method is one of the thin film deposition techniques and is widely used in the production of photovoltaic cells. This method offers advantages such as low cost, easy scalability and flexibility. The solution-based growth method can contribute to goals such as the development of clean energy technologies and increasing electricity generation from solar energy.

Spin coating technique (Spin Coating)

The spin coating process is based on dropping the solution drop into the center of the substrate and rotating the substrate at high speed (3000-4000 rpm). It is a process used to produce thin films on a hard layer or slightly inclined substrates. The thin film coating process with the spin coating technique takes place in 4 steps. These steps are coating, spinning, finishing spinning and evaporation. In the coating step, the prepared solution is poured into the center of the substrate. In the second step, rotation, the solution poured into the center of the substrate flows radially out of the surface under the effect of centripetal force. In the third step, the rotation process is terminated and the excess liquid remains outside the surface. As the film thickness decreases, the amount of liquid overflowing from the

surface decreases. The last step, evaporation, is the most important step in thinning the films.

An advantage of rotational coating is that the film that starts to form on the surface while the film is forming is evenly distributed. As a result, the film thickness shows a homogeneous feature along the surface (Bilgen, 2008).

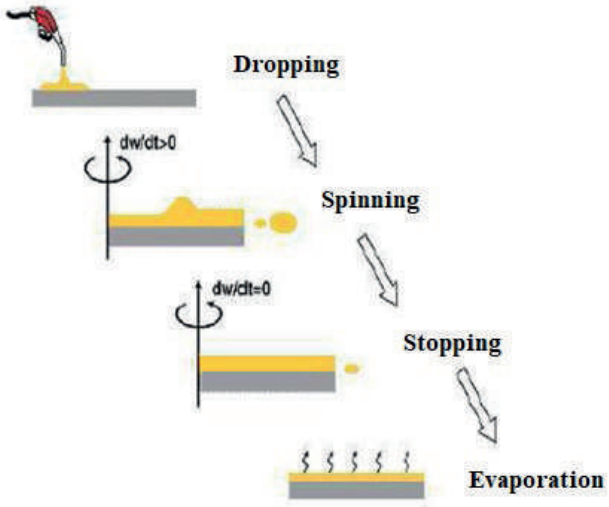

Figure 6. Schematic representation of the spin coating technique (Bilgen, 2008)

Dip coating technique (Dip Coating)

It is a coating technique in which the layer used in the immersion method is dipped into the solution several times and then slowly withdrawn. As the layer immersed in the solution is pulled outward, excess solvent is separated from the layer and the solvent evaporates and a thin film is obtained. The thickness of the ideal film obtained with a single immersion is between 0.1 - 0.45 μm on average (Bilgen, 2008). The dip coating technique consists of 5 stages. These are; dipping, pulling up, coating, percolation and evaporation. The material to be coated is dipped into the prepared sol and pulled upwards at the same speed (10-110 mm/min). In the coating stage, the parts in contact with the sol are coated. Gravitational force, friction force (between the sol and the material to be coated), surface tension force (the force generated by the sol adhering to the material) are effective in the coating part. In the percolation stage, some of the sol droplets leave the surface under the influence of gravity, friction force and surface tension force. In the

evaporation stage, the sol droplets that cannot be filtered during filtration evaporate and finally form a film with the baking process. Advantages and disadvantages of this method:

Advantages;

1. All shapes and sizes of samples can be coated (different samples such as tubes, pipes and rods can be coated).

2. Uniform thickness of the produced films can be obtained and the thickness of the film can be controlled.

3. It is easier to minimize the amount of additives with this technique.

4. It is not very sensitive to the properties of the solvent or solution.

5. Large quantities of samples can be coated economically at the same time.

6. It is an easy and inexpensive technique.

Disadvantages;

1. Large amounts of solution are used for large carriers. This technique is inconvenient if the cost of the solution is high or if the solution is not constant.

2. It is not a useful technique in multilayer systems due to cross doping (but it can be used).

3. Both sides of the carrier are coated during the process. If we want to coat one side of the carrier, we need to mask the other side.

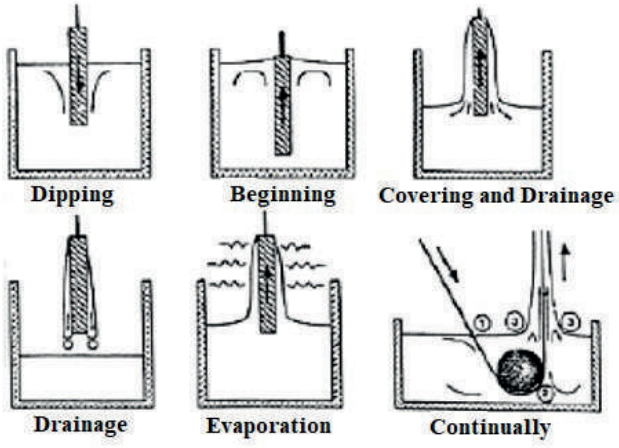

Figure 7. Schematic representation of the dip coating technique (Bilgen, 2008)

Spray coating technique (Spray Pyrolysis)

Spray coating method is the process of spraying the prepared solution onto the heated base by atomizing it with the help of air or argon gas. The particles sprayed on the heated base adhere to the substrate with the evaporation of the solution and a thin film is obtained. In general, the thin films obtained have a polycrystalline structure. This method is one of the most preferred methods because it is simple and economical. In addition to being simple and economical, the physical properties of the films to be produced can be regulated by preparing the solution as desired. At temperatures higher than 100°C, ethyl alcohol can be used in some cases of films. Solvent selection is made according to the values of the base temperature. Ethyl alcohol can be used as solvent from 80 °C to 250 °C. Different solvents are used for temperatures higher than 250 °C (Arabacı, 2001). Different parameters affect the thin films produced by this technique. These parameters are spraying speed and time, total amount of solution, carrier gas, atmosphere, starting solution, base temperature, distance between spray head and base, aerodynamics of sprayed solution droplets, cooling rate after deposition (Tosun, 2008). Advantages and disadvantages of this method:

Advantages;

1. High production rate and large area coverage
2. Ease of complex shape coating,
3. Low cost, (low temperature and no vacuum required)
4. Cheap equipment cost.

Disadvantages;

1. Reproducible thickness problems,
2. It is not always homogeneous.

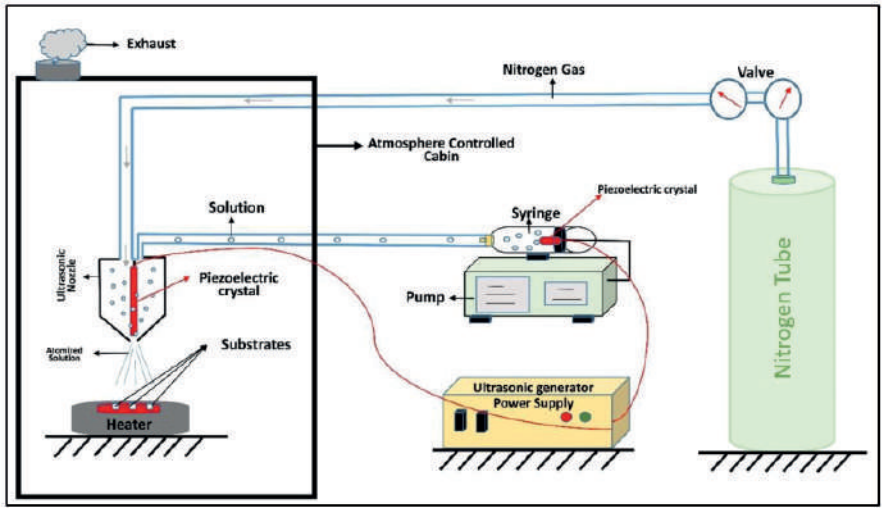

Figure 8. Schematic representation of the Spray Pyrolysis technique (Koç, 2018)

CONCLUSION

Thin film depositing techniques play a crucial role in various fields, including electronics, optoelectronics, and surface engineering. In this chapter, we discussed several commonly used techniques for depositing thin films. The physical vapor deposition (PVD) method, including sputter deposition and thermal evaporation, offers precise control over film thickness and composition. The electron beam method and flash evaporation method provide efficient and high-quality film deposition.

Another important technique is the chemical vapor deposition (CVD) method, which enables the growth of films with complex compositions and structures. Solution-based augmentation methods, such as spin coating, dip coating, and spray coating, offer simplicity and versatility for depositing thin films.

Each technique has its advantages and limitations, making them suitable for specific applications. The choice of deposition method depends on factors such as film material, desired properties, substrate type, and production scale. Researchers and engineers need to carefully select the appropriate technique to achieve the desired film quality and functionality.

In conclusion, this chapter provided an overview of various thin film depositing techniques, highlighting their principles, advantages, and applications. The continuous development of these techniques contributes to advancements in materials science and technology, enabling the fabrication of innovative devices and structures.

REFERENCES

Arabacı, E., 2001. Obtaining ZnS Semiconductor Compound by Spray Pyrolysis Method. Anadolu University Institute of Science and Technology, Master Thesis, 80s, Eskişehir.

Başkurt, E., 2010. Production and Characterization of Silicon Carbide Thin Films by Sputtering Method in Reactive Direct Current Magnetic Field. Istanbul Technical University, Institute of Science and Technology, Master Thesis, 107s, Istanbul.

Bilgen Y., 2008. Investigation of Optical and Microstructural Properties of Nanocrystalline Zno: Ga Thin Films Produced by Sol-Gel Method. Gebze University, Institute of Technology, Institute of Engineering and Science, Master Thesis, 59s, Gebze.

Ceylan H. M., 2013. Investigation of Structural Electrical and Optical Properties of CuGaSe2 Thin Films. Pamukkale University Institute of Science and Technology, Master Thesis, 58s, Denizli.

Gürlük, G., 2009. Production and Characterization of NiTi Memory Alloy Shaped Film Coatings. Istanbul Technical University, Institute of Science and Technology, Master Thesis, 105s, Istanbul.

Johnson, R. L., 2005. Characterization of Piesoelectric ZnO Thin Films and the Fabrication of Piezoelectric Micro-Cantilevers. Ames, IA (United States). 196.

Koç M, 2018. Investigation of Physical and Optical Properties Sn-Doped Indium Oxide Thin Films Fabricated by Ultrasonic Spray Pyrolysis Method and Heat Treatment under Different Nitrogen Flow Rate Atmospheres. Süleyman Demirel University, Graduate School of Natural and Applied Sciences, PhD Thesis.

Ozdemir, A. R., 1992. Investigation of Electrical Conductivity and Light Transmittance in Tin Oxide (SnO2) Thin Films. Ankara University Institute of Science and Technology, Master Thesis, 87s, Ankara

Sancar, M. R. & Altınkaynak, M. (2021). Isparta İli İçin Farklı Çatı Tiplerinde Tasarlanan Fotovoltaik Sistemlerin Karşılaştırılması . Avrupa Bilim ve Teknoloji Dergisi , Ejosat Özel Sayı 2021 (RDCONF) , 1024-1028 . DOI: 10.31590/ejosat.1047453

Sancar, M. R. (2023a). The Effect of Dust Deposition on Photovoltaic Systems' Electricity Generation and Its Economical Analysis. In: Çakoğlu, A. H. & Sancar, M. R. (eds.), Versatile Approaches to Engineering and Applied Sciences: Materials and Methods. Özgür Publications. DOI: https://doi.org/10.58830/ozgur.pub50.c43

Sancar, M. R. (2023b). Renewable Energy Sources and Energy Storage. In: Çakoğlu, A. H. & Sancar, M. R. (eds.), Versatile Approaches to Engi-

neering and Applied Sciences: Materials and Methods (pp. 131-140). Özgür Publications. DOI: https://doi.org/10.58830/ozgur.pub50.c69

Sancar, M. R., Yakut, A. K., "Comparative Analysis of SAM and PVsyst Simulations for a Rooftop Photovoltaic System," International Journal of Engineering and Innovative Research, pp. 60-76, 2022.

Tavsanoglu, T., 2009. Deposit and Characterization of Single and Multilayered Boron Carbide and Boron Carbonitride Thin Films By Different Sputtering Configurations. Istanbul Technical University, Institute of Science and Technology, Ph.D. Thesis, 235s, Istanbul.

Thornton, J. A., 1983. Plasma-Assisted Deposition Processes: Theory, Mechanisms and Applications. 107: 3–19.

Tosun, H., 2008. Investigation of Structural Properties of CdO Semiconductor Material Obtained by Ultrasonic Spray Pyrolysis Method Depending on Fluorine Additive. Anadolu University Institute of Science and Technology, Master Thesis, 95s, Eskişehir.

Chaphter 4

Ultrasonic Spray Pyrolysis Technique and Parameters

Ahmet Buğrahan Bayram[1]

INTRODUCTION

Due to technological advancements worldwide, the demand for energy has increased, leading to the establishment of energy generation plants (Sancar & Altınkaynak, 2021). The intensive use of fossil fuels in energy production has caused the issue of global warming to arise. In order to solve this problem, a transition to renewable energy systems has begun. One of the most commonly used systems among these is solar energy (Sancar, 2023a).

Electricity generation from solar energy is carried out in two different forms. One is through thermal systems, and the other is through photovoltaic systems. As the name suggests, thermal systems convert solar energy into thermal energy and produce electricity, while photovoltaic systems generate electricity through the photovoltaic effect (Sancar, 2023b).

Solar energy is gaining more and more attention worldwide as a sustainable and clean energy source. Solar cells, which are used to convert solar energy into electrical energy, are the basic building unit of photovoltaic Technologies (Sancar&Yakut, 2023). The production of these cells requires innovative production techniques and equipment. In this context, ULTRASONIC SPRAY PYROLIZING (USP) plays an important role in the production of solar cells.

Solar cells are devices that convert sunlight into electrical energy and are key components of photovoltaic systems. Ultrasonic Spray Pyrolysis (USP) devices play an important role in the manufacturing process of solar cells. In this chapter, we will examine the impact and advantages of USP on the production of solar cells.

1 Isparta University of Applied sciences, Institute of Postgraduate Education, Energy Systems Engineering, Isparta, Turkiye, ORCID Code: (0000-0002-7364-8559)
d1940640016@isparta.edu.tr

Ultrasonic Spray Pyrolysis is a method used in the production of thin film solar cells. This device sprays a liquid solution through ultrasonic waves to form a thin film of the desired material. This method is faster, more efficient and more economical than conventional methods.

One of the advantages of the USP device in the production of solar cells is the increased efficiency in material utilization. Ultrasonic waves transform the liquid solution into a very fine aerosol, which minimizes material loss. Furthermore, the solution is homogeneously dispersed during the spraying process and settles uniformly on the base, which improves film quality.

Another important advantage of the USP device is that the thickness of the thin film layer can be controlled. The distance between the spray head and the base determines the thickness of the film layer. This distance can be adjusted via the control panel of the USP device and the desired film thickness can be achieved. This feature is of great importance for optimizing the performance of solar cells.

Another influential parameter of the USP device on the production of solar cells is the base temperature. The base temperature affects the crystalline structure and electrical properties of the film layer. The USP device is equipped with a heating system to control the temperature of the base. In this way, the desired temperature value can be set and the quality of the film layer can be optimized.

ULTRASONIC SPRAY PYROLYSIS TECHNIQUE

Ultrasonic Spray Pyrolysis Technique (USP) is a process that plays an important role in the production of solar cells. This technique is a pyrolysis method using ultrasonic vibrations and aims to improve the quality of solar cells by creating a thin film of solution.

The USP process is performed using an ultrasonic spray device and a pyrolysis chamber. The process starts with the preparation of the solution. It is important to solutionize the solar cell materials in appropriate proportions and create a homogeneous structure. This solution is transferred to the ultrasonic spray device.

The ultrasonic spray device consists of a transducer and a spray head. The transducer converts electrical energy into mechanical vibrations. These vibrations are transmitted to the spray head to spray the solution at high frequency. The spray head sprays the solution onto a substrate in the form of a thin film.

During the USP process, the solution is broken into very small droplets by the action of the ultrasonic vibrations. The size and distribution of these droplets is an important factor affecting the performance of solar cells. The high frequency of the ultrasonic vibrations makes the solution droplets smaller and more homogeneous.

The Ultrasonic Spray Pyrolysis Technique optimizes the material utilization of solar cells and improves the energy conversion efficiency. Furthermore, it enables improvements in cell performance through the ability to control the solution film thickness.

This technique offers the potential to achieve high efficiency, low cost and thinner film layers in the production of solar cells. Ultrasonic Spray Pyrolysis Technique is an important area of research and development in the field of solar energy and is an area where more work will be done in the future to enable more efficient and sustainable production of solar cells.

Various materials with magnetic, optical, semiconductor and superconducting properties can be produced in thin film form by ultrasonic spray pyrolysis. This method is realized by applying the prepared solution to the line with a syringe and atomizing the solution coming to the nozzle with ultrasonic sound waves and spraying it onto the heated substrate. Thin films are obtained when the droplets atomized and sprayed on the heated substrate adhere to the substrate by the pyrolysis process without falling on the substrate. In general, the thin films obtained are polycrystalline. This method is one of the most preferred methods because it is simple, economical, large area coverage and does not require vacuum. Many parameters affect the thin films we produce in this technique. These parameters are; substrate temperature, nozzle frequency, flow rate, forming air pressure, distance between substrate and nozzle, spray time, solution concentration, solution amount, initial solution, number of passes, aerodynamics of solution droplets. All parameters of the films to be produced can be adjusted and the desired films can be obtained. Changing any parameter during production with this method changes all the properties of the film we will obtain. Parameters are determined according to the films we will produce and production is made accordingly. Advantages and disadvantages of this method;

Advantages

1. Low hardware cost
2. High coverage rate
3. Large area coverage

4. Adjust the properties of the film produced by adding the desired amount of additives to the prepared solution

Disadvantages

1. Affected by atmospheric conditions

2. Formation of uneven structures

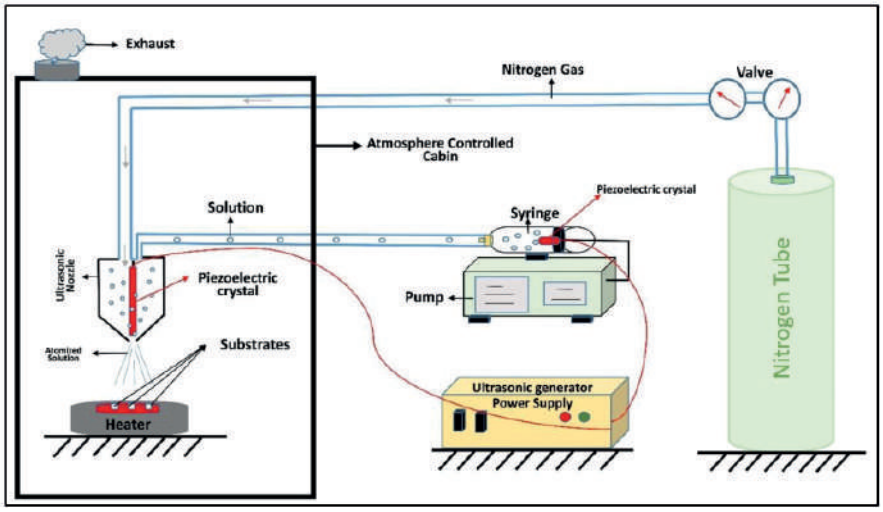

Figure 1. Schematic representation of the Spray Pyrolysis technique (Koç, 2018)

Ultrasonic Spray Pyrolysis Parameters

In this chapter, we will address various factors that play an important role in the production of solar cells, focusing on the Parameters of Ultrasonic Spray Pyrolysis. First, the concentration effect will be emphasized. The composition and concentration of the solution or suspension used has a decisive influence on the quality and properties of the sprayed thin film layers. This parameter is critical for the conversion efficiency and performance of solar cells.

Besides this, the frequency effect will also be studied. The frequency of ultrasonic waves has a direct impact on the homogeneity of thin film layers by affecting the dispersion and atomization of the solution during the spraying process. This parameter is an important factor in determining the structural and optical properties of the sputtered film layers.

The solution flow rate and duration will also be evaluated among the Ultrasonic Spray Pyrolysis Parameters. These parameters are used to control

the speed and duration of the spraying process. The flow rate and duration have a decisive influence on the thickness, uniformity and structure of the thin film layers. Therefore, determining the correct flow rate and duration is important to achieve the desired film layers.

Furthermore, the distance parameter between the sputtering nozzle and the base will also be addressed. This distance affects the efficiency of the sputtering process and the morphology of the resulting thin film layers. The choice of an ideal distance is important for obtaining homogeneous and desirable residual film layers. Accurate determination of the distance between the spray head and the base can improve the efficiency of the sputtering process and ensure the uniformity of the desired film layers

The effect of the base temperature is of particular importance among the parameters of ultrasonic spray pyrolysis. The temperature of the base has a decisive influence on the crystal structure, surface morphology and electrical properties of thin film layers during spraying. Choosing the right base temperature is a critical factor to obtain solar cells with the desired quality and performance.

Ultrasonic Spray Pyrolysis Parameters include a number of important factors that need to be controlled during the manufacturing process of solar cells. Proper tuning of these parameters can improve the conversion efficiency of solar cells by optimizing the quality, homogeneity and performance of thin film layers. However, the interactions between parameters and the determination of optimal combinations can be a complex process.

This book chapter aims to provide a comprehensive overview on the Parameters of Ultrasonic Spray Pyrolysis. The effects of each parameter on the production of solar cells will be examined through research and applications from existing literature. Furthermore, practical information on how to optimize the parameters, which values are preferred and methods to achieve process control will be presented.

Ultrasonic Spray Pyrolysis Parameters are an important factor that needs to be carefully managed in order to achieve advances in solar technologies and produce more efficient solar cells. This book chapter will be a valuable resource for researchers, engineers and industry experts and will help them to fully understand the potential of Ultrasonic Spray Pyrolysis in the production of solar cells.

Concentration effect

One of the most influential parameters on particle formation is the solution concentration. If the concentration at the center of the droplet produced in the USP technique is equal to or greater than the equilibrium state of the solution at the droplet temperature, the nucleation formed on the surface increases the rate of precipitation along the droplet and volumetric precipitation is observed. If the concentration in the center of the droplet is less than the equilibrium state, surface nucleation occurs. The solution concentration can be determined according to the properties we want in the product we will produce. High concentration is suitable for volumetric precipitation and low concentration is suitable for surface precipitation. In cases of volumetric precipitation, if the particles can remain in the heated zone for a sufficient time, small size distribution and dense solid particles are obtained. If the droplets cannot remain in the heated zone for a sufficient time, particles with a narrow size distribution are obtained. When surface precipitation occurs, hollow or dense structures with a small size distribution are obtained. This is not always the case. In some cases, they can also have large sizes (Ebin 2008; Jokanović, Spasić & Uskoković 2004). In the USP method, water or alcohol is usually used as the solvent while salts of the solute such as nitrate, chloride and acetate are used to prepare the starting solution. While the surface morphology of particles obtained from starting solutions prepared using different salts differs, their crystal structures remain the same (Wang et al. 2004).

Frequency effect

One of the parameters affecting production is frequency. Nozzle frequency affects the size of aerosol droplets. When the frequency is increased, the size of the aerosol droplets decreases. When the frequency is decreased, the droplet size increases. Frequency is inversely proportional to aerosol droplet size (Tsai et al., 2004). The expression between frequency and droplet size is expressed by the following formula (Peskin & Rajo, 1963).

$$D = 0{,}34\ x\left(\frac{8\pi\gamma}{\rho f^2}\right)^{\frac{1}{3}} \quad (1)$$

d: average droplet diameter

ρ: solution (liquid) density

γ: surface tension

f: frequency of the transmitted ultrasonic wave

Solution flow rate and time

The flow rate of the solution is an important parameter affecting the quality of the films to be produced. If the solution flow rate is above the normal value, porous films are formed and the control of the base temperature becomes difficult. If the solution flow rate is below the normal value, it causes loss of energy and time. A flow meter is used to determine the flow rate of the solutions to be sprayed. Each solution has its own appropriate flow rate. In addition to the flow rate, flow time is also an important factor. Long or short duration of the flow rate affects the thickness and physical properties of the films produced (Özer, 2010).

Distance between spray nozzle and substrate

The distance between the spray nozzle and the substrate affects the quality and thickness of the films produced. If the distance is above the normal value, the solution evaporates before reaching the substrate, the number of droplets decreases and uncoated areas remain on the substrate. If the distance is below the normal value, deposits can form on the substrate and thicker films are obtained. Generally, the distance is between 30 and 40 cm (Özer, 2010).

During the sputtering process, the solution is atomized by the sputtering nozzle and sprayed onto the base as thin film layers. The distance between the spray nozzle and the base affects the process of these atomized solution droplets falling to the base. A closer distance can result in the formation of larger droplets and a low dispersion, while a greater distance can result in the formation of smaller droplets.

The distance also has an impact on the uniformity of the spraying process. An optimal choice of distance ensures uniform and homogeneous spraying of thin film layers onto the base. A closer distance can lead to uneven spraying and fluctuations in the thickness of the layers. A greater distance may have negative effects on the uniformity of the layers.

Furthermore, the distance between the sputtering head and the base determines the morphology and structural properties of the thin film layers. Choosing an appropriate distance ensures the formation of film layers with the desired crystal structure, surface morphology and optical properties. For example, too close a distance can produce a denser and more irregular layer, while a greater distance can produce a thinner and more homogeneous layer.

The distance parameter between the spray nozzle and the base is an important factor to consider in order to optimize the spraying process in

the production of solar cells. Correct adjustment of this parameter ensures the formation of thin film layers that are homogeneous and of the desired quality. This improves the conversion efficiency and performance of solar cells.

Substrate temperature effect

Since it is difficult to keep the base temperature at a constant value, there is a deviation of ±5 °C from the base temperature. The solution and the forming air used during spraying cause the base temperature to drop slightly and the base must be preheated at high temperature in order to remain at the desired temperature values (Köse, 1993; Atay, 2001). Base temperature is an important parameter in production techniques using chemical spraying technique. The base temperature affects the physical properties and thickness of the film to be produced. When the base temperature is not at the temperature required for the formation of the thin film, the adhesion of the films to the surface is strong or weak. Low or high base temperature also affects the thickness of the films. High base temperatures cause thin films and low base temperatures cause thick films. The films we want to obtain have a base temperature suitable for the material used (Ceylan, 2012).

Spray pressure

Air with different pressure values according to the solution is used to atomize the solution that reaches the tip of the spray nozzle. A high pressure value causes the substrate to cool quickly and the temperature cannot be kept at a constant value. Low pressure value causes the sprayed solution not to be atomized and causes a damaged film to form. For this reason, the selected pressure value is one of the important factors. The air pressure is kept at a constant value by adjusting it with a manometer that can be controlled manually. The amount of air is controlled by another manometer connected to the air tube, which is between certain intervals (Polat, 2012).

Parts Of Ultrasonıc Spray Pyrolyzer

Ultrasonic transducer

Ultrasonic transducer is one of the key parts of ultrasonic spray pyrolysis device and converts electrical energy into mechanical vibrations. This transducer is usually made of piezoelectric materials. The piezoelectric effect is based on the principle that some crystalline and ceramic materials can accumulate electric charges under mechanical stresses, and these materials undergo mechanical vibrations under electric voltage.

The ultrasonic transducer generates high-frequency mechanical vibrations using electrical energy from the device's power supply. These vibrations cause deformation of the piezoelectric material of the transducer. During the deformation, a stress is generated on the material and this stress is used to atomize the liquid solution.

The ultrasonic transducer is typically enclosed in a metal container and comes into contact with a spray nozzle on the underside of the transducer. When electrical energy is applied to the transducer, the material vibrates rapidly and quickly breaks up the solution passing through the spray head.

The vibration of the transducer plays an important role when spraying the solution. The high-frequency vibrations break the solution into small droplets and create a homogeneous spray. Furthermore, the power and vibration frequency of the transducer can affect the size and distribution of the spray. Therefore, the correct transducer design and tuning is critical in achieving the desired solar cell quality.

The ultrasonic transducer is also important for energy efficiency. An efficient transducer can produce more solution spray by consuming less energy. This can reduce costs for solar cell production and increase production efficiency.

Calibration and maintenance of the ultrasonic transducer is also important. Checking the transducer regularly and cleaning it when necessary is important to ensure optimal performance. Here are some important points regarding the calibration and maintenance of the ultrasonic transducer:

Calibration: Periodic calibration should be performed to accurately set the vibration frequency and power of the ultrasonic transducer. This ensures that the device operates in accordance with the production parameters. The calibration process is usually performed using specialized equipment and test methods.

Cleaning: Dirt, oil or other debris accumulated on the transducer can reduce the efficiency of the vibrations. Therefore, it is important to clean the transducer regularly. Suitable cleaning solutions or ultrasonic cleaning baths can be used for the cleaning process. When cleaning the transducer, care should be taken to avoid damaging the material and the cleaning instructions recommended by the manufacturer should be followed.

Inspection and Replacement: The ultrasonic transducer may wear or fail over time. Therefore, the device should be checked regularly to ensure proper operation and replaced as necessary. A defective or worn transducer can adversely affect spray quality and reduce production efficiency. Therefore,

if any problems with the transducer are detected, they should be dealt with quickly and repaired or replaced as necessary.

Calibration and maintenance of the ultrasonic transducer is essential to achieve stable and high-quality results in solar cell production. The proper functioning of this part has a direct impact on the uniformity, size and distribution of the spray. Therefore, regular maintenance and calibration procedures ensure a long life and efficient operation of the device.

Liquid supply system

The liquid feeding system is an essential part of the ultrasonic spray pyrolysis device and ensures the supply of the solution to the device and the control of the spray formation. This system consists of the following components:

Feed Tank: The feed tank used for the liquid feed system provides a capacity where the solution is stored. The tank is usually made of a transparent or opaque material, allowing the level and quality of the solution to be visually monitored. The size of the feed tank can vary depending on the intended use of the device and production requirements.

Pump: One of the most important components of the liquid feed system is the pump. The pump is a mechanism that sucks the solution from the feed tank and pushes it towards the spray head. The pump controls the flow rate and pressure of the solution and ensures the desired spray formation. The pump is usually powered by an electric motor or compressed air.

Liquid Supply Line: A system of pipes or hoses that delivers the solution pushed by the pump to the spray head. The liquid supply line directs the flow of the solution and is designed according to the operating parameters of the device. In most cases, the diameter of the line is selected to match the flow rate and pressure.

The liquid feed system plays an important role for solar cell production. Controlling parameters such as the correct concentration, flow rate and duration of the solution makes it possible to achieve the desired quality and efficiency in production. The system can be adjusted according to user-specified parameters and modified as needed.

It is also important to maintain the liquid feed system. The feed tank should be cleaned regularly and replaced regularly to ensure that the solution remains fresh and clean. The pump and liquid supply line should also be cleaned and maintained as needed. This ensures the reliability and longevity of the instrument.

Nozzle

The spray nozzle of the ultrasonic spray pyrolysis device is an important component where the solution is atomized into a fine spray and sprayed onto the target surface. The spray nozzle is designed to ensure a homogeneous and stable spray formation. A functional and effective spray nozzle should have the following characteristics:

Atomization Capability: The spray head should have the ability to atomize the solution with the help of ultrasonic vibrations. Ultrasonic waves vibrate the solution, reducing surface tension and creating small particles. This results in a homogeneous spray formation and the solution particles are uniformly sprayed onto the target surface.

Adjustable Spray Features: The spray nozzle should allow adjustability of characteristics such as spray angle, spray intensity and distribution. This allows the spray to be controlled according to production requirements and the desired film thickness. The design of the spray head should be such that these characteristics can be optimized.

Material Compatibility: The spray head should be made of a material that is resistant to the solution used and the process temperature. Chemical resistance ensures the longevity and repeatable performance of the spray head. It is also important that the material does not cause unwanted reactions or contamination during the spraying process.

Easy Cleanability: The spray head should be easily cleanable after use. Solution residues or particles accumulated during operation can adversely affect the performance of the spray head. Therefore, the nozzle should be of a suitable design so that cleaning and maintenance can be easily performed.

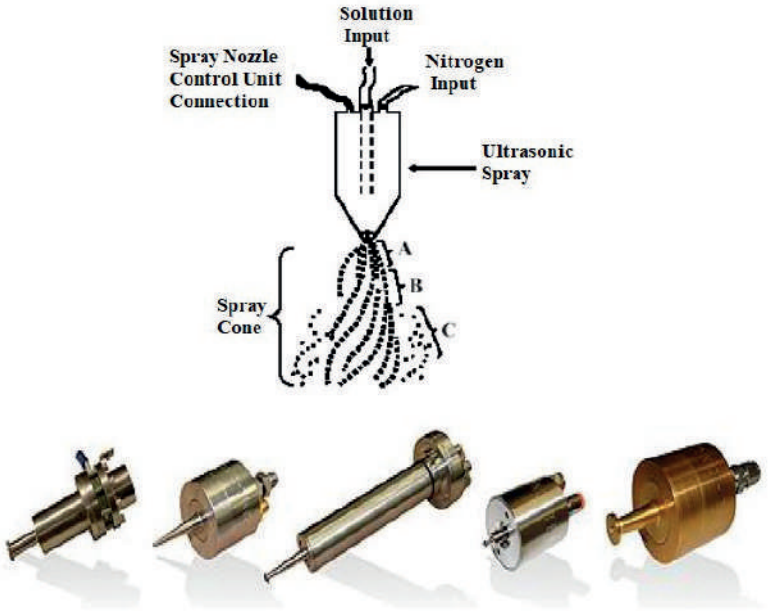

Figure 2. Spray nozzle schematic (Ozer, 2010: Sono-tek, 2023)

Heating system

In an ultrasonic spray pyrolysis device, maintaining the base or target surface at a suitable temperature is of great importance in the film formation process. Therefore, the heating system used as part of the device is important to achieve the desired film quality and performance. The heating system includes the following elements:

Heating Element: The basic component of the heating system is a heating element that converts energy into heat. Usually resistance wires pass an electric current that heats the air or liquid. The heating element must be correctly positioned to ensure a uniform and homogeneous heat distribution over the base or target surface.

Temperature Control System: The heating system is used in conjunction with a temperature control system to ensure that the target surface reaches and maintains the desired temperature. This system works in conjunction with components such as temperature sensors, thermocouples or thermal cameras. The temperature control system is used to set the temperature value via an adjustable control panel and automatically regulate it as needed.

Heat Distribution: The heating system must ensure a uniform heat distribution over the base or target surface. This is achieved by properly

positioning the heating element and ensuring effective heat transfer. Homogeneous heat distribution helps to avoid unwanted temperature variations and thermal stresses during film formation.

Controllability: The heating system must be adjustable so that the user can set the desired temperature range and control the process. This ensures that appropriate temperature conditions can be maintained for different film materials and thicknesses. The heating system is usually equipped with digital controls, giving the user the flexibility to set the desired temperature value.

CONCLUSION

In this chapter, we discussed the Ultrasonic Spray Pyrolysis technique and its parameters. The Ultrasonic Spray Pyrolysis process involves the conversion of liquid precursors into solid or powder form through the use of ultrasonic waves.

We examined the effect of various parameters on the Ultrasonic Spray Pyrolysis technique, including concentration, frequency, solution flow rate and time, distance between spray nozzle and substrate, substrate temperature, and spray pressure. These parameters play a crucial role in controlling the morphology, composition, and properties of the resulting materials.

Furthermore, we explored the different parts of an Ultrasonic Spray Pyrolyzer, which include the ultrasonic transducer, liquid supply system, nozzle, and heating system. Each component contributes to the efficient operation and optimization of the spray pyrolysis process.

Overall, the Ultrasonic Spray Pyrolysis technique offers a promising method for the synthesis of various materials with tailored properties. By understanding and controlling the parameters involved in this technique, researchers and engineers can achieve desired material characteristics and advance applications in fields such as nanotechnology, energy storage, and catalyst development.

Further research and development in the Ultrasonic Spray Pyrolysis technique are essential to explore its full potential and optimize its capabilities. With continuous advancements in this field, we can expect new and improved applications of this technique in the future.

In conclusion, the Ultrasonic Spray Pyrolysis technique provides a versatile and effective approach for material synthesis, and its parameters and equipment components are crucial for achieving desired results. Continued research and utilization of this technique will undoubtedly contribute to advancements in various scientific and technological domains.

REFERENCES

Atay, F., 2001. Investigation of Electrical, Optical, Structural and Surface Properties of Cd1-xNixS Films. Osmangazi University Institute of Science and Technology, Ph.D. Thesis, 145s, Eskişehir.

Ceylan E., 2012. Investigation of Some Physical and Surface Properties of Cd1-xBxS Films Obtained by Ultrasonic Chemical Sputtering Technique. Osmangazi University Institute of Science and Technology, Master Thesis, 55s, Eskisehir.

Ebin, B., 2008. Production of Iron Nano-Particles by Ultrasonic Spray Pyrolysis and Hydrogen Reduction Method. Istanbul Technical University, Institute of Science and Technology, Master Thesis, 107s, Istanbul.

Jokanović, V., Spasić, A. M., Uskoković, D., 2004. Designing of Nanostructured Hollow TiO2 Spheres Obtained by Ultrasonic Spray Pyrolysis. Journal of Colloid and Interface Science 278 (2): 342–352.

Koç M, 2018. Investigation of Physical and Optical Properties Sn-Doped Indium Oxide Thin Films Fabricated by Ultrasonic Spray Pyrolysis Method and Heat Treatment under Different Nitrogen Flow Rate Atmospheres. Süleyman Demirel University, Graduate School of Natural and Applied Sciences, PhD Thesis.

Kose, S., 1993. Investigation of Some Physical Properties of Cd1-xZnxS Films Obtained by Spray Pyrolysis Method. Osmangazi University Institute of Science and Technology, 112s, Eskisehir.

Ozer, T., 2010. Investigation of Some Physical, Structural and Surface Properties of Cd1-xSnxS Films Obtained by Ultrasonic Chemical Sputtering Technique. Osmangazi University Institute of Science and Technology, PhD Thesis, 91s, Eskişehir.

Peskin, R., Raco R., 1963. Ultrasonic Atomization of Liquids. Journal of Acoustical Society of America, 33, 1010-1014.

Polat M., 2012. Investigation of Some Physical Properties of Mn Doped CdS Films Obtained by Ultrasonic Chemical Sputtering, PhD Thesis, Eskişehir Osmangazi University, Institute of Science, 108s, Eskişehir.

Sancar, M. R. & Altınkaynak, M. (2021). Isparta İli İçin Farklı Çatı Tiplerinde Tasarlanan Fotovoltaik Sistemlerin Karşılaştırılması . Avrupa Bilim ve Teknoloji Dergisi , Ejosat Özel Sayı 2021 (RDCONF) , 1024-1028 . DOI: 10.31590/ejosat.1047453

Sancar, M. R. (2023a). Renewable Energy Sources and Energy Storage. In: Çakoğlu, A. H. & Sancar, M. R. (eds.), Versatile Approaches to Engineering and Applied Sciences: Materials and Methods (pp. 131-140). Özgür Publications. DOI: https://doi.org/10.58830/ozgur.pub50.c69

Sancar, M. R. (2023b). The Effect of Dust Deposition on Photovoltaic Systems' Electricity Generation and Its Economical Analysis. In: Çakoğlu, A. H.

& Sancar, M. R. (eds.), Versatile Approaches to Engineering and Applied Sciences: Materials and Methods. Özgür Publications. DOI: https://doi.org/10.58830/ozgur.pub50.c43

Sancar, M. R., Yakut, A. K., "Comparative Analysis of SAM and PVsyst Simulations for a Rooftop Photovoltaic System," International Journal of Engineering and Innovative Research, pp. 60-76, 2022.

Sono-Tek, Access date: 27.06.2023 http://www.sono-tek.com/ultrasonic-nozzle-technology/

Tsai, S. C., Song Y. L., Tsai, C. S., Yang, C. C., Chiu, W. Y., Lin, H. M., 2004. Ultrasonic Spray Pyrolysis for Nanoparticles Synthesis. Journal of Materials Science, 39, 3647-3657.

Wang, W. N., Itoh, Y., Lenggoro, I. W., Okuyama, K., 2004. Nickel and Nickel Oxide Nanoparticles Prepared from Nickel Nitrate Hexahydrate by a Low Pressure Spray Pyrolysis. Materials Science and Engineering B: SolidState Materials for Advanced Technology 111 (1): 69–76

Chaphter 5

CdTe (Cadmium Telluride) Thin Film Solar Cell Structures and Production Methods

Dr. Muhammet Raşit Sancar[1]

INTRODUCTION

İt is possible to classify them according to some parameters such as the materials used in production and the production process, in order to examine and compare photovoltaic solar cells in more detail, and these classifications are given in Table 1.

Table 1: Classification of Photovoltaic Solar Cells.

First generation crystalline cells	Monocrystalline silicon cells
	Polycrystalline silicon cells
Second generation thin film cells	Amorphous silicon cells
	CuInSe2 (CIS) or CuInGaSe2 (CIGS)
	Cadmium Telluride (CdTe) et al.
Third generation organic cells	Dye-sensitized solar cells (DSSC)
	Perovskite cells
	Organic solar cells (OPV)

First-generation silicon solar cells, among other disadvantages, require expensive processes and techniques in their production and also require large areas for power generation. In addition, these silicon solar cells experience significant performance degradation at high temperatures, making them less efficient in hot regions. For these reasons, scientists have begun research on second-generation thin-film solar cells that offer higher efficiency and are less affected (or minimally affected) by environmental conditions compared to first-generation silicon crystal-based solar cells.

1 Isparta University of Applied Sciences, Institute of Postgraduate Education, Energy Systems Engineering, Isparta, Turkiye, ORCID Code: (0000-0002-4488-8393), d1840640001@isparta.edu.tr

Silicon, the second most abundant element in the Earth's crust after oxygen, is widely used in the production of solar cells (27% abundance). Silicon with a purity of 98% is obtained by reacting silicon dioxide (SiO_2), also known as sand, with carbon at high temperatures. After various purification processes, silicon is further refined to reach a purity of over 99.99%. The high-purity silicon material is then cut into thin slices to obtain wafers that are subjected to a doping process. During the doping process, boron (B) doped (P-type) silicon wafers are heated at 850-900 °C under a gas containing phosphorus (P), which causes the front surface of the wafers to be doped with phosphorus and become N-type. After all these processes, a P-N junction is formed in the silicon wafers (Turan&Es, 2011). As shown in Figure 1, monocrystalline solar cells have a regular crystal structure, while polycrystalline solar cells have a more irregular crystal structure.

Figure 1. Structural characteristics of polycrystalline (left) and monocrystalline (right) solar cells appearances (Kuzdere, 2019)

In today's market, crystalline silicon solar cells are the most dominant and widely used solar cell model. In general, the efficiency of crystalline silicon cells on the market ranges from 14% to 18%. However, advances have been made in recent years to achieve efficiencies above 22%.

2nd generation thin film solar cells are currently considered as the best alternative to crystalline silicon cells. Studies show that the optimum energy band gap (Eg) for the solar spectrum is around 1.5 eV (Burgelman, 2006). The values closest to this range can be obtained from CdTe, $Cu(In,Ga)Se_2$ and a-Si thin film cells.

Thin film solar cells can be manufactured to be much thinner (in the nanometre or micrometre range) compared to crystalline cells by using

materials with better light absorption ability. The main reasons for focusing on thin-film photovoltaic cells are the high energy consumption and the material requirements for purification of silicon, resulting in high costs. Thin film solar cells, besides being low cost and easy to manufacture, offer the advantage of being structured on inexpensive materials such as glass and plastic and can even enable the production of flexible cells. Thin film solar cells can also be produced as semi-transparent, making them highly suitable for Building Integrated Photovoltaic (BIPV) applications.

Thanks to their high absorption capacity (100-500 times less material consumption), thin film solar cells can be manufactured using significantly less material compared to first generation crystalline silicon cells. They can achieve high efficiencies with an absorber layer only 1 μm thick. Furthermore, while the purification process of silicon requires high temperatures of 1400-1900 °C, resulting in significant energy consumption (Turan&Es, 2011), thin films can be easily fabricated at temperatures generally below 500 °C.

Some of the methods used for the production of thin films are listed below:

- Chemical Vapor Deposition (CVD)
- Electrochemical Deposition (ED)
- Close-Spaced Sublimation (CSS)
- Metal Organic Chemical Vapor Deposition (MOCVD)
- Spray Method (Spray Pyrolysis)
- Sol-Gel Coating
- Spin Coating

In third generation organic cells, the absorber layer consists of organic materials such as solar inks, nanotubes, silicon wires, organic paints, etc. The high absorption rates and their ability to be produced in a flexible structure make these organic materials a good alternative for cell production. An organic solar cell with flexibility is shown in Figure 2.

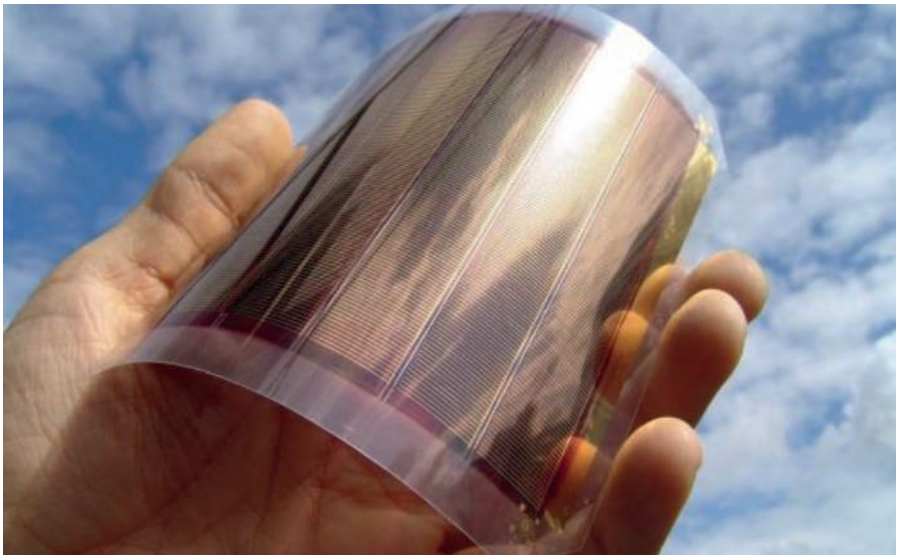

Figure 2. Organic solar cell with flexibility capability (Fraunhofer ISE, 2019)

The first organic solar cell was produced by Tang et al. The efficiency of this two-layer cell was 1.1%, but the efficiency remained low because the separation of electron-hole pairs produced by solar radiation occurs only at the interface of the layers (Toppare vd., 2011).

Until recent years, the highest efficiency reported in the literature for third generation organic cells was around 7.4% as reported in a study by Yongye Liang and colleagues (Brabec vd., 2001). In 2017, the National Renewable Energy Laboratory (NREL) reported on its official website that they achieved an efficiency of approximately 13.2% in their research on organic photovoltaic cells (NREL, 2017). However, many studies on third generation organic cells have not yet moved from the laboratory environment to commercialisation due to high costs, low efficiency and stability issues.

CdTe (CADMIUM TELLURIDE) THIN FILM SOLAR CELLS AND THEIR STRUCTURES

Thanks to their high absorption capacity, thin film solar cells can be produced with significantly less material consumption (100-500 times less) compared to first generation crystalline silicon cells. They can achieve high efficiencies with an absorber layer only 1 μm thick. Furthermore, the purification process for silicon requires high temperatures of 1400-1900 °C, which leads to high energy consumption (Turan&Es, 2011), whereas thin films can be easily produced at temperatures generally below 500 °C.

The most widely used thin film solar cells today are CdTe cells. What distinguishes CdTe solar cells from other thin-film cells is the bandgap energy value, which falls in the most efficient range of the solar spectrum (1.2 eV to 1.5 eV). CdTe thin film cells have an ideal bandgap energy value of 1.47 eV, while other thin film cells such as CuInSe2 have values around 1.20 eV and amorphous silicon cells around 1.70 eV (Burgelman, 2006). As a result, non-CdTe thin film cells cannot effectively utilise the most efficient regions of the solar spectrum, resulting in lower efficiency. For these reasons, CdTe solar cells are the most common thin film cells today.

The most common CdTe thin film solar cells consist of a CdTe absorber layer and a CdS (cadmium sulphide) window layer. The first cell with this structure was prepared by Bonnet and Rabenhorst in 1972 and an efficiency of 6% was obtained (Bonnet, 1972). The highest efficiency obtained from CdTe thin film solar cells to date is 22.1% and was obtained by First Solar in 2016 under laboratory conditions (Wesoff, 2016).

Table 2. Key data for CdTe and CdS molecules

Molecular Formula	**CdTe**	**CdS**
Molecular Weight	240.01 g/mol	144.48 g/mol
Density	6.2 g/cm³	4.82 g/cm³
Melting Point	1092 °C	1750 °C
Band Gap	1.47 eV	2.42 eV

Transparent Conductive Oxide (TCO)

Transparent conductive oxide (TCO) plays a very important role in the production of thin film solar cells. This layer must have high conductivity (low resistivity) and transparency to the solar spectrum. To obtain highly efficient cells, the layer resistance of the front contact coating must be below 10 ohms/square metre. Tin oxide is commonly used as a 500 nm thick material. Tin oxide alone has low conductivity for a good contact, so it is often combined with indium to form indium tin oxide (ITO) (Aydin, 2013). TCO pre-contacts can be applied to rigid substrates such as glass and metal as well as flexible plastic materials. Figure 3 shows the appearance of glass and PET surfaces coated with an ITO layer.

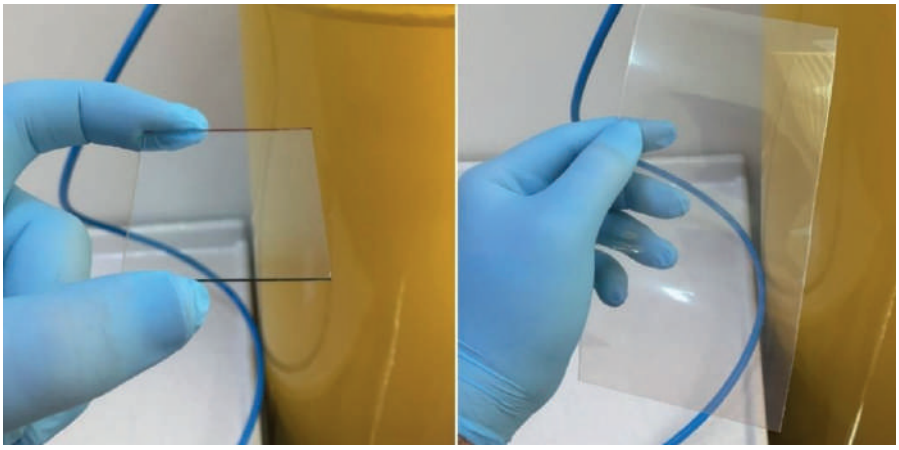

Figure 3. Appearance of glass (left) and PET (right) substrates coated with ITO (Kuzdere, 2019).

CdS Window Layer

Window layer materials must have two key properties: low resistivity and high transparency. Cadmium sulphide (CdS) is a commonly used window layer in thin film solar cells. With a bandgap of Eg = 2.42 eV, CdS has a direct band structure and has gained considerable popularity in thin-film solar cells due to its stability and low cost. The CdS layer grows as an N-type layer and forms the N-type region of the P-N junction.

The thickness of the CdS layer used in thin-film cells ranges from 10 nm to 500 nm. The CdS layer should absorb as few photons from the sunlight as possible to allow more electron energy to be transferred to the CdTe layer. Therefore, the CdS layer needs to be as thin as possible. This is because according to the principles of semiconductor and photovoltaic absorption, a photon can only be transmitted through the material without being absorbed if its energy is smaller than the bandgap of the semiconductor. However, an excessively thin CdS window layer can lead to a decrease in open-circuit voltage and fill factor, resulting in lower efficiency, as seen in equation (1).

$$\eta = \frac{P_{max}}{P_{\text{ışık}}} = \frac{I_{sc} * V_{oc} * FF}{P_{\text{ışık}}} \tag{1}$$

J. Pantoja Enriquez and Xavier Mathew reported band gap energies of 2.46 eV, 2.42 eV and 2.40 eV for CdS window layers of 26 nm, 40 nm and 95 nm thickness, respectively. They observed that the band gap energy value decreases as the layer thickness increases. These findings suggest that the CdS layer thickness should be as thin as possible and ideally optimised. This

is due to the desired balance between absorbing as little sunlight as possible while maintaining efficient electron energy transfer to the CdTe layer.

CdTe Absorber Layer

The CdTe absorber layer is the most important layer in thin-film solar cells as it absorbs incoming sunlight and generates current. To form a P-N junction with the N-type CdS layer, it must be P-type. P-type CdTe has a bandgap energy of 1.47 eV, which is lower than the bandgap energy of CdS (2.42 eV). This allows photons with energies lower than 2.42 eV but greater than 1.47 eV to pass through the CdS window layer and be absorbed in the CdTe layer.

The high absorption coefficient and direct bandgap of the CdTe absorber layer make it possible to achieve high efficiency with a thickness of only 1-2 μm. This thickness is sufficient to absorb the most valuable region of the solar spectrum. The CdTe absorber layer can be produced at low temperatures (<500 °C) using various methods.

The commonly used methods among these are listed below:

Electrodeposition (ED)

Spray method (SP)

Close-spaced sublimation (CSS)

Chemical vapor deposition (CVD)

The resistance of P-type CdTe layers is usually high (107-108 Ω.cm), which results in low conductivity. This negatively affects the overall efficiency of the solar cell. Various applications and additives can be used to reduce this resistance. Dopants such as P, Cu, Ag and excessive amounts of Te can be used to reduce the resistance of the P-type CdTe layer (Çalışkan, 2006).

Back Contact

The rear contact in thin-film solar cells serves the purpose of completing the circuit and facilitating the flow of electric current. It is desirable that both the transparent conductive oxide (TCO) front contact and the rear contact have low resistance, as these resistance parameters directly affect cell performance.

It is difficult to make ohmic contacts with P-type CdTe. In order to make ohmic contacts on P-type semiconductors, the work function of the metal used in the back contact must be higher than the work function of the semiconductor. The work function value for the CdTe absorber layer is 5.7 eV and metals with higher work function values are not available (Öztürk &

Kaya, 2013). Therefore, a Schottky contact is formed in which electron flow from one side to the other is highly favourable, while electron and hole flow in the opposite direction is almost negligible. In order to obtain an ohmic contact between the CdTe layer and the back contact, measures and additives that reduce the 5.7 eV work function value of the CdTe absorber layer as described in the "CdTe absorber layer" section can be used to facilitate the formation of a quasi-ohmic contact.

PRODUCTION METHODS OF CdTe/CdS THIN FILMS

CdTe/CdS thin film solar cells can be easily fabricated using various simple methods, which gives them an advantage over other semiconductors. Some of the fabrication techniques are as follows and detailed explanations will be given under the following headings: Electrodeposition (ED) method, close spaced sublimation (CSS) method, chemical vapour deposition (CVD) method, spray method (SP).

Electrodeposition Method (ED)

Electrodeposition (electrolysis) is a deposition technique in which thin films are coated from solutions by depositing the material on substrates. This method provides great convenience in applications with large coating areas. There are various parameters that affect the characterisation of thin films produced by electrodeposition. Some of these parameters are deposition potential, type and amount of additives added to the electrolyte, solution pH, current density, electrolyte temperature and chemical additives added to the solution (Sönmezoğlu vd., 2012). This method is suitable for both CdTe and CdS thin film growth. In general, $Cd(OH)_2$ as Cd source and thiourea ($(NH_2)2CS$) as S source are used for CdS thin film growth, while $CdCl_2$ as Cd source and sodium tellurite (Na_2TeO_3) as Te source are used for CdTe thin film growth.

Close-Spaced Sublimation Method (CSS)

An illustration of the close range sublimation (CSS) method is presented in Figure 4. In this method, solid CdS and CdTe materials in powder or granules are sublimated in vacuum. A pressure of 10 Torr is sufficient to sublimate these materials onto a glass substrate. The substrate temperature typically ranges from 400 °C to 600 °C. The distance between the substrate and the weld is very small, usually around 1 or 2 cm. The fact that the substrate temperature is lower than the weld temperature ensures that sublimated materials are deposited on the substrate surface. With this method, production rates of 1 μm to 5 μm/min can be easily achieved and large surface areas can be coated (Çalışkan, 2006).

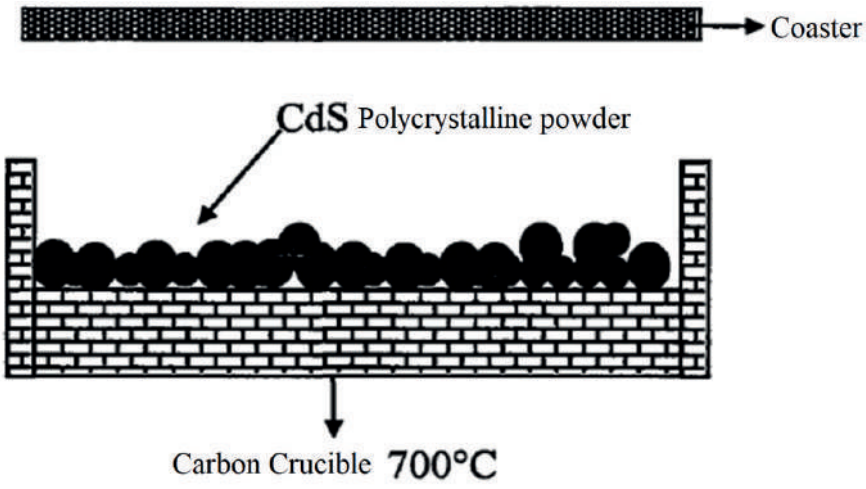

Figure 4. Close-range sublimation setup (Bonnet, 2000)

Chemical Vapor Deposition Method (CVD)

The Chemical Vapor Deposition method (CVD) is used to create high purity thin films. This method starts by placing the substrate to be coated in a reactor tube that is exposed to volatile gases. Through interactions between the volatile gases and the substrate, the solid material used for coating begins to deposit on the substrate. The CVD method can be used for the synthesis of both CdS and CdTe materials. Despite the slow production rate (~1μm/h), this technique enables the low-cost production of CdS/CdTe thin films (Bacaksız, 2002). The CVD method is particularly used for doping processes in semiconductor silicon wafers as it allows easy doping with boron and phosphorus.

Spray Pyrolysis Method (SP)

The spray pyrolysis method, also known as chemical spray deposition, is a widely used technique in many sources. An illustration of this technique is presented in Figure 5. It is the easiest and most cost-effective thin film deposition method for both CdS and CdTe films. In this method, a solution containing atomized sources of the desired material is prepared and then sprayed onto a heated substrate using a pressurized carrier gas (such as nitrogen or air). Solvents such as pure water, ethanol, methanol or hydrazine hydrate can be used.

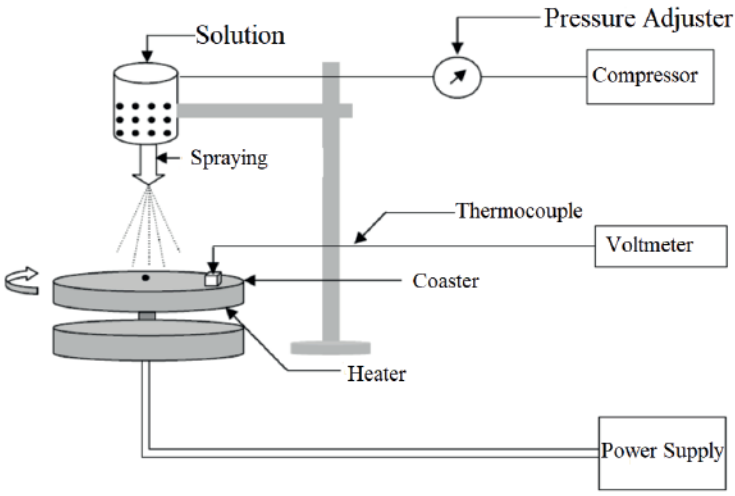

Figure 5. Spray pyrolysis setup (Yılmaz, 2007)

To obtain CdTe thin films using the spray pyrolysis method, the production is typically carried out in the substrate temperature range of 300°C to 400°C. In this method, $CdCl_2$ is usually used as the Cd source and TeO_2 as the Te source, while solvents for these materials can include distilled water, ammonium hydroxide (NH_4OH), hydrochloric acid (HCl) and hydrazine hydrate (NH_2NH_2). These components are mixed to prepare the solution to be sprayed.

For the production of CdS thin films using the sputtering pyrolysis method, $CdCl_2$ or $CdSO_4$ is typically used as the Cd source and thiourea ($(NH_2)2CS$) as the S source. Both $CdCl_2$ and thiourea are highly soluble in distilled water, so no additional solvent is usually needed in the solution containing these materials.

To obtain CdS thin films using the spray pyrolysis method, the substrate temperature is typically around 400 °C. At lower temperatures, NH4CdCl3 phase can form on the substrate, while at extremely high temperatures CdO phases can form. The synthesis of CdS thin films by spray pyrolysis is realized by the following reaction:

$$CdCl_2 + (NH_2)2CS + 2H_2O \rightarrow CdS + 2NH_4Cl + CO_2$$

The parameters that affect the characterization of thin films obtained by the spray pyrolysis method are as follows:

- Substrate temperature

- Nozzle distance
- Composition ratios of the solution
- Solution flow rate
- Spray deposition time
- Total amount of solution sprayed onto the surface
- Cooling time of the surface after the spray process

During this reaction, CdS thin film is formed on the substrate while NH_4Cl (Ammonium chloride) and CO_2 (Carbon dioxide) leave the environment in the gas phase.

The ideal thin film production process in the spray pyrolysis method is that the solution droplets sprayed from the nozzle evaporate completely before reaching the substrate, forming a film. Premature evaporation before reaching the substrate or large droplets contacting the substrate without evaporating are undesirable. The droplets sprayed from the nozzle undergo a heterogeneous reaction and evaporate completely before reaching the substrate. During this reaction process,

- The diffusion of reaction molecules to the lower regions,
- Adsorption or dissociation of many molecules on the surface,
- Combination of certain molecules within the lattice structure,
- Evaporation of some molecules reaching the surface with the surface temperature, leaving the structure from the surface layer.

As a result of these physical and chemical events, heterogeneous reactions occur (Tatar, 2015). As seen above, the production and characterization of thin films is the result of a delicate and balanced process. Parameters such as substrate temperature, nozzle distance, solution flow rate and deposition time play a crucial role in reaching optimum values that directly affect cell efficiency.

CONCLUSION

This book chapter focuses on the structures and fabrication methods of thin film solar cells using CdTe (Cadmium Telluride) material. CdTe stands out as a material with the potential to convert solar energy into electrical energy. In this chapter, the basic structure and fabrication process of CdTe thin film solar cells are comprehensively discussed.

The basic structure of CdTe thin film solar cells starts with a layer of CdTe deposited on a glass or other substrate. The CdTe layer forms the active region that absorbs sunlight and facilitates the conversion into electrical energy. Typically, buffer layers such as CdS (Cadmium Sulfide) or ZnxCd1-xS (Zinc-Cadmium Sulfide) are applied on top of this layer. The buffer layers improve the surface morphology of the CdTe layer and provide electrical contact. Finally, front and rear contacts are installed to serve as the electrical contacts of the solar cell.

The production methods of CdTe thin-film solar cells involve several steps. First, the CdTe layer is formed using deposition methods such as Chemical Vapor Deposition (CVD), Physical Vapor Deposition (PVD) or Electrochemical Deposition. Next, the buffer layer is applied and the electrical contacts of the solar cell are formed. These steps are typically performed by chemical deposition or atomic layer deposition methods. Finally, the front surface of the solar cell is treated with anti-reflective coatings to enhance the absorption of sunlight.

The aim of this book chapter is to provide readers with an understanding of the basic principles of CdTe thin-film solar cells by explaining their structure and fabrication methods. CdTe-based solar cells will continue to play an important role in the field of solar energy in the future due to their advantages such as high efficiency, low cost and commercial viability.

REFERENCES

Aydın, S., 2013. Elektrokimyasal Yolla CdS/CdTe Güneş Gözesinin Fabrikasyonu ve Karakterizasyonu. Atatürk Üniversitesi, Fen Bilimleri Enstitüsü, Doktora Tezi, 137s, Erzurum.

Burgelman, M. (2006). Cadmium telluride thin film solar cells: characterization, fabrication and modeling. Thin Film Solar Cells: Fabrication, Characterization and Applications, 277-324.

Brabec, C. J., Sariciftci, N. S., & Hummelen, J. C. (2001). Plastic solar cells. Advanced functional materials, 11(1), 15-26.

Bonnet, D., & Rabenhorst, H. (1972). New results on the development of a thin-film p-CdTe-n-CdS heterojunction solar cell. In Photovoltaic Specialists Conference, 9 th, Silver Spring, Md (pp. 129-132).

Bonnet, D., 2000. Manufacturing of CSS CdTe solar cells. Thin Solid Films, 361, 547-552.

Çalışkan, M., 2006. Au/CdTe ve Ag/CdTe Eklemlerin Yapısal ve Opto-Elektronik Özellikleri. Yıldız Teknik Üniversitesi, Fen Bilimleri Enstitüsü, Doktora Tezi, 100s, İstanbul.

Öztürk, H. H., & Kaya, D. (2013). Güneş enerjisinden elektrik üretimi: Fotovoltaik teknoloji. Umuttepe Yayınları.

Sönmezoğlu, S., Mehmed, Koç., & Seçkin, Akın. (2012). İnce film üretim teknikleri. Erciyes Üniversitesi Fen Bilimleri Enstitüsü Fen Bilimleri Dergisi, 28(5), 389-404.

Turan, R., Es, F., 2011. Kristal Silisyum Güneş Gözeleri, Bilim Teknik Dergisi, sayı: 523, 52-53s.

Toppare, L., Çırpan, A., Apaydın, D.H., 2011. Akpınar, H.Z., Organik Güneş Gözeleri, Bilim Teknik Dergisi, sayı: 523, 56-57s.

Tatar, D., 2015. Spray Pyrolysis Yöntemi ile Farklı Altlık Sıcaklığında Elde Edilen SnO2 ve SnO2:F İnce Filmlerin Bazı Fiziksel Özelliklerine, Altlık Sıcaklığının Etkisinin Araştırılması. Atatürk Üniversitesi, Fen Bilimleri Enstitüsü, Doktora Tezi, 154s, Erzurum.

NREL (The National Renewable Energy Laboratory), 2017. Photovoltaic Research. Erişim Tarihi: 14.03.2019. https://www.nrel.gov/pv/organicphotovoltaic-solar-cells.html

Wesoff, E., 2016. First Solar Hits Record 22.1% Conversion Efficiency for CdTe Solar Cell. Green Tech Media (PV Modules).

Bacaksız, E., 2002. CdS İnce Filmlerinin Farklı Yöntemlerle Büyütülmesi, Yapısal, Elektriksel ve Optiksel Özelliklerinin İncelenmesi. Karadeniz Teknik Üniversitesi, Fen Bilimleri Enstitüsü, Doktora Tezi, 74s, Trabzon.

Yılmaz, S., 2007. Düşük Altlık Sıcaklıklarında Üretilen CdTe İnce Filmlere Cd-Cl2'ün Etkisinin İncelenmesi. Karadeniz Teknik Üniversitesi, Fen Bilimleri Enstitüsü, Yüksek Lisans Tezi, 55s, Trabzon

Kuzdere, E., 2019. Farklı Katman Kalınlıklarına Sahip İnce Film Cdte/Cds Güneş Hücrelerinin İncelenmesi. Süleyman Demirel Üniversitesi, Fen Bilimleri Enstitüsü, Yüksek Lisans Tezi, 80s, Isparta

Fraunhofer ISE, 2019. Entwicklung Organischer Solarzellen. Erişim Tarihi: 01.04.2019. https://www.ise.fraunhofer.de/de/geschaeftsfelder/photovoltaik/neuar tige-photovoltaik-technologien/organische-solarzellen/organischesolarzellen.html

Chaphter 6

Dye Sensitized Solar Cells (DSSCs) And Working Principle

Dr. Muhammet Raşit Sancar[1]

INTRODUCTION

The classification of photovoltaic cells is shown in Table 1. The cells evaluated as three separate categories are classified as first generation, second generation and third generation cells.

Table 1. Classification of photovoltaic cells (Ranabhat et al., 2016)

First Generation Cells
•Monocrystalline Silicon Cells (Mono c-Si) •Polycrystalline (Poly c-Si) Silicon Cells •Amorphous Silicon Cells
Second Generation Cells
•Amorphous Silicon (a-Si and a-Si/μc-Si) •CuInSe2 (CIS), CIGS (CuInGaSe2) •Cadmium Telluride (CdTe)
Third Generation Cells
•Dye Sensitized Solar Cells (DSSC) •Perovskite (cell) •Organic Solar Cells (OPV)

First generation photovoltaic cells are conventional solar cells. Silicon is the most widely studied material. Conventional cells are made of monocrystalline or polycrystalline silicon. They are made by cutting silicon into thin slices and doping them. They are currently the most efficient photovoltaic cells

1 Isparta University of Applied Sciences, Institute of Postgraduate Education, Energy Systems Engineering, Isparta, Turkiye, ORCID Code: (0000-0002-4488-8393), d1840640001@isparta.edu.tr

used in residential buildings. These cells account for approximately 90% of the photovoltaic cell market (Kabadayı, 2011).

Second-generation solar cells are often referred to as thin-film solar cells because, compared to silicon-based cells, they have a very small thickness and are only a few micrometers thick. They are structured on low-cost materials such as glass, plastic and metal, allowing cells produced with this technology to be produced and sold more cost-effectively. However, their efficiency is low.

Third generation photovoltaic cells are made from many different materials other than silicon, including nanotubes, silicon wires, conventional printing technologies, organic dyes and solar inks using conductive plastics. The aim is to make solar energy more efficient over a wider solar spectrum (including, for example, infrared), less expensive so that it can be used by more people, and to develop more and different uses. Most of the work on third generation solar cells is being done in the laboratory. Research and development is being carried out by many companies. However, they are mostly not commercially available. Work for commercialization is still ongoing and many studies are being carried out on their development.

There are six parameters used to compare solar cells among themselves and these parameters are important for calculating cell efficiency. These parameters are open circuit voltage (VOC), short circuit current (ISC), fill factor (FF), maximum power point (MPP) and power conversion efficiency (PCE).

Under the standard conditions set by IEC (AM=1.5, 1000 W/m2, 25°C), it is possible to maximize efficiency by optimizing each of these three parameters (VOC, ISC and FF). For higher open circuit voltage, the redox couple with better redox potential can be used. Similarly, the short-circuit current can be improved by increasing sunlight absorption with dye sensitizers that help absorb sunlight. Increasing the parallel circuit resistance and reducing the series resistance, reducing the over-voltage for diffusion and electron transfer, leads to a higher FF value, thus providing higher efficiency and output power value closer to the theoretical power. Material properties and physical processes inside the cell have an impact on the variation of these parameters. Therefore, theoretical models that can capture the characteristics of the physical process and material properties are critical to optimize various operating parameters and cell configurations (Gong et al., 2017).

The open circuit voltage is the maximum voltage obtained from a solar cell. It occurs at the moment when the net current in the device is zero (I=0).

This electrical potential difference represents the energy difference between the Fermi level of the semiconductor and the electrolyte redox potential. The high voltage is generated by the open circuit voltage of the device.

In a photovoltaic battery, it is the current observed at the moment when the voltage is zero. It varies depending on the material used, the amount of light and the design of the terminals. The short circuit current is equal to the photovoltaic current which depends on the brightness. By operating the photovoltaic cell at a current close to the short-circuit current, the current, which is directly proportional to the solar radiation falling on the battery, can be measured. The short circuit current density (Isc) is the short circuit current divided by the photoactive surface area (Kabadayı, 2011).

In a solar cell, it is the ratio of maximum power to ISC and VOC products. It is an important parameter that determines the maximum power in solar cells under weak beam conditions.

$$FF = \frac{I_{max} V_{max}}{I_{SC} V_{OC}} = \frac{P_{max}}{I_{SC} V_{OC}} \quad (1)$$

Where; I_{max} is maximum current, V_{max} is maximum voltage, P_{max} is maximum power point, I_{SC} is short circuit current, V_{OC} is open circuit voltage. The values of the filling factor determine the quality of the solar cell. In order to characterize a solar cell as good, the filling factor of the cell should be between 0.75-0.8.

The maximum power point is the point of maximum current and voltage depending on the amount of light coming into the cell.

$$P_{max} = V_{max} \; x \; I_{max} \quad (2)$$

Power conversion efficiency is a parameter used to compare cell performance. It is the ratio of the maximum power obtained to the power of the light energy incident on the surface (Plight).

$$\eta = \frac{P_{max}}{P_{ışık}} = \frac{I_{SC} x V_{OC} x FF}{P_{ışık}} \quad (3)$$

The power conversion efficiency depends on the solar spectrum, the intensity of the received light energy and the cell temperature. Therefore, the standard conditions mentioned before (AM=1.5, 1000 W/m2, 25°C) are applied.

DYE SENSİTİZED SOLAR CELLS (DSSCs)

Dye sensitized solar cells (DSSCs) are one of the cells belonging to the third generation of solar cells, with a working principle quite different from conventional photovoltaic cells. They were developed to improve the efficiency of photovoltaic cells. Its working principle is similar to artificial photosynthesis as it resembles the process of absorption of radiation energy by plant leaves. DSSCs can also be called artificial chloroplasts because one of their components, the dye-sensitized semiconductor material, acts as a kind of chlorophyll. Understanding the working principle of this new generation of cells requires knowing their components, each of which has its own importance. These components are the working electrode, semiconductor material, sensitizing dye, electrolyte and counter electrode. It was first designed by O'Regan and Grätzel in 1991. Cells with a dye-sensitized porous TiO_2 semiconductor were reported to exhibit efficiencies of 7.1-7.9% in simulated sunlight and 12% in diffuse daylight (O'Regan and Grätzel, 1991). DSSCs, also known as Grätzel cells, are named after their designer Michael Grätzel.

If the superior features of DSSCs are listed, they are;

- Stable structure,
- Robust and lightweight construction,
- Less toxic substances,
- Ability to operate in high temperature and low irradiance conditions,
- Not having complex production processes,
- High efficiency with low energy,
- Easy modification of production conditions.

These superior features make DSSCs an alternative to conventional photovoltaic cells. However, they have the disadvantage of absorbing only UV radiation from the sun. In addition, it shows low efficiency and stability in terms of commercialization.

In 2014, Yang et al. found that the addition of Nb significantly increased the power conversion efficiency of Dye-sensitized Solar Cells (DSSCs). Similarly, in 2015, Shakir et al. observed that Cu-doped TiO_2 films improved the performance of DSSCs, and their porosity was further enhanced by the addition of carbon microspheres. Su et al. (2015) discovered that Nb doping prevented surface recombination at the TiO_2 electrolyte interface, leading to an increase in open-circuit voltage and improved long-

term stability of DSSCs. Arunachalam et al. (2015) determined that the substrate temperature and precursor concentration of TiO_2 films had an impact on their physical properties, and they achieved the highest power conversion efficiency in cells containing anatase-phase TiO_2. Furthermore, Dhanapandian et al. (2016) found that Zn-doped TiO_2 films enhanced DSSC efficiency, with an increase in the dopant concentration leading to a decrease in the energy bandgap. Akar (2016) obtained TiO_2 films of different thicknesses using an electrochemical deposition method and examined the effect of various surface enhancers on photovoltaic performance. Liu et al. (2016) demonstrated that Nb-doped TiO_2 films improved the photovoltaic properties of DSSCs, as the dopant accelerated the transfer of solar radiation and reduced electron recombination losses. Lastly, Shaban et al. (2016) found that ZnO thin films deposited using the ultrasonic spray pyrolysis method yielded the best results. Collectively, these studies highlight the positive effects of Nb, Cu, and Zn dopants on DSSC performance, the influence of substrate temperature and precursor concentration on TiO_2 film properties, and the significance of surface enhancers in enhancing the photovoltaic performance. These findings underscore the importance of using dopants and surface enhancers to improve the power conversion efficiency and long-term stability of DSSCs. Furthermore, enhancing the performance and optimizing the efficiency of DSSCs remains a focal point of research and development in the field of solar energy.

Operating Principle

As mentioned, the working principle of DSSCs is quite different from the working structure of conventional photovoltaic cells. In conventional photovoltaic cells, silicon, which provides an electric field for charge separation, acts both as a photoelectron source and generates current. In DSSCs, semiconductor materials provide the charge transport and the redox couple provides the vacancy transport. The source of photoelectrons is the sensitizing dye. Charge separation takes place between the dye-sensitized semiconductor and the electrolyte used as a redox mediator. In order for the dye, which acts as a light absorber, to absorb more light, the semiconductor material needs to adsorb more dye. To improve this situation, metal doping is added to semiconductor materials.

The working stages of DSSCs are as follows (Figure 1);

1. The radiation from the sun is absorbed by the dye molecules adsorbed on the semiconductor material.

2. The dye that absorbs the solar radiation becomes excited.

3. An electron in the excited dye molecule moves towards the conduction band of the semiconductor material with the energy of the radiation.

4. The electrons reaching the conduction band travel to the working electrode and pass to the external circuit.

5. The gap created by one electron of the dye molecule passing into the conduction band of TiO_2 is reduced by the electrolyte giving one electron.

6. The electrolyte, which is oxidized by giving one electron to the dye molecule, is reduced by the low-energy electron coming to the opposite electrode. Thus the circuit is completed and current is generated as a result of this process.

During the electron transfer process of DSSCs, the net charge is always zero and no chemical change occurs (Zafer, 2006).

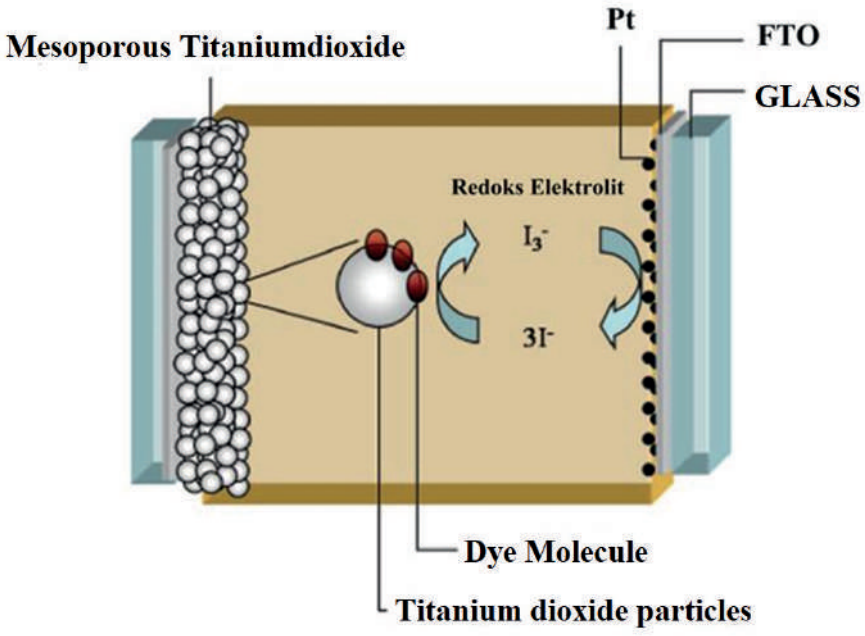

Figure1. Working principle of DSSC (Hagfeldt et al., 2010)

Cell Structure

DSSC consists of a conductive glass coated with a dye-adsorbed semiconductor as working electrode, a counter electrode and a liquid interlayer with a redox couple ($I^-/I3^-$) between them. The most commonly

used material as semiconductor is TiO_2. Iodide triiodide ($I^-/I3^-$) is used as the redox couple and ruthenium complex dyes are used for the dye. Conductive and permeable glass coated with fluorine-doped tin oxide (FTO) is used for the working electrode. Platinum-coated FTO glass is used for the counter electrode. Figure 2. shows the components and structure of a DSSC.

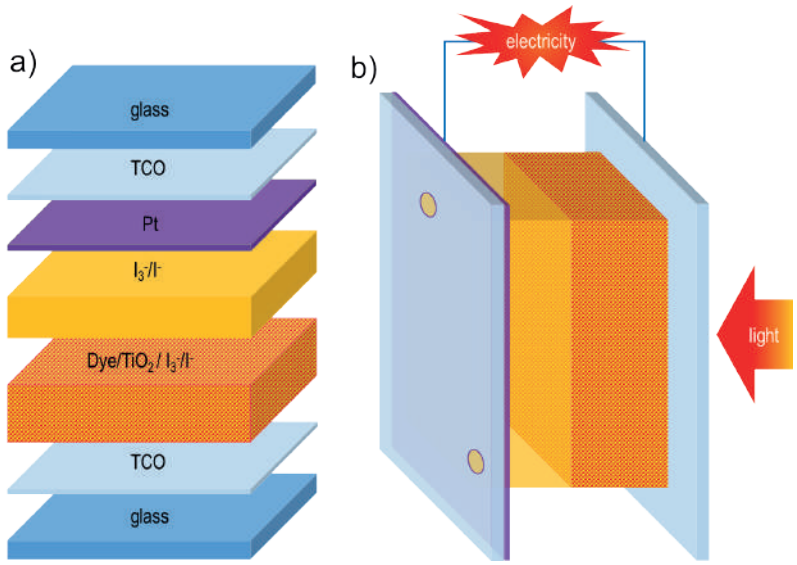

Figure 2. Schematic representation of DSSC components and structure (Sarker, 2017)

Working electrode

One of the important components in Sensitized Solar Cells (DSSCs) is the working electrode. The working electrode is designed to capture sunlight and initiate the photoelectric conversion process. In DSSCs, transparent conductive oxide (TCO) materials are used as working electrodes to absorb and transmit solar radiation. Fluorine-doped tin oxide (FTO) and indium tin oxide (ITO) are the most widely used TCO materials in DSSC applications. Although ITO has better performance in terms of transparency and sheet resistance, its resistance increases at high temperatures. Therefore, FTO is preferred in DSSC applications requiring high temperatures.

The working electrode is usually made on a transparent conductive layer on which layers of semiconductor material and sensitizing dye are applied. These layers form an interface to release electrons and generate electric current when exposed to sunlight.

The first layer is a structure called a transparent electrode, a layer usually made of transparent conductive materials such as glass or indium tin oxide (ITO). This layer allows sunlight to reach the working electrode and also provides a way to collect electrons.

The second layer is the semiconductor material layer of the working electrode. Titanium dioxide (TiO_2) is commonly used as the semiconductor material. The TiO_2 layer must have a high effective surface area for light absorption and at the same time have a structure suitable for electron transport. High surface area nanostructures applied to this layer enhance light absorption and facilitate the release of electrons.

The third layer is a layer known as a sensitizing dye. The sensitizing dye excites electrons by absorbing sunlight and binds to its surface on the semiconductor material. This dye can usually be made of organic dyes or inorganic materials such as perovskite. The sensitizing dye should have properties that can absorb sunlight at different wavelengths and provide higher efficiency.

The working electrode releases electrons by absorbing sunlight and provides a way to collect electrons. The electrons flow through the semiconductor material to the sensitizing dye layer and from there to the circuit, thus generating an electric current. This current is converted into electrical energy by the DSSC.

The working electrode has several factors that have a direct impact on the efficiency of the DSSC. These factors include:

Light Absorption and Surface Area: The working electrode should absorb sunlight as well as possible. Therefore, a structure with a high surface area is preferred. A high surface area allows more sunlight to be absorbed and more electrons to be produced.

Electron Mobility: The semiconductor material in the working electrode must have high electron mobility. This ensures that the released electrons can be quickly and efficiently delivered to the sensitizing dye layer. Semiconductor materials such as titanium dioxide (TiO_2) are a suitable option for electron mobility.

Sensitizer Dye Efficiency: The sensitizing dye in the working electrode must be able to effectively absorb sunlight and excite electrons. This can be achieved by choosing a suitable dye material that provides a high absorption efficiency over a broad spectrum of sunlight.

Electron Collection Efficiency: The working electrode must collect the released electrons quickly and efficiently. This can be achieved by optimizing the electronic connections and contacts that collect electrons with the working electrode.

Designing the working electrode with all these factors in mind is important to improve the performance of the DSSC. A working electrode that provides high light absorption, electron mobility, sensitizer dye efficiency and electron collection efficiency can help the DSSC achieve higher efficiency and energy conversion.

In this way, the working electrode, as a key component of DSSC, plays a critical role in the process of converting solar energy into electrical energy.

Semiconductor Material

Materials can be classified based on different properties, and one common classification is based on their ability to conduct electricity. In this classification, materials are categorized as conductors, insulators, and semiconductors. Conductors are materials that have the highest electrical conductivity. Insulators, on the other hand, are materials that either lack electrical conductivity or have very weak conductivity and exhibit resistance to electric current. Semiconductors are materials that exhibit the properties of insulators at absolute zero temperature (T=0 K) but show increased conductivity as temperature rises. This behavior of semiconductors in response to temperature, light, or electrical voltage provides an advantage over conductive materials in the production of photovoltaic cells. When external influences such as heat, light, or electrical voltage are applied to semiconductor materials, they exhibit the characteristics of conductive materials. When these influences are removed, they return to their insulating properties.

The electrical conductivity of materials varies based on their energy band structures. The energy band structure, which provides information about the electrical, magnetic, and optical properties of a material, is determined by the behavior of the outermost electrons located in the material's structure. These electrons are referred to as valence electrons and have specific energy levels. The band in which valence electrons reside is called the valence band, and the energy possessed by the electrons in this band is known as the valence band energy. The energy band that is not occupied by electrons is called the conduction band, and the energy required for valence electrons to transition from the valence band to the conduction band is referred to as the conduction band energy. Insulating and semiconducting materials have

energy band structures that include energy ranges (Eg) in which electrons cannot occupy, and these ranges are called band gaps. The level at which the probability of the energy range being filled with electrons reaches 50% is referred to as the Fermi energy level.

A larger band gap makes electron transition more difficult. Looking at the band structure of materials, conductors have the valence band and conduction band adjacent to each other (Figure 2.(a)). Therefore, a low-level energy is sufficient for electrons to transition to the conduction band in conductive materials. Electrons in conductive materials can move freely and directly transition to the conduction band, resulting in their excellent electrical conductivity. In contrast, insulating materials have a significantly wider band gap and either lack or possess very weak electrical conductivity (Figure 2.(b)). In insulating materials, a significantly higher energy level is required to enable electrons to become free.

The energy band structures of semiconductors resemble those of insulators. However, the energy band gap in semiconductors is narrower than that of insulating materials (Figure 2.(c)). At absolute zero temperature, the valence bands of semiconductors are filled with electrons, and no electrons are present in the conduction band. Therefore, semiconductors exhibit weak conductive properties at low temperatures. At higher temperatures, the narrow band gap of semiconductors leads to increased conductivity. With the influence of temperature, electrons in the valence band of semiconductors transition to the conduction band, leaving behind vacancies or "holes." These vacancies in the valence band are seen as positive charges. This behavior indicates that semiconductors contain both positive and negative charges within their structure. When an electron from the valence band fills the nearby vacancy, and the vacancy is occupied by another electron, the vacancy behaves as a charge carrier (Serway and Beichner, 2005).

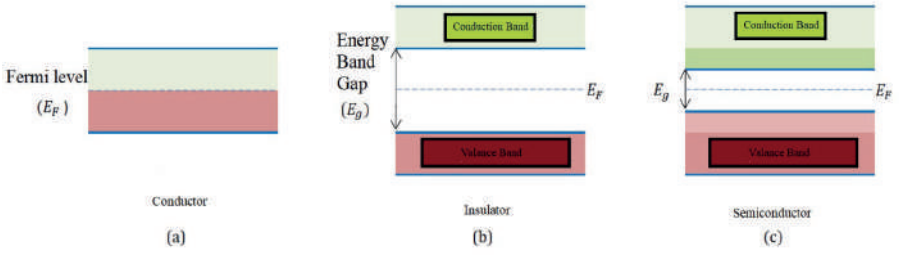

Figure 2. Energy band structures of (a) conducting, (b) insulating and (c) semiconducting materials

With increasing temperature, the resistance of semiconductors decreases and their conductivity increases. The opposite is the case with conductive materials. For this reason, it is more advantageous to use semiconductor materials rather than conductor materials in photovoltaic cell construction.

If the number of electrons in the conduction band of a semiconductor is equal to the number of vacancies they leave in the valence band, these semiconductors are called pure (prime) semiconductors. In a material of this definition, at absolute zero (T=0 K) all electrons are in the valence band and there are no free electrons in the conduction band (Tatar, 2015).

Since semiconductor materials cannot be used in pure form in solar cell production, these materials need to be doped. With doping, n-type or p-type semiconductor is obtained. The structure of the semiconductor changes according to the doping. Semiconductors in which the valence band energy level is raised by doping are called p-type semiconductors, while semiconductors in which the conduction band energy level is lowered are called n-type semiconductors. To obtain n-type silicon from silicon, the most widely used semiconductor in solar cells, an element from the 5th group of the periodic table is doped. For example, phosphorus, a group 5 element, has 5 electrons in its outer orbit. Silicon, on the other hand, has 4 electrons in its outer orbit. When phosphorus is doped into silicon, one electron is left out in phosphorus and this is called a free electron. These free electrons can move towards other atoms. The semiconductor formed by such doping is called an n-type semiconductor. To obtain p-type silicon, an element from group 3 of the periodic table is doped. For example, the indium atom has 3 electrons in its outer orbit and when doped into silicon, it is 1 electron less. In this case, the deficiency created by indium is called a vacancy. Electrons can move in these vacancies. Vacancies are defined as positive charges and semiconductors formed by such doping are called p-type semiconductors (Öztürk and Kaya, 2013)

There are many materials for semiconductor materials, one of the main components of DSSC. These are semiconductors such as TiO_2, SnO_2, ZnO, Nb_2O_5, ZrO_2. Among these, TiO_2, which is transparent in visible light, has a wide band gap, stable structure and non-toxic, is frequently used in DSSC applications. TiO_2 has a wide range of applications due to its pigment function. TiO_2 is used in the paint and coating industry, in the food industry, in products such as paper, plastics and pharmaceuticals, as well as in self-cleaning systems. TiO_2 has three different crystal structures: rutile, anatase and brocite. Rutile is the most thermodynamically stable structure. In addition, the anatase structure, which has both a wide band gap and high

conductivity band energy, is the most preferred crystal structure in DSSCs (Boz, 2015).

It is formed by the combination of titanium atoms in group 4A of the periodic table and oxygen (O) atoms in group 6B. Its melting temperature is 1858 °C and it is a stable phase at high temperatures. Anatase also crystallizes in the tetragonal system. Hardness is 5-6 and specific gravity is 4-4.5. It is semi-metallic and metallic polished. Anatase, which has a stable phase structure at lower temperatures, turns into rutile phase at high temperatures (Akar, 2016).

Sensitizing Dye

A sensitizing dye is a component used in Dye-Sensitized Solar Cells (DSSCs) to absorb incoming radiation on the surface of the semiconductor material. The excited dye molecules, upon absorption of the incident radiation, act as a source of photoelectrons. After excitation, they transfer the absorbed radiation by donating electrons to the semiconductor material, thus becoming oxidized. On the other hand, they can accept electrons from the redox couple in the electrolyte, leading to their reduction.

In DSSC production, various ruthenium (Ru) complexes, porphyrins, phthalocyanines, and organic dyes have been used. Among them, Ru complex dyes exhibit the best photovoltaic properties due to their specific characteristics. However, they are not ideal dyes, and many studies have been conducted to approach the ideal dye. The synthesis of ruthenium dyes is not easy, and the materials used during synthesis are quite expensive. Additionally, their absorption is limited to a certain range of the solar spectrum, which hinders their ideal characteristics.

The choice of dye for sensitizing the semiconductor material depends on the type of semiconductor used. For the TiO_2 semiconductor, the highest efficiency has been achieved with N3 (10%) and Z907 (11%) dyes, while for the ZnO semiconductor, N719 (5%), a ruthenium complex dye, has been employed (Mori and Yanagida, 2006).

The desirable characteristics of dyes to be used in DSSC cells are listed below:

- Should have a broad absorption spectrum, preferably extending to the IR region.
- Should strongly adhere to the surface of the semiconductor layer.
- Energy levels should be compatible with both the conductivity band of the semiconductor and the redox couple.

- Should be easily synthesized on a large scale and have a well-understood synthesis pathway.
- Should have the possibility of recyclability and low toxicity.
- Should exhibit high stability under light.
- Should not cause agglomeration on the semiconductor surface.
- Should be electrochemically stable.
- Should be resistant to light and heat (Boz, 2015).

Redox couple

In DSSC, the redox couple is the component that undertakes the task of gap transport in the current generation process. The vacancies created by the electrons leaving the excited dye are filled by the oxidation of the redox couple and electron circulation is ensured. Many types of electrolytes have been developed for the electrolyte. In DSSCs, iodide/triiodide (I^-/ $I3^-$) liquid redox couple is generally used. Liquid electrolytes have a sealing problem. Solid electrolytes have been developed as a solution to this problem. However, it was emphasized that solid electrolyte is not suitable due to its low electron mobility (Giray, 2010).

The redox couple, an important component for Sensitized Solar Cells (DSSCs), is a system in which electrochemical reactions take place. The redox couple provides the interaction between the semiconductor material in the working electrode and the electrolyte.

The redox couple consists of two components that facilitate electron transfer between oxidation and reduction reactions. The most commonly used redox couple in DSSCs is a platinum (Pt) electrode and an iodide/iodine (I-/I2) pair, often used as a metal-ion pair to carry out the electrochemical reaction.

The redox couple facilitates the transition of electrons excited by sunlight from the semiconductor material (usually titanium dioxide - TiO_2) to the electrolyte (usually an iodine-based electrolyte solution). Electrons excited by sunlight are captured by the sensitizing dye on the surface of the semiconductor material and then transferred to the electrolyte solution.

Meanwhile, the Pt electrode in the redox couple undergoes oxidation reaction while transferring electrons to the electrolyte solution. At the same time, the I-/I2 pair also undergoes a reduction reaction and receives electrons back.

As a result of these electrochemical reactions, electrons circulate through the electrolyte solution and flow into the external circuit, resulting in an electric current. The electric current carries out the energy conversion of the DSSC and usable electrical energy is obtained.

The redox couple has a significant impact on the efficiency of the DSSC. The electron transfer rate depends on the structure and properties of the redox couple. An efficient redox couple ensures a faster and more efficient electron transfer and therefore improves the performance of the DSSC.

The redox couple can also be optimized by chemical reactions between ions in the electrolyte solution. Factors such as the concentration of ions, pH value, redox potential can affect the performance of the redox couple. For example, proper control of the iodine concentration and pH value in the electrolyte solution can improve the efficiency of the redox couple.

Also of great importance is the choice of materials used as the redox couple. The platinum (Pt) electrode should have high conductivity and catalytic activity. It is also important that the redox reaction between iodine (I2) and iodide (I-) is fast and reversible.

Optimizing the redox couple can improve the efficiency and stability of DSSCs. Higher electron transfer rate and efficiency leads to higher electric current generation and higher energy conversion efficiency. In addition, the stability of the redox couple helps to maintain the performance of the DSSC during its long-term use.

As a result, the redox couple plays a critical role in the working principle of the DSSC. It ensures that electron transfer is fast, efficient and reversible, increasing efficiency in the process of converting solar energy into electrical energy. Structuring and optimizing the redox couple helps DSSCs achieve higher performance and stability.

Opposite electrode

The counter electrode consists of a conductive layer coated on a glass or plastic surface. The task of the counter electrodes is to allow photoelectrons to complete the circuit cycle during the current flow in the cell and to reintroduce low-level electrons back into the system. The dye molecule, which is oxidized by giving up an electron, allows the triiodide to be reduced by taking an electron. After the reduction of the triiodide, iodide is formed, which is used for the dye molecule to take electrons again. For an ideal cell, the reaction at the working electrode (anode) should be slow and the reaction at the counter electrode (cathode) should be fast (Giray, 2010). In DSSCs, stable and noble conductors such as Pt, Au or carbon are generally

used as counter electrodes. Due to its high light reflectivity, platinum is frequently used as a counter electrode in DSSCs.

Duyarlaştırılmış Güneş Hücreleri (DSSCs) için karşıt elektrot, çalışma elektroduyla birlikte güneş enerjisini elektrik enerjisine dönüştürmek için kullanılan bir bileşendir. Karşıt elektrot, elektron akışının tamamlanmasını sağlar ve elektrokimyasal reaksiyonlarda rol oynar.

Karşıt elektrot, genellikle platinyum (Pt) veya karbon gibi yüksek iletkenliğe sahip malzemelerden yapılmış bir elektrodun kullanılmasıyla oluşturulur. Bu elektrot, çalışma elektrodundaki elektron akışını kabul eder ve dış devreye ileterek elektrik akımının tamamlanmasını sağlar.

Karşıt elektrotun görevi, elektronları toplamak ve elektronik devre üzerinden akışını sağlamaktır. Bu akım, DSSC'nin elektrik enerjisine dönüşüm sürecini tamamlar ve kullanılabilir elektrik enerjisi elde edilir.

Karşıt elektrotun seçimi, DSSC'nin performansını etkileyebilir. İyi bir iletkenlik, katalitik aktivite ve kimyasal stabiliteye sahip malzemeler tercih edilir. Platinyum elektrotlar, yüksek iletkenlik ve katalitik aktiviteye sahip olmaları nedeniyle yaygın olarak kullanılan bir seçenektir.

Karşıt elektrot aynı zamanda DSSC'nin kararlılığı için de önemlidir. Elektrokimyasal reaksiyonlar sırasında elektrotta herhangi bir değişiklik veya bozulma olmamalıdır. Malzemenin kimyasal ve fiziksel stabilitesi, DSSC'nin uzun süreli kullanımı ve dayanıklılığı için önemlidir.

Karşıt elektrot, DSSC'nin çalışma prensibinde kritik bir bileşen olarak işlev görür. Elektron akışının tamamlanması ve elektrik akımının sağlanması için önemlidir. Karşıt elektrotun uygun malzeme seçimi ve yapılandırılması, DSSC'nin performansını artırabilir ve uzun ömürlü, kararlı bir enerji dönüşüm sistemi sağlayabilir.

Bu şekilde, karşıt elektrot, DSSC teknolojisinin gelişimi ve güneş enerjisinin etkin şekilde kullanılması için önemli bir bileşen olarak karşımıza çıkmaktadır.

Metal Doping

The working electrode produced by various methods in DSSCs is an important factor to improve cell efficiency. The semiconductors used to form the working electrode must have a very good ability to conduct electricity well. One of the most widely used methods to improve the ability of semiconductors to conduct electricity is metal doping of the semiconductor. As mentioned in TiO_2 with its wide band gap is the most preferred semiconductor in DSSCs. Alkaline earth metals (Li, Ca and Ba),

transition metals (Co, Cr, Fe, Cu, Nb and Ru), lanthanide and rare earth metals (Eu, La, Nd and Pr) can be doped to improve the conductivity of TiO_2 (Iwasaki et al., 2000; Rodrriguez et al., 1997).

Metal doping is a method used in Dye-Sensitized Solar Cells (DSSCs) to enhance the performance of the semiconductor material and improve the efficiency of the solar cell. Metal doping involves introducing small amounts of metal into the semiconductor material to modify its electronic and optical properties.

Metal doping is commonly performed on titanium dioxide (TiO_2), which is widely used as the semiconductor material in DSSCs. The addition of metal doping enhances the electron mobility of the semiconductor and enables more efficient absorption of sunlight.

One of the advantages of metal doping is that it allows for the manipulation of the electronic structure of the semiconductor material. By introducing metal atoms into the semiconductor, the electronic band structure of the material is altered. This enables electrons to move more freely and rapidly, thereby increasing electron mobility.

Furthermore, metal doping can improve the optical properties of semiconductor materials. The doping process can modify the absorption and reflection spectra of the semiconductor, enabling effective absorption over a wider range of the light spectrum. This allows DSSCs to harness sunlight more efficiently and achieve higher overall efficiency.

Metal doping involves the use of different metal dopants to enhance the performance of DSSCs. Metals such as niobium (Nb), selenium (Se), copper (Cu), and iron (Fe) are commonly employed as doping agents to improve the properties of the semiconductor material. The amount and method of metal doping are critical factors that determine the characteristics of the semiconductor material and the performance of the DSSC.

In conclusion, metal doping is a strategy used to enhance the efficiency and performance of DSSCs. By introducing metal dopants into the semiconductor material, electron mobility and optical properties can be improved. Metal doping represents an important research area in the development of DSSC technology and the effective utilization of solar energy.

CONCLUSION

In this chapter, we summarize the information presented on Sensitized Solar Cells (DSSCs). We have covered various important topics ranging from the working principle of DSSCs to the cell structure, materials, redox

couple and metal doping. This information will help to understand the working mechanism and components of DSSC technology.

DSSCs are photoelectrochemical devices that convert solar energy into electrical energy. The principle of operation is realized through interactions between the basic components of the cell structure: working electrode, semiconductor material, sensitizing dye, redox couple and counter electrode. DSSCs perform an electrochemical reaction, usually with an inorganic electrolyte solution.

The cell structure consists of basic components such as working electrode, semiconductor material, sensitizing dye, redox couple and counter electrode. The working electrode is designed to capture sunlight and is made of semiconductor material. The semiconductor material is usually titanium dioxide (TiO2) based and is ideal for light absorption and electron transport. The sensitizing dye excites electrons by absorbing sunlight and binds to its surface on the semiconductor material. The redox couple performs the electrochemical reaction, allowing electrons to circulate. The counter electrode allows the electrons to return back to the cell.

Metal doping is a method used to improve the performance of DSSCs. Metal doping can improve the cell's electron transport efficiency and photochemical reaction rate. For example, platinum (Pt) doping can improve efficiency by increasing the electrochemical reaction rate.

In conclusion, Sensitized Solar Cells (DSSCs) are photoelectrochemical devices that convert solar energy into electrical energy. In this chapter, detailed information about the working principle, cell structure and components of DSSCs is given. It also explains how metal doping can improve the performance of DSSCs.

REFERENCES

Akar, V. (2016). Elektrokimyasal Depolama Yöntemi İle Boyar Maddeli Güneş Pili Üretimi [Production of Dye-Sensitized Solar Cells with Electrochemical Storage Method]. Süleyman Demirel Üniversitesi, Fen Bilimleri Enstitüsü, Yüksek Lisans Tezi, 85s, Isparta.

Akar, V., 2016. Elektrokimyasal Depolama Yöntemi İle Boyar Maddeli Güneş Pili Üretimi. Süleyman Demirel Üniversitesi, Fen Bilimleri Enstitüsü, Yüksek Lisans Tezi, 85s, Isparta.

Arunachalam, A., Dhanapandian, S., Manoharan, C., & Sivakumar, G. (2015). Physical properties of Zn doped TiO_2 thin films with spray pyrolysis technique and its effects in antibacterial activity. Spectrochimica Acta Part A: Molecular and Biomolecular Spectroscopy, 138, 105-112.

Boz, M. (2015). Katkılandırılmış TiO_2 İnce Filmlerin Üretilmesi, Karakterizasyonu ve Boya Katkılı Güneş Pili Aygıtlarının Geliştirilmesi [Production, Characterization, and Development of Dye-Sensitized Solar Cell Devices with Doped TiO_2 Thin Films]. Ege Üniversitesi, Fen Bilimleri Enstitüsü, Yüksek Lisans Tezi, 56s, İzmir.

Dhanapandian, S., Arunachalam, A., & Manoharan, C. (2016). Highly oriented and physical properties of sprayed anatase Sn-doped TiO_2 thin films with an enhanced antibacterial activity. Applied Nanoscience, 6, 387-397.

Giray, H. B. (2010). The Effects of Platinum Particle Size to the Efficiency of a Dye Sensitized Solar Cell (Dssc). [Doctoral dissertation, Orta Doğu Teknik Üniversitesi, Fen Bilimleri Enstitüsü]. Ankara.

Gong, J., Sumathy, K., Qiao, Q., & Zhou, Z. (2017). Review on Dye-sensitized Solar Cells (DSSCs): Advanced Techniques and Research Trends. Renewable and Sustainable Energy Reviews, 68, 234-246.

Hagfeldt, A., Boschloo, G., Sun, L., Kloo, L., & Pettersson, H. (2010). Dye-sensitized Solar Cells. Chemical Reviews, 110(11), 6595-6663.

Iwasaki, M., Hara, M., Kawada, H., Tada, H., & Ito, S. (2000). Cobalt ion-doped TiO_2 photocatalyst response to visible light. Journal of Colloid and Interface Science, 224(1), 202-204.

Kabadayı, K. (2011). Esnek Yüzeyde Boya İle Duyarlaştırılmış Fotovoltaik Hücre Üretimi Ve Performans İncelenmesi [Production and Performance Analysis of Dye-Sensitized Photovoltaic Cells on Flexible Substrates]. Ege Üniversitesi, Fen Bilimleri Enstitüsü, Yüksek Lisans Tezi, 96s, İzmir.

Liu, W., Wang, H. G., Wang, X., Zhang, M., & Guo, M. (2016). Titanium mesh supported TiO_2 nanowire arrays/Nb-doped TiO_2 nanoparticles for fully flexible dye-sensitized solar cells with improved photovoltaic properties. Journal of Materials Chemistry C, 4(47), 11118-11128.

Mori, S., & Yanagida, S. (2006). TiO_2-Based Dye-Sensitized Solar Cell. In T. Soga (Ed.), Nanostructured Materials for Solar Energy Conversion (pp. -). Elsevier, Amsterdam.

O'Regan, B., & Grätzel, M. (1991). A Low-cost, High-efficiency Solar Cell Based on Dye-sensitized Colloidal TiO_2 Films. Nature, 353(6346), 737-740.

Öztürk, H. H., & Kaya, D. (2013). Güneş Enerjisinden Elektrik Üretimi: Fotovoltaik Teknoloji [Electricity Generation from Solar Energy: Photovoltaic Technology]. Umuttepe Yayınları, 417s, Kocaeli.

Ranabhat, K., Patrikeev, L., Antal'evna-Revina, A., Andrianov, K., Lapshinsky, V., & Sofronova, E. (2016). An Introduction to Solar Cell Technology. Journal of Applied Engineering Science, 14(4), 481-491.

Rodriguez-Talavera, R., Vargas, S., Arroyo-Murillo, R., Montiel-Campos, R., & Haro-Poniatowski, E. (1997). Modification of the phase transition temperatures in titania doped with various cations. Journal of Materials Research, 12(2), 439-443.

Sarker, S. (2017). Dye-sensitized solar cells (DSSCs). Retrieved November 22, 2018, from https://www.jvanalysis.com/about

Serway, R. A., & Beichner R. J. (2005). Çev. Ed. Çolakoğlu, K. [Translation Ed. Çolakoğlu, K.]. Palme Yayıncılık, 392s, Ankara.

Shakir, S., Khan, Z. S., Ali, A., Akbar, N., & Musthaq, W. (2015). Development of copper doped titania based photoanode and its performance for dye sensitized solar cell applications. Journal of Alloys and Compounds, 652, 331-340.

Su, H., Huang, Y. T., Chang, Y. H., Zhai, P., Hau, N. Y., Cheung, P. C. H., ... & Feng, S. P. (2015). The synthesis of Nb-doped TiO_2 nanoparticles for improved-performance dye sensitized solar cells. Electrochimica Acta, 182, 230-237.

Tatar, D. (2015). Spray Pyrolysis Yöntemi ile Farklı Altlık Sıcaklığında Elde Edilen SnO_2 ve SnO_2:F İnce Filmlerin Bazı Fiziksel Özelliklerine, Altlık Sıcaklığının Etkisinin Araştırılması [Investigation of the Effect of Substrate Temperature on Some Physical Properties of SnO_2 and SnO_2:F Thin Films Obtained by Spray Pyrolysis Method]. Atatürk Üniversitesi, Fen Bilimleri Enstitüsü, Doktora Tezi, 154s, Erzurum.

Yang, M., Ding, B., & Lee, J. K. (2014). Surface electrochemical properties of niobium-doped titanium dioxide nanorods and their effect on carrier collection efficiency of dye sensitized solar cells. Journal of Power Sources, 245, 301-307.

Zafer, C. (2006). Organik Boya Esaslı Nanokristal Yapılı İnce Film Güneş Pili Üretimi [Production of Organic Dye-Based Nanocrystalline Thin Film Solar Cells]. Ege Üniversitesi, Fen Bilimleri Enstitüsü, Doktora Tezi, 132s, İzmir.

Chaphter 7

Dual Active Bridge DC/DC Converter

Samet Yalçın[1]

INTRODUCTION

Renewable energy such as solar energy (Sancar & Yakut, 2023) (Sancar & Bayram, 2023) and electric vehicle technologies such as battery management system (Krismer & Kolar, 2009) have been widely studied. the intersection points of these topics are usually converters that can transmit bidirectional energy. the structure of the DAB (Dual Active Bridge DC/DC Converter) circuit, one of these converters, is described in this section.

DAB DC/DC converter consists of eight power switch elements, one transformer, two DC bus capacitors at the input and output of the circuit and one inductor to be used when the transformer leakage inductance is not sufficient. DAB converters, which have high power transmission capability due to its double full bridge feature, can also perform bidirectional power transmission since it has a symmetrical structure. The $L_{leakage}$ value plays an important role in the soft switching of the DAB circuit shown in Figure 1 in power transmission (Zengin S. , 2019) (Kenny, 2015).

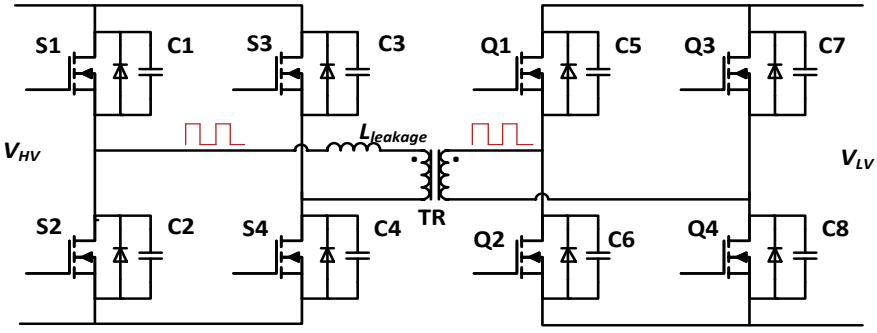

Figure 1. DAB DC/DC Converter

1 Isparta University of Applied Sciences, Faculty of Technology, Department of Electrical and Electronics Engineering, Isparta, Türkiye, ORCID: 0000-0002-1097-981X
E-mail: sametyalcin@isparta.edu.tr

When the literature is analysed in terms of efficiency, it is seen that DAB circuits have an important place in high power DA/DA converter circuits. (Texas Instruments, 2019) (Kumar, H.Bhat, & Agarwal, 2017) (Fei, Feng, PuQi, & Xuhui, 2018) (Gorji, Sahebi, Ektesabi, & Rad, 2019). The benefits of the DAB converter compared to conventional converters are in the literature:

- Galvanic isolation,

- Wide soft switching band,

- Modular structure,

- High power density (Texas Instruments 2019),

- Providing bidirectional energy transmission (Bai and Mi 2008),

- High power density (Harrye, et al. 2014),

- Switching losses can be reduced and

- The success of the balance between EMI and productivity (Hoang and Wang 2012).

In addition to its advantages, the DAB inverter topology has a complex structure at the control point since it has an eight-switch structure (Hoang and Wang 2012). The DAB converter has phase-shifted control methods according to the switching order of the power switches. Mathematical modelling of these methods is important to reduce the efficiency, noise, power density and control complexity of the circuit.

MATHEMATICAL ANALYSIS OF DAB CONVERTER

The power transferred through the leakage inductance in DAB converter is the same as the power transferred through an inductance between two voltage sources with phase difference between them as shown in Figure 2. The direction and intensity of the power depends on the intensity of the voltage sources and the phase difference between them as in Equation (1).

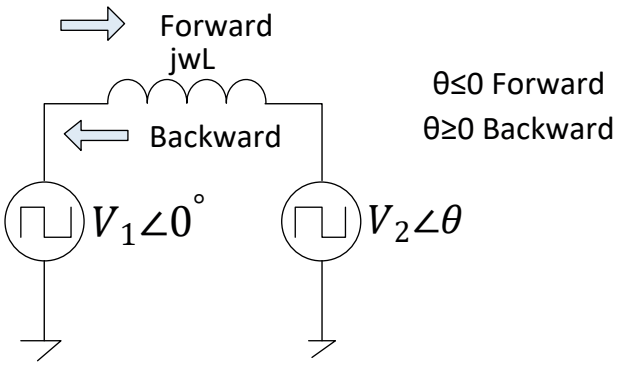

Figure 2. Power Transfer Between Voltage Sources

$$P_o = \frac{V_1 V_2 \sin\varphi}{\omega L} \quad (1)$$

Here P_o is the transferred or in other words the output power. V_1 is the voltage of the DC voltage source on the high voltage side and V_2 is the voltage of the DC voltage source on the low voltage side. φ is the phase difference between V_1 and V_2, ω is the radial switching frequency and L is the total leakage inductance. It should be noted that the total leakage inductance is the sum of the transformer leakage inductance and the inductance connected in series with the transformer (Zhang, et al. 2019).

Power transfer is carried out in the DAB circuit by square waves generated by full-bridge MOSFETs in the high voltage and low voltage sections. If the phase difference between the square waves is increased, the direction and intensity of the transferred power are also controlled (Yıldız 2019), similar to the phase difference shown in Equation (1) (Texas Instruments 2019).

For soft switching applications, the voltage cycling ratio (d) should be considered in the DAB circuit. The voltage conversion ratio d defines the voltage ratios on both sides of the leakage inductance as given in Equation (2). Although the conditions of the voltage conversion ratio and phase shift ratio for soft switching are specified in the literature, it is accepted in many publications that the DAB circuit operates under soft switching conditions regardless of the value of the phase shift ratio if the voltage conversion ratio is equal to one (S. Zengin 2019) (A. Kızıcı 2019) (Texas Instruments 2019) (Huang, et al. 2016) (Zhang, et al. 2019).

$$d = \frac{V_{HV}}{N_{ps} \times V_{LV}} \tag{2}$$

In this equation, d is the voltage conversion ratio, V_{HV} is the DC voltage on the high voltage side of the first full bridge, V_{LV} is the DC voltage on the low voltage side of the second full bridge, N_{ps} is the ratio of the primary winding to the secondary winding of the transformer.

In addition, there are two conditions for the soft switching capability to occur in the DAB circuit when the voltage conversion ratio is not equal to one. These conditions can be explained as given in Equations (3) and (4).

$$D_3 > \frac{1}{2}(1 - d) \tag{3}$$

$$D_3 > \frac{1}{2}\left(1 - \frac{1}{d}\right) \tag{4}$$

In these equations, D_3 is the phase shift interval between two full bridges and d is the voltage conversion ratio. If the parameters of the DAB circuit can fulfil Equation (3), the high voltage section of the circuit structure given in Figure 1 is capable of soft switching. Likewise, if the parameters of the circuit can fulfil Equation (4), the low voltage section is also capable of soft switching (Texas Instruments 2019) (S. Zengin 2019). However, it should be noted that even if the DAB circuit operates under soft switching conditions, the total loss may not be minimal (Oggier, Garcia, and Oliva 2009).

There are several critical factors in the power transmission stages of the DAB converter. The important factors are the value of the leakage inductor, the phase shift method, the phase shift ratio, the value of the output capacities, the switching elements and the switching frequency. Almost all of these design parameters are interrelated. For example, the variation of the leakage inductance amount will change the power transfer value, and the variation of the switching frequency will affect the power transfer as it will change the switching speed, inductor and capacitor impedance.

Since some of the factors mentioned in the above paragraph cannot be changed for the designed DAB circuit, the most important way to control the direction and magnitude of the transmitted power in the following stages is to change the phase differences between the square waves generated by the switching elements. This change is known as phase shifting and, depending

on the method chosen, it can significantly change the amount of power, efficiency, soft switching region and EMI level.

PHASE SHIFT MODULATION METHODS

DAB converters are capable of soft switching and high power density operation (Doncker, Divan and Kheraluwala 1991) without the need for any extra circuit components (Kheraluwala, et al. 1992). Phase shifting methods have been developed to realize soft switching under varying load conditions (R.T.Naayagi, A.J.Forsyth and R.Shuttleworth 2011). The phase shift methods in the literature are divided into four as Single Phase Shift (SPS), Extended Phase Shift (EPS), Dual Phase Shift (DPS) and Triple Phase Shift (TPS).

The phase shift modulation methods depend on phase shift ratios. These ratios are three. The first phase shift ratio is *D3* outer phase shift ratio that is between *S1* and *Q1* switches in Figure 1. The second phase shift ratio is *D1* high voltage side inner phase shift ratio that is between *S1* and *S3* switches in Figure 1. The last phase shift ratio is *D2* low voltage inner phase shift ratio that is between Q1 and Q3 switches in Figure 1.

Waveforms of phase shift methods are shown in Figure 3. In this figure, the x-axes in the graphs are time. The voltages on the y-axes are the gate voltages of the switches in Figure 1. *Vh1* and *Vh2* are the voltages at the high and low voltage ends of the leakage inductance in Figure 1, respectively. As can be seen by looking at these waveforms, for the SPS method, *D1* and *D2* should be zero while *D3* should be at a value other than zero. For the EPS method, only *D2* should be zero, *D1* and *D3* should be different from zero. In the DPS method, all phase shift ratios are required to be different from zero, but *D1* and *D2* must be equal to each other. In the TPS method, all three phase shift ratios are expected to be different from zero and from each other (Zhao, Song, et al. 2014) (Harrye, et al. 2014) (Huang, et al. 2016).

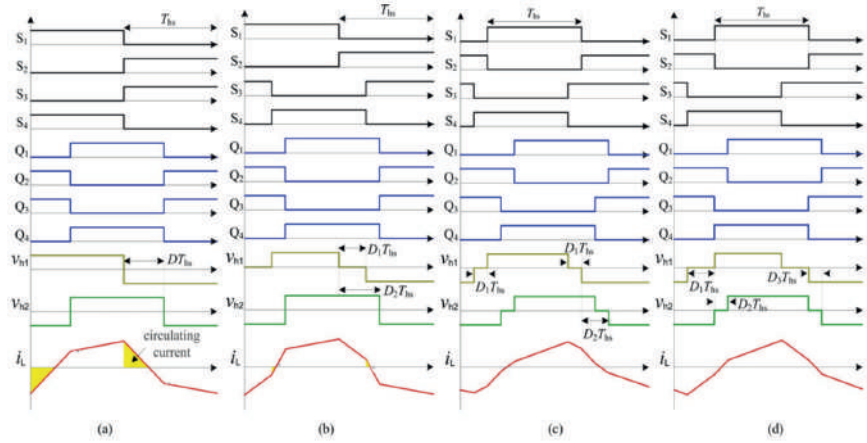

Figure 3. DAB Phase Shifting Methods (a) SPS method, (b) EPS method, (c) DPS method and (d) TPS method (Zhao, Song, et al. 2014)

In DAB converter, the power transmission direction depends on the parameter *Df* whose equation is given in Equation (6). If *Df* is greater than zero, the power transmission direction is to the right, and if it is less than zero, the power transmission direction is to the left (Huang, et al. 2016). It should be noted that since *D1* and *D2* are equal to each other in SPS and DPS conditions, the power transmission direction depends on whether *D3* is positive or negative. However, if the circuit operates in one of the EPS or TPS conditions, the *Df* value must be known in order to determine the power transmission direction.

$$D_f = D_3 + \frac{D_2}{2} - \frac{D_1}{2} \tag{6}$$

The TPS method also includes other three phase shift methods. These methods work as a mode of TPS. The conditions given in the modes also include the conditions of the other phase shift methods.

In the SPS method, the internal phase shift ratios are zero ($D_1 = D_2 = 0$). This means that the occupancy rate of H bridges is 1 ($k_1 = k_2 = 1$). In addition, in the SPS method, the external phase shift ratio can vary between 0 and 1. This condition is also expressed as $0 \leq k_3 \leq 1$. Since these conditions are the conditions in Mode 6, the operating conditions and mathematical expressions of the SPS method can also be explained with the conditions and mathematical expressions of Mode 6.

In the EPS method, one H bridge will produce a square wave while the other will produce a three-stage wave as AC output. Thus, we should look at the conditions of the EPS method by dividing them into four.

- The EPS method with conditions $k_1 = 1$, $k_2 \geq 1$, $(1 - k_2) \leq k_3 \leq 1$ is in Mode 6,
- In EPS Mode 6 with conditions $k_2 = 1$, $k_1 \geq 1$, $0 \leq k_3 \leq k_1$,
- EPS Mode 1 with conditions $k_1 = 1$, $k_2 \leq 0$, $0 \leq k_3 \leq 1 - k_2$ and
- The EPS with conditions $k_2 = 1$, $k_1 \leq 0$, $k_1 \leq k_3 \leq 1$ operates in Mode 2.

The DPS method is conditioned as $k_1 = k_2 < 1$. When analysed depending on this condition

- $k_1 \geq 0.5$, $(1 - k_1) \leq k_3 \leq k_1$ in DPS Mode 6,
- DPS operates in Mode 3 for $k_1 \leq 0.5$, $k_1 \leq k_3 \leq (1 - k_1)$ conditions.

Two separate MATLAB codes were written about the TPS method of the DAB converters. With these codes, it is possible to calculate how much leakage inductance should be used when the circuit is to be operated at specified phase shift ratios or how much external phase shift ratio should be used for a circuit whose leakage inductance and internal phase shift ratios are determined.

CURRENT MODULATION IN DUAL ACTIVE BRIDGE CONVERTER

In DAB circuits, a current flow through the leakage inductance with square wave and multilevel waves generated at the AC outputs of H bridges. This current can be in triangular, trapezoidal or multifractal shapes proportional to the differences of the voltages on both sides of the inductance. At this point in phase shifting methods, when the alternation of the current on the inductor changes, hard switching of the switching elements may occur (Oggier, Leidhold, et al. 2006), which is undesirable (Oggier, Garcia, and Oliva 2009). In addition, the phase-shifted DAB circuit operates under Continous Condution Mode (CCM). CCM mode, whose sample waveform is shown in Figure 4, causes power losses along with circulating currents in the DAB circuit. DCM (Discontinous Conduction Mode) is used to eliminate these losses (Zengin, Deveci and Boztepe 2013) (Rehman, Hassan and Zaffar 2013). The voltage V1 given in Figure 4 is the voltage on the

high voltage side of the leakage inductance given in Figure 1, the voltage *V2* is the voltage on the low voltage side of the leakage inductance given in Figure 1, the voltage *Vlk* is the voltage across the leakage inductance given in Figure 1, and the current Ilk is the current across the leakage inductance given in Figure 1.

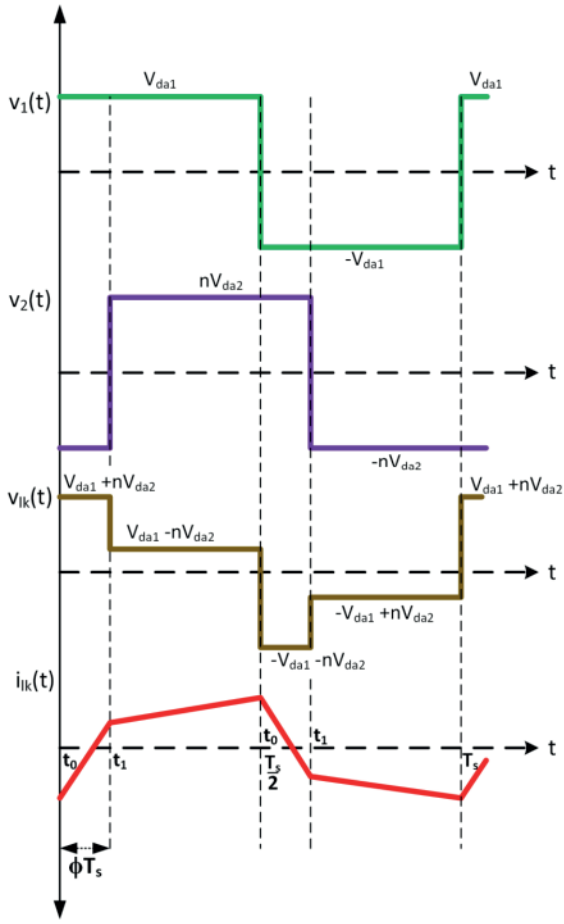

Figure 4. DCM in TPS method (Zengin S. , 2019)

DAB circuits can operate under DCM with triangular current modulation as shown in Figure 5 or trapezoidal current modulation as shown in Figure 6 (Wang, Haan and Ferreira 2009). The trapezoidal modulation technique of these two techniques is known to be more efficient at high loads (Zengin and Boztepe 2014).

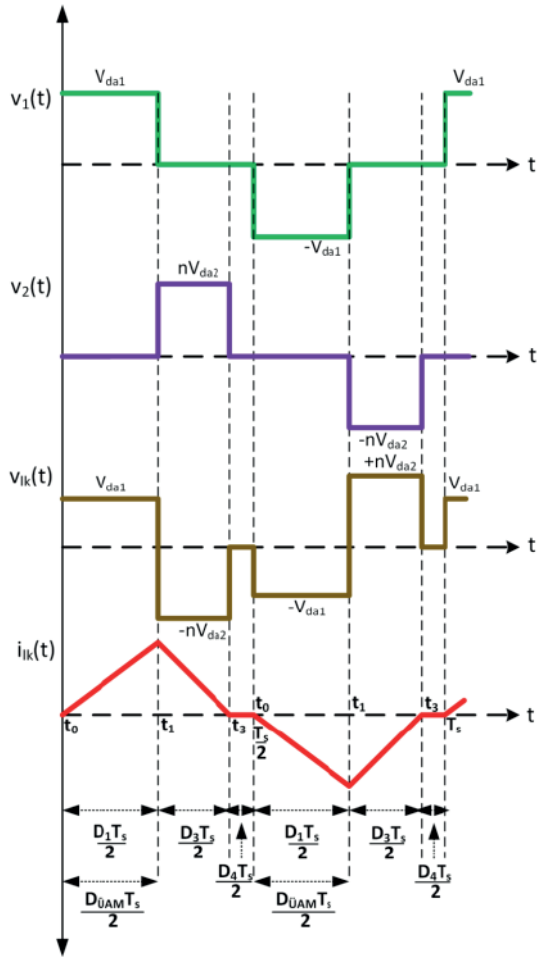

Figure 5. Discrete Current Mode Triangular Current Modulation in TPS Method

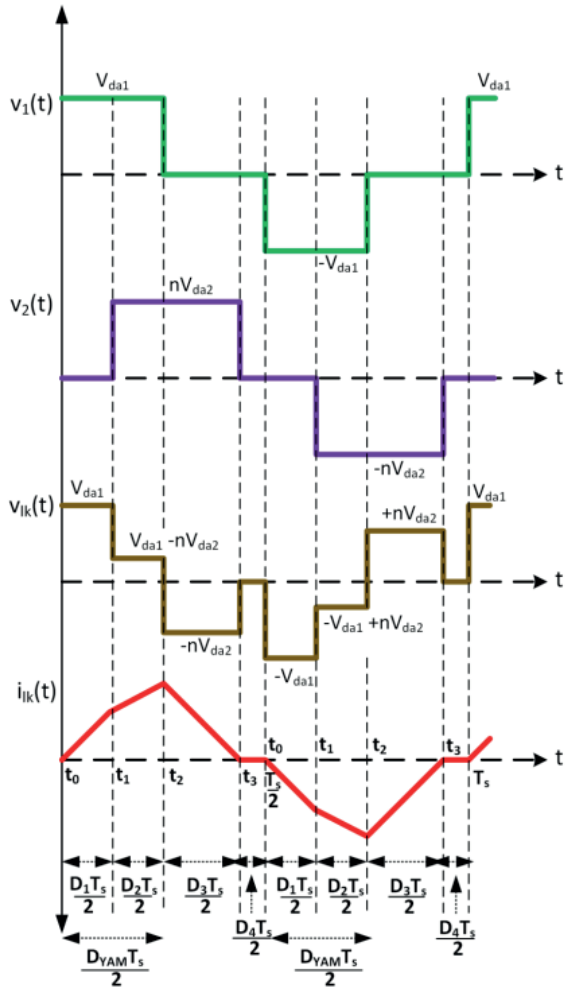

Figure 6. Discrete current mode trapezoidal current modulation in TPS method

When DCM is analyzed in the TPS method, it is found through MATLAB codes that the inductor current can be reduced to zero in 11 conditions with Mode 6 and in 18 different conditions with Mode 5.

CONCLUSION

The Dual Active Bridge (DAB) DC-DC converter offers a highly efficient and versatile solution for power conversion in a variety of applications. With the ability to handle high power levels and wide voltage ranges, the DAB converter offers significant advantages in terms of improved power quality, reduced losses and enhanced controllability.

One of the key features of the DAB converter is the phase shift modulation method, which provides efficient voltage conversion and power transfer between the primary and secondary sides of the converter. By controlling the phase shift angles between the bridge legs, the DAB converter performs smooth switching operation, minimising switching losses and improving overall efficiency. Furthermore, phase shift modulation allows bidirectional power flow, making the DAB converter suitable for applications such as renewable energy systems, electric vehicles and energy storage systems.

In addition, current modulation techniques play a crucial role in optimising the performance of the DAB converter. By using techniques such as phase-shifted carrier-based modulation or phase-shifted pulse width modulation (PWM), the converter can achieve better current sharing between the bridge legs, reduce the load on individual switches and improve converter efficiency. These techniques also enable precise control of output voltage and current waveforms, resulting in stable and accurate power conversion.

Overall, the combination of the Dual Active Bridge (DAB) converter, phase shift modulation methods and current modulation techniques provides a robust and efficient solution for high power DC-DC conversion. With their numerous advantages, these technologies have the potential to revolutionize various industries and pave the way for more sustainable and advanced power systems.

REFERENCES

Bai, H., & Mi, C. (2008). Eliminate Reactive Power and Increase System Efficiency of Isolated Bidirectional Dual-Active-Bridge DC–DC Converters Using Novel Dual-Phase-Shift Control. *IEEE Transactions on Power Electronics, 23*(6), 2905 - 2914.

Costinett, D., Maksimovic, D., & Zane, R. (2013). Design and control for high efficiency in high step-down dual active bridge converters operating at high switching frequency. *IEEE Transaction on Power Electronics*, 3931–3940.

Doncker, R. W., Divan, D. M., & Kheraluwala, M. H. (1991). A three-phase soft-switched high-power-density DC/DC converter for high-power applications. *IEEE Transactions on Industry Applications*, 63-73.

Fei, X., Feng, Z., PuQi, N., & Xuhui, W. (2018). Analyzing ZVS Soft Switching Using Single Phase Shift Control Strategy of Dual Active Bridge Isolated DC-DC Converters. *2018 21st International Conference on Electrical Machines and Systems (ICEMS)*, 2378-2381.

Gorji, S. A., Sahebi, H. G., Ektesabi, M., & Rad, A. B. (2019). Topologies and Control Schemes of Bidirectional DC–DC Power Converters: An Overview. *IEEE Access, 7*(7).

Harrye, Y. A., Ahmed, K., Adam, G., & Aboushady, A. (2014). Comprehensive steady state analysis of bidirectional dual active bridge DC/DC converter using triple phase shift control. *2014 IEEE 23rd International Symposium on Industrial Electronics (ISIE)* (s. 437-442). Istanbul, Turkey: IEEE.

Hoang, K. D., & Wang, J. (2012). Design Optimization of High Frequency Transformer for Dual Active Bridge DC-DC Converter. *2012 XXth International Conference on Electrical Machines* (pp. 2311-2317). Marseille, France: IEEE.

Hua, B., Mi, C. C., & Gargies, S. (2008). The short-time-scale transient processes in high-voltage and high-power isolated bidirectional dc-dc converters. *IEEE Transactions on Power Electronics*, 2648-2656.

Huang, J., Wang, Y., Li, Z., & Lei, W. (2016). Unified Triple-Phase-Shift Control to Minimize Current Stress and Achieve Full Soft-Switching of Isolated Bidirectional DC–DC Converter. *IEEE Transactions on Industrial Electronics, 63*(7), 4169 - 4179.

Huiqing, W., & dong, X. W. (2013). Bidirectional Dual-Active-Bridge DCDC Converter with Triple-Phase-Shift Control. *Applied Power Electronics Conference and Exposition (APEC)*. IEEE.

Inoue, S., & Akagi, H. (2007). A bidirectional dc-dc converter for an energy storage system with galvanic isolation. *IEEE Trans. Power Electronics*, 2299–2306.

Kenny, G. (2015). *Design and Control of a Bidirectional Dual Active Bridge DC-DC Converter to Interface Solar, Battery Storage, and Grid-Tied Inverters.* Fayetteville: University of Arkansas.

Kheraluwala, M. N., Gascoigne, R. W., Divan, D. M., & Baumann, E. D. (1992). Performance characterization of a high-power dual active bridge DC-to-DC converter. *IEEE Transactions on Industry Applications*, 1294-1301.

Kızıcı, A. (2019). *Design and Implementation of A Hıgh Power Density Dual Active Bridge DC/DC Converter With GaN Power Transistors.* Ankara, Turkey: Hacettepe University.

Kızıcı, A. (2019). *Gan Güç Tranzistörüne Dayali Yüksek Güç Yoğunluklu Çift Aktif Köprü DA/DA Çevirgeç Tasarimi Ve Gerçekleştirilmesi.* Ankara, TURKIYE.

Krismer, F., & Kolar, J. (2009). Accurate small-signal model for the digital control of an automotive bidirectional dual active bridge. *IEEE Transactions on Power Electronics*, 2756–2768.

Krismer, F., & Kolar, J. (2012). Closed Form Solution for Minimum Conduction Loss Modulation of DAB Converters. *IEEE Transaction on Power Electronics*, 174-188.

Kuiyuan, W., Silva, C. W., & Dunford, W. G. (2012). Stability analysis of isolated bidirectional dual active full-bridge dc-dc converter with triple phase shift control. *IEEE Transaction on Power Electronics*, 2007-2017.

Kumar, A., Bhat, A. H., & Agarwal, P. (2017). Comparative analysis of dual active bridge isolated DC to DC converter with single phase shift and dual phase shift control techniques. *2017 6th International Conference on Computer Applications In Electrical Engineering-Recent Advances (CERA)*. Roorkee, India.

Kumar, A., H.Bhat, A., & Agarwal, P. (2017). Comparative Analysis Of Dual Active Bridge Isolated Dc To Dc Converter With Single Phase Shift And Extended Phase Shift Control Techniques. *2017 6th International Conference on Computer Applications In Electrical Engineering-Recent Advances (CERA)*. doi:10.1109/CERA.2017.8343363

Muthuraj, S. S., Kanakesh, V. K., Das, P., & Panda, S. K. (2017). Triple Phase Shift Control of an LLL Tank Based Bidirectional Dual Active Bridge Converter. *IEEE Transactions on Power Electronics*, 8035-8053.

Naayagi, R. T., Forsyth, A. J., & RShuttleworth. (2015). Performance analysis of extended phase-shift control of DAB DC-DC converter for aerospace energy storage system. *11th International Conference on Power Electronics* (s. 514-517). Australia: IEEE .

Oggier, G. G., Garcia, G. O., & Oliva, A. R. (2009). Switching control strategy to minimize dual active bridge converter losses. *IEEE Trans. Power Electronics*, 1826–1838.

Oggier, G. G., Garcia, G. O., & Oliva, A. R. (2011). Modulation strategy to operate the dual active bridge dc-dc converter under soft switching in the whole operating range. *IEEE Trans. Power Electronics*, 1228–1236.

Oggier, G. G., Leidhold, R., Garcia, G. O., Oliva, A. R., Balda, J. C., & Barlow, F. (2006). Extending the ZVS operating range of dual active bridge high-power DC-DC converters. *37th IEEE Power Electronics Specialists Conference* (s. 1-7). Jeju, Korea (South): IEEE.

Qin, H., & Kimball, J. W. (2012). Generalized Average Modeling of Dual Active Bridge DC–DC Converter. *IEEE Transactions on Power Electronics*, 2078-2084.

R.T.Naayagi, A.J.Forsyth, & R.Shuttleworth. (2011). Performance Analysis of DAB DC-DC Converter under Zero Voltage Switching. *1st International Conference on Electrical Energy Systems.* IEEE.

Rehman, M. M., Hassan, R., & Zaffar, N. (2013). High efficiency modified dual-active bridge converter for photovoltaic integration. *2013 IEEE Grenoble Conf.* (s. 1-5). IEEE.

Sancar, M. R., & Bayram, A. B. (2023). Modeling and Economic Analysis of Greenhouse Top Solar Power Plant with Pvsyst Software. *International Journal of Engineering and Innovative Research*, 48 - 59.

Sancar, M. R., & Yakut, K. (2023). Comparative Analysis of SAM and PVsyst Simulations for a Rooftop Photovoltaic System. *International Journal of Engineering and Innovative Research*, 60 - 76.

Texas Instruments. (2019). *Bi-Directional, Dual Active Bridge Reference Design for Level 3 Electric Vehicle Charging Stations.* ti.com.

Wang, Y., Haan, S. W., & Ferreira, J. a. (2009). Optimal operating ranges of three modulation methods in dual active bridge converters. *6th International Power Electronics and Motion Control Conference* (s. 1397–1401). IEEE.

Ye, Z., Jain, P., & Sen, P. (2007). Circulating current minimization in high frequency AC power distribution architectures with multiple inverter modules operated in parallel . *IEEE Trans. Ind. Electron*, 2673–2687.

Yıldız, N. (2019). *Makine öğrenimi tabanlı PID optimizasyonu ile çift aktif köprülü doğru akım güç çeviricilerinin denetimi.* Denizli: Pamukkale Üniversitesi.

Zengin, S. (2019). *Silisyum Karbür (Sic) Güç Anahtari Kullanan Tek Aşamali Çift Aktif Köprü Aa-Da Dönüştürücü.* İzmir: Ege Üniversitesi Fen Bilimleri Enstitüsü.

Zengin, S. (2019). *Silisyum Karbür (SiC) Güç Anahtari Kullanan Tek Aşamali Çift Aktif Köprü AA-DA Dönüştürücü.* İzmir: Ege Üniversitesi.

Zengin, S., & Boztepe, M. (2014). Modified Dual Active Bridge Photovoltaic Inverter for Solid State Transformer Applications. *International Symposium on Fundamentals of Electrical Engineering (ISFEE)*, (s. 3-6).

Zengin, S., Deveci, F., & Boztepe, M. (2013). Decoupling Capacitor Selection in DCM Flyback PV Microinverters Considering Harmonic Distortion. *IEEE Transaction on Power Electronics*, 816–825.

Zhang, Z., Sun, J., Wang, P., Cai, Z., Kong, J., Bai, X., & Ma, D. (2019). An Improved DC Bias Elimination Strategy with Extended Phase Shift Control for Dual-Active-Bridge DC-DC. *2019 Chinese Automation Congress*. Hangzhou, China: IEEE.

Zhao, B., Song, Q., & Liu, W. (2012). Power Characterization of Isolated Bidirectional Dual-Active-Bridge DC–DC Converter With Dual-Phase-Shift Control. *IEEE Transactions on Power Electronics, 27*(9), 4172 - 4176.

Zhao, B., Song, Q., Liu, W., & Sun, Y. (2014). Overview of Dual-Active-Bridge Isolated Bidirectional DC-DC Converter for High-Frequency-Link Power-Conversion System. *29*(8).

Zhao, B., Song, Q., Liu, W., & Sun, Y. (2014). Overview of Dual-Active-Bridge Isolated Bidirectional DC-DC Converter for High-Frequency-Link Power-Conversion System. *IEEE TRANSACTIONS ON POWER ELECTRONICS*, 4091 - 4106.

Zhao, B., Yu, Q., & Sun, W. (2012). Extended-Phase-Shift Control of Isolated Bidirectional DC–DC Converter for Power Distribution in Microgrid. *IEEE Transactions on Power Electronics*, 4667-4680.

Chaphter 8

Phase Shift Modulation Methods on Dual Active Bridge Dc/Dc Converter

Samet Yalçın[1]

Tuna Göksu[2]

INTRODUCTION

The phase shift methods in the literature are divided into four as Single Phase Shift (SPS), Extended Phase Shift (EPS), Dual Phase Shift (DPS) and Triple Phase Shift (TPS).

Three different phase phase shift ratios between the DAB converter switching elements are used when constructing the phase shift methods. The first one is the HV internal phase shift ratio between the high voltage full bridge switches (between S_1 and S_3 shown in Figure 1), which will be denoted as D_1 in this thesis. The second one is the LV internal phase shift ratio between the low voltage full bridge switches (between Q_1 and Q_3 shown in Figure 1), denoted as *D2*, and the last one is the external phase shift ratio between the bridges (between *S1* and *Q1* shown in Figure 1), denoted as *D3*. In some references, the phase shift between bridges is given as φ phase shift angle instead of *D3* phase shift ratio (Texas Instruments 2019) (Bai and Mi 2008) (A. Kızıcı 2019) (S. Zengin 2019) (Zhao, Song, et al. 2014). The ratio between the phase shift ratio *D3* and the phase shift angle φ, which is generally used in the literature and also used in this study, is as shown in Equation (1). The first one is the HV internal phase shift ratio between the high voltage full bridge switches (between *S1* and *S3* shown in Figure 1), which will be denoted as *D1* in this thesis. The second one is the LV internal phase shift ratio between the low voltage full bridge

1 Isparta University of Applied Sciences, Faculty of Technology, Department of Electrical and Electronics Engineering, Isparta, Türkiye, ORCID: 0000-0002-1097-981X
E-mail: sametyalcin@isparta.edu.tr

2 Dr. Öğr. Üyesi, Isparta University of Applied Sciences, Faculty of Technology, Department of Electrical and Electronics Engineering, Isparta, Türkiye, ORCID: 0000-0002-2334-1698
E-mail: tunagoksu@isparta.edu.tr

switches (between *Q1* and *Q3* shown in Figure 1), denoted as *D2*, and the last one is the external phase shift ratio between the bridges (between *S1* and *Q1* shown in Figure 1), denoted as *D3*. In some references, the phase shift between bridges is given as φ phase shift angle instead of *D3* phase shift ratio (Texas Instruments 2019) (Bai and Mi 2008) (A. Kızıcı 2019) (S. Zengin 2019) (Zhao, Song, et al. 2014). The ratio between *D3* phase shift ratio and *φ* phase shift angle, which is generally used in the literature and also used in this study, is as shown in Equation (1).

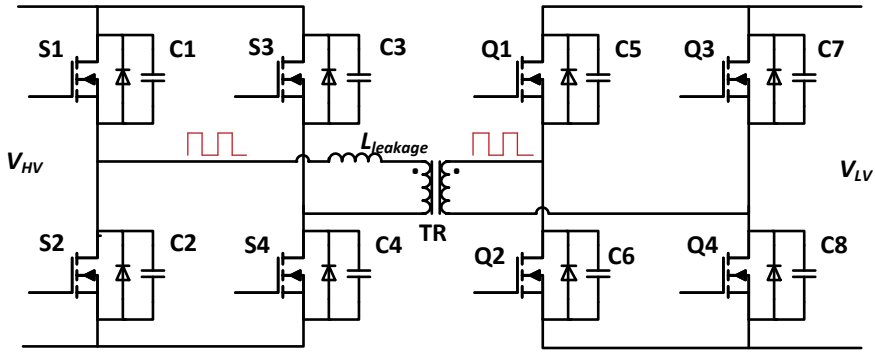

Figure 1. Dual Active Bridge DC/DC Converter

$$D_3 = \frac{\varphi}{\pi} \tag{1}$$

SINGLE PHASE SHIFT METHOD

The SPS method is the first and currently the most widely used phase shifting method (Doncker, Divan and Kheraluwala 1991) (Zhao, Song and Liu 2012) (Inoue and Akagi 2007) (Costinett, Maksimovic and Zane 2013). As can be seen in Figure 3.3(a), no phase shift ratio is applied within the H bridges in the eight switching elements, only the external phase shift ratio between the bridges is controlled ($D_1 = 0, D_2 = 0, D_3 \neq 0$). For this reason, it is much easier to implement than other phase shift methods.

In the SPS method, in both full bridge circuits, the transformer primary and secondary windings are switched to generate square waves with 50% occupancy rate with a phase difference between them. By controlling the phase difference of the voltage square waves to the right and left of the leakage inductance, the current passing through the inductance is controlled.

Thus, the direction and magnitude of the transmitted power can be adjusted (Zhao, Song, et al. 2014).

The basic power transmission equation shown in Equation 2.1 of the power transmission in the DAB circuit is transformed into the equation shown below (Bai and Mi 2008) when the SPS modulation method is used (Kumar, H.Bhat and Agarwal 2017).

$$P_o = \frac{V_{HV} * N * V_{LV}}{2 * f_{sw} * L_{leakage}} D_3(1 - D_3) \tag{2}$$

Where P_o is the output power, V_{HV} is the DC voltage at the high voltage section of the first H bridge of the DAB circuit, N is the ratio of the primary winding to the secondary winding of the transformer, V_{LV} is the DC voltage at the low voltage section of the second H bridge of the DAB circuit, f_{SW} is the switching frequency of the switching elements, $L_{leakage}$ is the leakage inductance value and D_3 is the phase shift ratio between H bridges. As can be seen from the equation, the highest value of the output power - in other words, the power that can be transmitted - will be achieved when D_3 is 0.5. In this way, the equation can be shown as follows (Zhao, Song and Liu 2012) (Harrye, et al. 2014).

$$P_o = \frac{V_{HV} * N * V_{LV}}{8 * f_{sw} * L_{leakage}} \tag{3}$$

SPS control has a great importance in the literature due to its small volume and high dynamic characteristics. In addition, since the full bridges are operated symmetrically without changing the internal phase shifts and the power is controlled only by the phase difference between the bridges, complex mathematical equations are not required. However, the SPS method also has disadvantages that lead to the use of other phase shifting methods.

The SPS method is not suitable for operation under variable load conditions. Since the phase shift ratio for ZVS is limited, ZVS cannot be achieved most of the time at variable loads. Thus, power losses increase. In addition, under conditions where the voltages between the two ends of the transformer do not match, circulating currents occur on the leakage inductance. This increases both the effective (Root Mean Square - RMS) and peak values of the total current (Zhao, Song, et al. 2014). Thus, switching current stresses also increase (Oggier, Leidhold, et al. 2006). In addition, it has been shown in the literature that the reactive power in the circuit increases due to high peak currents in this method (Bai & Mi, 2008). These problems have pushed users to other phase shifting methods.

EXTENDED PHASE SHIFT METHOD

The EPS control method is a typical development of the SPS method. As can be observed in Figure 3.3 (b), in this method, one full bridge circuit is switched simultaneously without phase shift ratio while the other full bridge circuit is switched by waiting for a certain phase shift ratio. Thus, the AC output of one bridge is a two-stage square wave at 50% occupancy rate, while the AC output of the other bridge is a three-stage wave. In the interval where the three-stage wave goes down to zero voltage, the power in the reverse direction also becomes zero. Thus, the circulating current and circulating power are reduced for the transmitted power (Bai and Mi 2008) (Zhao, Song, et al. 2014).

In the literature, the performance of EPS control in terms of transmitted power, current stress, power loss and soft switching has been widely compared with SPS (Oggier, Garcia, and Oliva 2011) (Oggier, Garcia, and Oliva 2009) (Zhao, Song, et al. 2014). Comparisons have shown that the EPS method reduces current stress as well as increasing the ZVS range and increasing efficiency.

Compared to SPS control, EPS control performs an external phase shift ratio (D3) as well as an internal phase shift ratio (D1 or D2) within one of the H bridges. The external phase shift ratio controls the direction and amount of transmitted power, while the internal phase shift ratio reduces the circulating current and expands the ZVS region (Naayagi, Forsyth, and RShuttleworth 2015).

The mathematical equation of the EPS method and its switching sequences are more complex than the SPS method. Although there are studies in the literature that try to explain EPS with shorter equations (Kumar, H.Bhat and Agarwal 2017), the waveforms and mathematical expressions shown in Figure 2 depending on the relationship between the internal phase shift ratio and the external phase shift ratio of the EPS control are as follows (Zhang, et al. 2019) (Qin and Kimball 2012). The voltage *Uab* shown in this figure is the voltage on the high voltage side of the leakage inductance given in Figure 1. The *Ucd* voltage shown in the same figure is the voltage on the low voltage side of the leakage inductance given in Figure 1. The current i_L given in the figure is the current on the leakage inductance given in Figure 1.

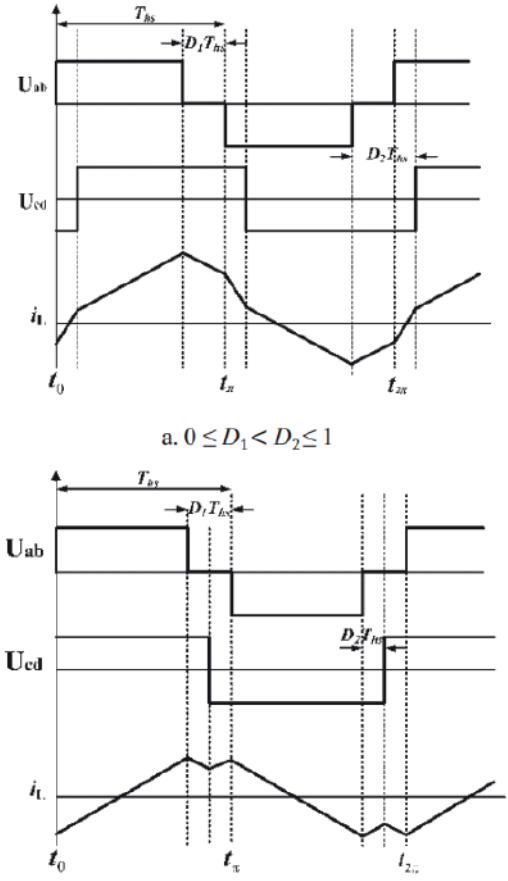

a. $0 \leq D_1 < D_2 \leq 1$

b. $0 \leq D_2 \leq D_1 \leq 1$

Figure 2. EPS waveforms under a) $0 \leq D_1 \leq D_3 \leq 1$, *b)* $0 \leq D_3 \leq D_1 \leq 1$ *conditions (Zhang, et al. 2019)*

$$P = \frac{V_{HV} * N * V_{LV}}{2 * f_{sw} * L_{leakage}} \times \begin{cases} 2D_1D_3 - D_1 - {D_1}^2 - 2{D_3}^2 + 2D_3, & 0 \leq D_1 \leq D_3 \leq 1 \\ {D_1}^2 - D_1 + 2D_3 - 2D_1D_3, & 0 \leq D_3 \leq D_1 \leq 1 \end{cases} \quad (4)$$

There is a point to be noted in these equations and conditions. In studies focusing only on EPS in the literature (Zhang, et al. 2019) (Kumar, Bhat, and Agarwal 2017), Equation 4 is formed by considering the internal phase shift ratio D_1 as the internal phase shift ratio of the H bridge in the direction the power is coming from. However, in EPS control, the ZVS region can be adjusted and the current stress can be reduced by controlling the internal phase shift ratio of the H bridge in the direction of power transmission

(Harrye, et al. 2014). It should also be noted that since the DAB circuit operates bidirectionally, the H-bridge on the receiving side of the power will become the H-bridge in the transmitted direction when the power direction changes. Therefore, it will be necessary to extend this equation expression. This point will be addressed in more detail in Section of TPS by referring to phase shifting modes.

As explained, the EPS method provides lower switching loss and lower current stress than the SPS method. However, there are also some difficulties with the EPS method. First of all, although one of the H bridges works with phase shift ratio, the other one will work symmetrically as in the SPS method, which will give the losses experienced in SPS again. In addition, the conditions and mathematical expressions in EPS control make the circuit more complex. In addition, when the direction of the transmitted power is changed in this phase shift method, the internal phase shifted and non-phase shifted H bridges must be changed. Therefore, it is expected that the control board should be prepared for this asymmetric situation and be able to update itself quickly when the power direction changes. In order to overcome these problems, the DPS method has been developed.

DUAL PHASE SHIFT METHOD

As shown in Figure 3.3 (c), the DPS phase shift method differs from EPS control in that the external phase shift ratio D_3 as well as the internal phase shift ratios are different from zero and equal to each other ($D_1 = D_2 \neq 0$). Therefore, the AC output of both bridges is a three-level waveform.

When the literature is examined, it is known that the DPS method shows advantages over the SPS method as follows:

- Peak currents are reduced,
- Current stress is reduced,
- Instantaneous currents are limited,
- Reactive power is suppressed,
- The efficiency of the system increases,
- The value of the output capacities is reduced (Zhao, Yu and Sun 2012) (Zhao, Song, et al. 2014) (Kumar, H.Bhat and Agarwal 2017),
- Since the reactive power is reduced, the voltage fluctuation is less,
- Zero Current Switching (ZCS) range can be analysed in the DPS control,

- It is more stable in instantaneous changes in load quantity (Bai and Mi 2008)

Compared to EPS, in DPS control, since both H bridges have the same internal phase shift ratios, the processor is not expected to expect any different performance in any voltage or power transmission direction change. Thus, it is understood that DPS control has a simpler implementation and more dynamic performance (Zhao, Song, et al. 2014).

In the literature, there are inverter studies with parallel connection for balancing reactive power and active power (Ye, Jain and Sen 2007). In the DPS method, it is possible to completely suppress the reactive current beyond controlling it. Reducing the peak and circulation values of the current enables the reactive power to be suppressed.

Since the internal phase shift ratios are equal to each other in the DPS control method, both of their values are called D_1 and conditions and mathematical expressions are formed as follows (Bai and Mi 2008).

$$D_1 \leq \frac{1}{2} \rightarrow P = \frac{V_{HV} * N * V_{LV}}{2 * f_{sw} * L_{leakage}} \times \begin{cases} D_3(2 - 2D_1 - D_3), & 0 \leq D_3 \leq D_1 \\ D_3(1 - D_1 - D_3) + D_1 - {D_1}^2, & D_1 \leq D_3 \leq 1 - D_1 \\ (1 - D_1)(1 - D_3,), & 1 - D_1 \leq D_2 \leq 1 \end{cases} \quad (5)$$

$$D_1 > \frac{1}{2} \rightarrow P = \frac{V_{HV} * N * V_{LV}}{2 * f_{sw} * L_{leakage}} \times \begin{cases} D_3(2 - 2D_1 - D_3), & 0 \leq D_3 \leq 1 - D_1 \\ (1 - D_1)^2, & 1 - D_1 \leq D_3 \leq D_1 \\ (1 - D_1)(1 - D_3,), & D_1 \leq D_3 \leq 1 \end{cases} \quad (6)$$

In a study by Bai in 2008 (Bai and Mi 2008), it was reported that the DPS method can give 4/3 times more output power than the SPS method. However, in a paper published by Zhao in 2012 (Zhao, Yu and Sun 2012), it was shown that this information is purely theoretical and erroneous. Because, regardless of the phase shift method, the maximum output power value that the DAB circuit can give is constant. In addition, Zhao also showed the DPS conditions and mathematical expressions in his study, but it was seen that the formulas in Bai's study cover these expressions. All switching types and the mode of operation of the DPS method are explained in more detail in Section of TPS.

TRIPLE PHASE SHIFT METHOD

As shown in Figure 1.3 (d), the TPS method is realised by using all three phase shift ratios different from each other ($D_1 \neq D_2 \neq D_3 \neq 0$). For the TPS phase-shifting method, studies have been carried out in the literature mainly on the improvement of ZVS and current stresses (Kuiyuan, Silva, and Dunford 2012) (Krismer and Kolar 2012) (Zhao, Song, et al. 2014).

In fact, TPS was proposed after the other phase-shifting methods. Considering its structure, SPS can be used with only one phase shift control, EPS and DPS can be used with two phase shift controls, while TPS requires three phase shift controls to control the transmitted power. Therefore, the TPS method is the most complex method. However, it should be noted that other methods are special cases of the TPS method. Therefore, if the conditions and mathematical equations of the TPS method are known, other phase shift methods can be easily expressed with these equations. For this reason, ZVS, ZCS, current stress and reactive power issues cover all the features of other methods and the soft switching region is wider than others.

The TPS method was first introduced in Kuiyuan's study in 2012 (Kuiyuan, Silva, & Dunford, 2012). Huiqing (Huiqing & dong 2013) used the fourth mode in this method to expand the ZVS region and increase efficiency. In the literature (Krismer and Kolar 2012) (Oggier, Garcia and Oliva 2009) (Krismer and Kolar 2009) (Hua, Mi and Gargies 2008) (Doncker, Divan and Kheraluwala 1991) (Huang, et al. 2016), the TPS phase shift method has been demonstrated in many modes. However, the most ideal mathematical expression in this method is realised over six modes (Harrye, et al. 2014). When Harrye's study is examined, it is seen that it covers the equations given in Huang's and Muthuraj's 2016 study (Muthuraj, et al. 2017).

In the TPS method, the six modes are defined as shown in Table 3 1. In this figure, the x-axes are in time. The voltages shown in red in the figure are the voltages of the high voltage side of the leakage inductance shown in Figure 1. The voltages shown in blue in the figure are the voltage of the low voltage side of the leakage inductance shown in Figure 1. The currents shown in black in the figure are the current of the leakage inductance shown in Figure 1. In addition, the modes shown with exponential numbers are the graphs drawn for the power flow in the other direction. The conditions of these modes are determined according to the occupancy ratios (k_1, k_2) of the AC three-level signals generated within the H bridges and the phase difference (k_3) of these signals at the rising moments. The relationship between the occupancy ratios and phase difference with the phase shift ratios used in the phase shift methods are shown in the following Equations.

$$k_1 = 1 - D_1 \tag{7}$$

$$k_2 = 1 - D_2 \tag{8}$$

$$k_3 = D_3 + D_2 - D_1 \tag{9}$$

Table 1. DAB Operating Modes with TPS Method (Harrye, et al. 2014)

Waveform	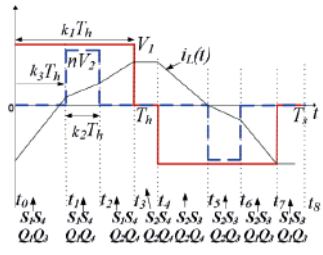	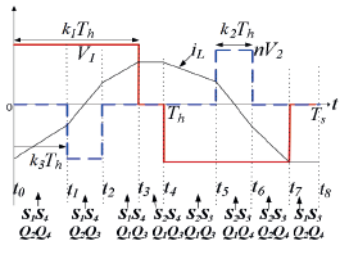
Mode	Mode 1 - Forward Energy Transmission	Mode 1 - Backward Energy Transmission
Conditions	$k_1 \geq k_2, 0 \leq k_3 \leq (k_1 - k_2)$	
Waveform	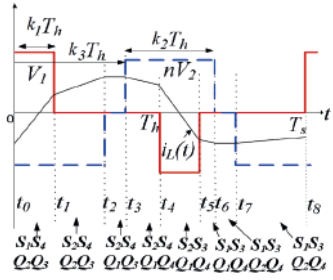	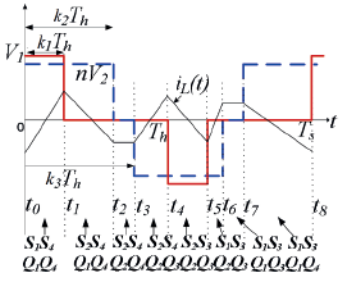
Mode	Mode 2 - Forward Energy Transmission	Mode 2 - Backward Energy Transmission
Conditions	$k_2 \geq k_1, \quad (1 + k_1 - k_2) \leq k_3 \leq 1$	
Waveform	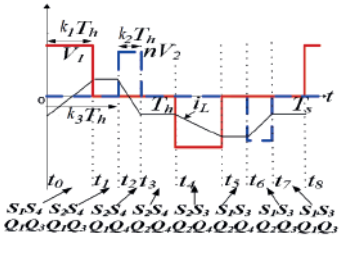	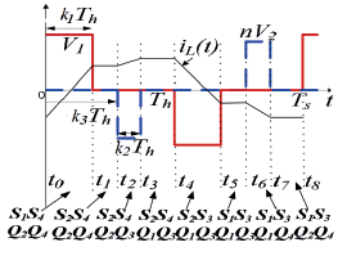
Mode	Mode 3 - Forward Energy Transmission	Mode 3 - Backward Energy Transmission
Conditions	$(k_1 + 1) \geq k_2, \ k_1 \leq k_3 \leq (1 - k_2)$	

Waveform	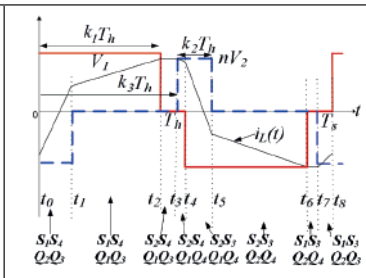	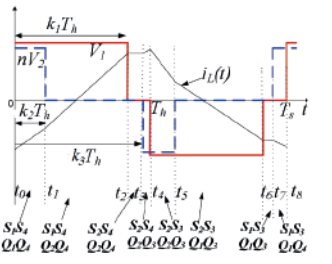
Mode	Mode 4 - Forward Energy Transmission	Mode 4 - Backward Energy Transmission
Conditions	$k_1 \leq k_3 \leq 1, \quad (1-k_3) \leq k_2 \leq (1-k_3+k_1)$	
Waveform	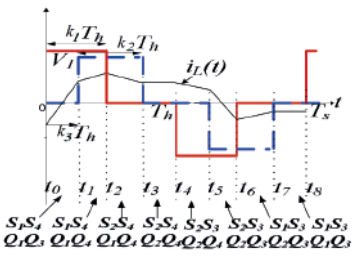	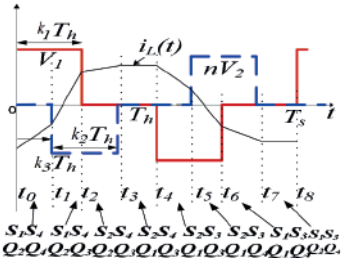
Mode	Mode 5 - Forward Energy Transmission	Mode 5 - Backward Energy Transmission
Conditions	$0 \leq k_3 \leq k_1, \quad (k_1-k_3) \leq k_2 \leq (1-k_3)$	
Waveform	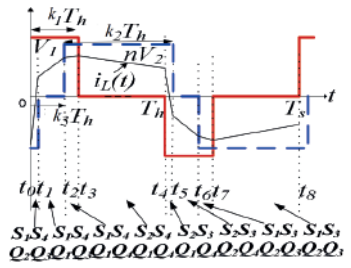	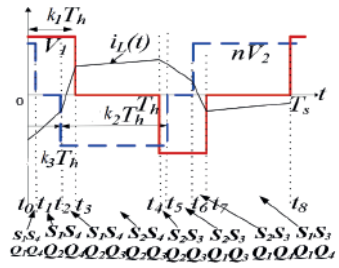
Mode	Mode 6 - Forward Energy Transmission	Mode 6 - Backward Energy Transmission
Conditions	$(1-k_2) \leq k_1, \quad (1-k_2) \leq k_3 \leq k_1$	

Mode 1: If the selected phase shifting method works under the conditions $k_1 \geq k_2$ and $0 \leq k_3 \leq (k_1 - k_2)$, it means that the method works in Mode 1 and the transmitted power equation is expressed mathematically as shown in Equation 10.

$$P = \frac{V_{HV} * N * V_{LV}}{2 * f_{SW} * L_{leakage}} (k_2{}^2 - k_1 k_2 + 2 k_2 k_3) \tag{10}$$

Mode 2: If the selected phase shifting method works under the conditions $k_2 \geq k_1$ and $(1 + k_1 - k_2) \leq k_3 \leq 1$, it means that the method works in Mode 2. The expression of the transmitted power equation is as shown in Equation 11.

$$P = \frac{V_{HV} * N * V_{LV}}{2 * f_{SW} * L_{leakage}} (k_1{}^2 - k_1 k_2 + 2k_1 - 2k_1 k_3) \tag{11}$$

Mode 3: If the selected phase shifting method works under the conditions $(k_1 + 1) \geq k_2$ and $k_1 \leq k_3 \leq (1 - k_2)$, it means that the method works in Mode 3. The mathematical expression of the transmitted power is shown in Equation 12.

$$P = \frac{V_{HV} * N * V_{LV}}{2 * f_{SW} * L_{leakage}} k_1 k_2 \tag{12}$$

Mode 4: If the selected phase shifting method operates in the conditions $k_1 \leq k_3 \leq 1$ and $(1 - k_3) \leq k_2 \leq (1 - k_3 + k_1)$, it means that the method operates in Mode 4 and mathematically the transmitted power equation is expressed as shown in Equation 13.

$$P = \frac{V_{HV} * N * V_{LV}}{2 * f_{SW} * L_{leakage}} (2k_2 - k_2{}^2 - k_3{}^2 + 2k_3 + k_1 k_2 - 2k_2 k_3 - 1) \tag{13}$$

Mode 5: If the selected phase shifting method operates in the conditions $0 \leq k_3 \leq k_1$ and $(k_1 - k_3) \leq k_2 \leq (1 - k_3)$, it means that the method operates in Mode 4 and mathematically the transmitted power equation is expressed as shown in Equation 14.

$$P = \frac{V_{HV} * N * V_{LV}}{2 * f_{SW} * L_{leakage}} (k_1 k_2 + 2k_1 k_3 - k_1{}^2 - k_3{}^2) \tag{14}$$

Mode 6: If the selected phase shifting method operates in the conditions $(1 - k_2) \leq k_1$ and $(1 - k_2) \leq k_3 \leq k_1$, it means that the method operates in Mode 4 and mathematically the transmitted power equation is expressed as shown in Equation 15.

$$P = \frac{V_{HV} * N * V_{LV}}{2 * f_{SW} * L_{leakage}} (k_1 k_2 + 2k_1 k_3 + 2k_2 - k_1{}^2 - k_2{}^2 - 2k_3{}^2 + 2k_3 - 2k_2 k_3 - 1) \tag{15}$$

When the DAB converters are operated with the TPS method, the direction of the transmitted power can be adjusted by *k3* or by increasing the phase difference of the second H bridge by 180 degrees. Thus, the resulting transmitted power is negative even if it is considered forward (Harrye, et al. 2014). In the modes given above, Mode 6 is the only mode that covers the entire operating power range. Modes 1 and 2 provide half of the power range. Modes 3, 4 and 5 are used for unidirectional power transfer.

In a study conducted by Zhao in 2012 (Zhao, Yu and Sun 2012), it was shown that the reactive power is reduced in the EPS method compared to the SPS method. However, in this study, the reactive power is given as back-flow power. However, Harrye mentioned in his 2014 article (Harrye, et al. 2014) that this situation is not clear. Because according to the definition, reactive power occurs when the current and voltage are opposite (in negative flow). However, it is certain that regardless of the level, the DAB with coupling inductances can attract reactive power. This reactive power can be reduced to a level that can be suppressed, especially with TPS techniques.

CONCLUSION

The choice of phase shift modulation method in dual active bridge (DAB) converters significantly impacts their performance, efficiency, and control characteristics. Various phase-shift modulation techniques offer different advantages and trade-offs, enabling specific applications according to specific application requirements.

One of the commonly used phase shift modulation method is the single phase shift modulation. This method uses a phase shift angle between the primary and secondary bridges throughout the operating range. Single phase shift modulation provides simplicity in control and eliminates the need for complex feedback systems. However, it can result in sub-optimal efficiency under light load conditions due to constant phase shift angles that do not adapt to varying power levels.

Another approach is variable phase shift modulation, which allows the phase shift angle to be adjusted dynamically depending on the load conditions. This method optimizes the efficiency of the converter at different power levels by adapting phase shifts to minimize switching losses and improve overall performance. Variable phase shift modulation requires sophisticated control algorithms and real-time feedback systems to continuously adjust phase shift angles.

Consequently, the selection of phase shift modulation methods in dual active bridge converters requires careful consideration of efficiency, control complexity and load range characteristics. Fixed, variable and hybrid modulation techniques offer distinct advantages, allowing designers to tailor their applications to specific application requirements. By understanding the differences between these modulation methods, engineers can optimize the performance and efficiency of dual active bridge converters in a variety of power conversion applications.

REFERENCES

Bai, H., ve C. Mi. «Eliminate Reactive Power and Increase System Efficiency of Isolated Bidirectional Dual-Active-Bridge DC–DC Converters Using Novel Dual-Phase-Shift Control.» *IEEE Transactions on Power Electronics* (IEEE) 23, no. 6 (2008): 2905 - 2914.

Doncker, R. W. A. A. De, D. M. Divan, ve M. H. Kheraluwala. «A three-phase soft-switched high-power-density DC/DC converter for high-power applications.» *IEEE Transactions on Industry Applications*, 1991: 63-73.

Harrye, Yasen A., K.H Ahmed, G.P Adam, ve A.A Aboushady. «Comprehensive steady state analysis of bidirectional dual active bridge DC/DC converter using triple phase shift control.» *2014 IEEE 23rd International Symposium on Industrial Electronics (ISIE)*. Istanbul, Turkey: IEEE, 2014. 437-442.

Hua, B., C. C. Mi, ve S. Gargies. «The short-time-scale transient processes in high-voltage and high-power isolated bidirectional dc-dc converters.» *IEEE Transactions on Power Electronics*, 2008: 2648-2656.

Huang, Jun, Yue Wang, Zhuoqiang Li, ve Wanjun Lei. «Unified Triple-Phase-Shift Control to Minimize Current Stress and Achieve Full Soft-Switching of Isolated Bidirectional DC–DC Converter.» *IEEE Transactions on Industrial Electronics* (IEEE) 63, no. 7 (2016): 4169 - 4179.

Huiqing, W., ve X. Wei dong. «Bidirectional Dual-Active-Bridge DCDC Converter with Triple-Phase-Shift Control.» *Applied Power Electronics Conference and Exposition (APEC)*. IEEE, 2013.

Inoue, S., ve H. Akagi. «A bidirectional dc-dc converter for an energy storage system with galvanic isolation.» *IEEE Trans. Power Electronics*, 2007: 2299–2306.

Kızıcı, Aykut. *Design and Implementation of A High Power Density Dual Active Bridge DC/DC Converter With GaN Power Transistors.* Ankara, Turkey: Hacettepe University, 2019.

Krismer, F., ve J.W. Kolar. «Closed Form Solution for Minimum Conduction Loss Modulation of DAB Converters.» *IEEE Transaction on Power Electronics*, 2012: 174-188.

Kuiyuan, W., C. W. Silva, ve W. G. Dunford. «Stability analysis of isolated bidirectional dual active full-bridge dc-dc converter with triple phase shift control.» *IEEE Transaction on Power Electronics*, 2012: 2007-2017.

Kumar, A., A. H.Bhat, and P. Agarwal. "Comparative Analysis Of Dual Active Bridge Isolated Dc To Dc Converter With Single Phase Shift And Extended Phase Shift Control Techniques." *2017 6th International Conference on Computer Applications In Electrical Engineering-Recent Advances (CERA)*. 2017.

Muthuraj, S. S., V. K. Kanakesh, P. Das, ve S. K. Panda. «Triple Phase Shift Control of an LLL Tank Based Bidirectional Dual Active Bridge Converter.» *IEEE Transactions on Power Electronics*, 2017: 8035-8053.

Naayagi, R. T., A. J. Forsyth, ve RShuttleworth. «Performance analysis of extended phase-shift control of DAB DC-DC converter for aerospace energy storage system.» *11th International Conference on Power Electronics*. Australia: IEEE , 2015. 514-517.

Oggier, G. G., G. O. Garcia, ve A. R. Oliva. «Modulation strategy to operate the dual active bridge dc-dc converter under soft switching in the whole operating range.» *IEEE Trans. Power Electronics*, 2011: 1228–1236.

Oggier, G. G., G. O. Garcia, ve A. R. Oliva. «Switching control strategy to minimize dual active bridge converter losses.» *IEEE Trans. Power Electronics*, 2009: 1826–1838.

Texas Instruments. *Bi-Directional, Dual Active Bridge Reference Design for Level 3 Electric Vehicle Charging Stations*. ti.com, 2019.

Ye, Z., P. Jain, ve P. Sen. «Circulating current minimization in high frequency AC power distribution architectures with multiple inverter modules operated in parallel .» *IEEE Trans. Ind. Electron*, 2007: 2673–2687.

Zengin, S. *Silisyum Karbür (SiC) Güç Anahtari Kullanan Tek Aşamali Çift Aktif Köprü AA-DA Dönüştürücü*. İzmir: Ege Üniversitesi, 2019.

Zhang, Zhao, et al. "An Improved DC Bias Elimination Strategy with Extended Phase Shift Control for Dual-Active-Bridge DC-DC." *2019 Chinese Automation Congress*. Hangzhou, China: IEEE, 2019.

Zhao, B., Q. Song, ve W. Liu. «Power Characterization of Isolated Bidirectional Dual-Active-Bridge DC–DC Converter With Dual-Phase-Shift Control.» *IEEE Transactions on Power Electronics* (IEEE) 27, no. 9 (2012): 4172 - 4176.

Zhao, B., Q. Song, W. Liu, ve Y. Sun. «Overview of Dual-Active-Bridge Isolated Bidirectional DC-DC Converter for High-Frequency-Link Power-Conversion System.» *IEEE TRANSACTIONS ON POWER ELECTRONICS*, 2014: 4091 - 4106.

Zhao, B., Q. Yu, ve W. Sun. «Extended-Phase-Shift Control of Isolated Bidirectional DC–DC Converter for Power Distribution in Microgrid.» *IEEE Transactions on Power Electronics*, 2012: 4667-4680.

CV

Dr. Sancar graduated from Süleyman Demirel University with a degree in Energy Systems Engineering in 2015. During his university years, he actively participated in TÜBİTAK projects in the field of energy recovery and renewable energy. In the same year, he assumed the role of founding president of the Energy Systems Engineering Project and Solution Association, where he conducted research on resolving Turkey's energy dependency and promoting renewable energy production. He continued his education by pursuing a master's degree in Energy Systems Engineering at the Department of Energy Systems Engineering at Süleyman Demirel University's Faculty of Science and Letters. In the same year, he was selected as a young energy leader by BEC. Throughout his master's studies, he continued his involvement in the association's activities and academic research. In 2018, he completed his master's degree and started his doctoral studies in the same field of study at Süleyman Demirel University, focusing on the priority areas of YÖK 100/2000. Due to university changes, he is currently pursuing his doctoral studies at Isparta Applied Sciences University, conducting academic research on electric vehicles and photovoltaic systems.

In summary, Dr. Sancar's career has been shaped by his active participation in research projects, his leadership role in the Energy Systems Engineering Project and Solution Association, and his academic contributions to the field of energy systems engineering. He specializes in electric vehicles and photovoltaic systems.

Renewable Energy Systems and Power Electronics: Advances, Applications, and Integration

Editor:
Dr. Muhammet Raşit Sancar

ÖZGÜR YAYINLARI

ISBN 978-975-447-675-0